National Library of Canada
Acquisitions and Bibliographic Services Branch
395 Wellington Street
Ottawa, Ontario
K1A 0N4

Bibliothèque nationale du Canada
Direction des acquisitions et des services bibliographiques
395, rue Wellington
Ottawa (Ontario)
K1A 0N4

Your file Votre référence

Our file Notre référence

NOTICE

The quality of this microform is heavily dependent upon the quality of the original thesis submitted for microfilming. Every effort has been made to ensure the highest quality of reproduction possible.

If pages are missing, contact the university which granted the degree.

Some pages may have indistinct print especially if the original pages were typed with a poor typewriter ribbon or if the university sent us an inferior photocopy.

Reproduction in full or in part of this microform is governed by the Canadian Copyright Act, R.S.C. 1970, c. C-30, and subsequent amendments.

AVIS

La qualité de cette microforme dépend grandement de la qualité de la thèse soumise au microfilmage. Nous avons tout fait pour assurer une qualité supérieure de reproduction.

S'il manque des pages, veuillez communiquer avec l'université qui a conféré le grade.

La qualité d'impression de certaines pages peut laisser à désirer, surtout si les pages originales ont été dactylographiées à l'aide d'un ruban usé ou si l'université nous a fait parvenir une photocopie de qualité inférieure.

La reproduction, même partielle, de cette microforme est soumise à la Loi canadienne sur le droit d'auteur, SRC 1970, c. C-30, et ses amendements subséquents.

Canada

Multi-Reception Techniques in CDMA Networks

Ehsan Rezaaifar

A Thesis

in

The Department

of

Electrical and Computer Engineering

Presented in Partial Fulfillment of the Requirements
for the Degree of Master of Applied Science at
Concordia University
Montreal, Quebec, Canada

September 1995

©Ehsan Rezaaifar, 1995

National Library of Canada
Acquisitions and Bibliographic Services Branch
395 Wellington Street
Ottawa, Ontario
K1A 0N4

Bibliothèque nationale du Canada
Direction des acquisitions et des services bibliographiques
395, rue Wellington
Ottawa (Ontario)
K1A 0N4

Your file Votre référence

Our file Notre référence

THE AUTHOR HAS GRANTED AN IRREVOCABLE NON-EXCLUSIVE LICENCE ALLOWING THE NATIONAL LIBRARY OF CANADA TO REPRODUCE, LOAN, DISTRIBUTE OR SELL COPIES OF HIS/HER THESIS BY ANY MEANS AND IN ANY FORM OR FORMAT, MAKING THIS THESIS AVAILABLE TO INTERESTED PERSONS.

L'AUTEUR A ACCORDE UNE LICENCE IRREVOCABLE ET NON EXCLUSIVE PERMETTANT A LA BIBLIOTHEQUE NATIONALE DU CANADA DE REPRODUIRE, PRETER, DISTRIBUER OU VENDRE DES COPIES DE SA THESE DE QUELQUE MANIERE ET SOUS QUELQUE FORME QUE CE SOIT POUR METTRE DES EXEMPLAIRES DE CETTE THESE A LA DISPOSITION DES PERSONNE INTERESSEES.

THE AUTHOR RETAINS OWNERSHIP OF THE COPYRIGHT IN HIS/HER THESIS. NEITHER THE THESIS NOR SUBSTANTIAL EXTRACTS FROM IT MAY BE PRINTED OR OTHERWISE REPRODUCED WITHOUT HIS/HER PERMISSION.

L'AUTEUR CONSERVE LA PROPRIETE DU DROIT D'AUTEUR QUI PROTEGE SA THESE. NI LA THESE NI DES EXTRAITS SUBSTANTIELS DE CELLE-CI NE DOIVENT ETRE IMPRIMES OU AUTREMENT REPRODUITS SANS SON AUTORISATION.

ISBN 0-612-05134-X

Canada

ABSTRACT

MULTI-RECEPTION TECHNIQUES IN CDMA NETWORKS

Ehsan Rezaaifar

Nowadays the application of Spread Spectrum Multiple Access, or more specifically Code Division Multiple Access, in civil and commercial communication systems, is a hot research topic. In the conventional single user systems co-channel interference and the necessity of power control (because of near-far problem) are the major problems. The multi-user detection scheme as a possible way to overcome these problems is under investigation. There are numerous papers proposing different types of multi-user detection. Besides the receiver, selecting appropriate codes for signature codes plays an important role to eliminate the interference.

In the first part of the thesis, the effects of choosing different kinds of codes as signature codes on SNR and BER of CDMA systems employing multi-user detection, are studied. Results, obtained by simulations, for different kinds of codes are brought and compared.

In the second part, a new hybrid single user/multi-user receiver for CDMA systems is proposed. By computer simulations, it has been shown that in some noise environments single user detection might perform better than sub-optimum multi-user detection. So the hybrid system, by taking advantage of both single user and multi-user detection, is able to perform better than both of them in all cases.

Finally, the performance of multi-user detection in voice transmission is examined and the results of computer simulations are reported.

Dedicated to My Parents

ACKNOWLEDGEMENT

I would like to express my sincere gratitude to my thesis supervisor, Professor A. K. Elhakeem, for his continued guidance, suggestions and encouragement during the course of this thesis.

My special thanks and appreciations to my parents, who always made everything so easy for me, and to my beloved wife and my best friend, Shadia, for her moral support, love, and help in typing the thesis.

I also like to use this opportunity to thank two wonderful people, two of my best friends, Mr. Hamid-Reza Mehrvar and Mr. Sayed Hossein Saboksayr, for whatever they did for me, specially during last few months.

TABLE OF CONTENTS

LIST OF SYMBOLS AND ABBREVIATIONS

α	the probability of going from active to silent mode
β	the probability of going from silent to active mode
b_k	the information symbol sequence of user k
E_k	received energy of user k
ϕ	phase
G	Processing Gain
$\boldsymbol{H}$	matrix of cross-correlations
$\boldsymbol{H}_N$	Hadamard matrix of order N
K	total number of users
L	code length
n	number of stages in linear feedback shift register
$n(t)$ or $w(t)$	Gaussian noise with power spectral density σ_n^2 or σ_w^2
P_A	steady state probability of active period
P_S	steady state probability of silent period
$\boldsymbol{R}$	matrix of normalized cross-correlations
$R_c(\tau)$	autocorrelation function of code sequence
$r(t)$	received signal at the receiver
$S_c(f)$	power spectral density of code sequence
sgn(.)	sign function
$s_k(t)$	signature waveform for user k
τ	time delay
T_c	chip duration
T_P	packet transmission time

T_P	packet transmission time
T_S or T	data symbol duration
$WAL(n,T)$	Walsh function of order n
A/D	Analog to Digital convertor
AWGN	Additive White Gaussian Noise
BER	Bit Error Rate
BPSK	Binary Phase Shift Keying
BS	Base Station
CDMA	Code Division Multiple Access
CRAD	Coherent Receiver Antenna Diversity
D/A	Digital to Analog convertor
DS	Direct Sequence
FDMA	Frequency Division Multiple Access
FH	Frequency Hopping
IC	Interference Cancellation
JD	Joint Detection
MS	Mobile Station
PN	pseudonoise sequence
RLS	Recursive Least Square
SNR	Signal to Noise Ratio
SSMA	Spread Spectrum Multiple Access
TDMA	Time Division Multiple Access
TH	Time Hopping

LIST OF FIGURES

CHAPTER 1

INTRODUCTION

1.1 Spread Spectrum Communications

Most of the modulation and the demodulation techniques in digital communications have been designed to communicate digital information from one place to another as efficient as possible in a stationary Additive White Gaussian Noise (AWGN) environment. The transmitted signals have been selected to be relatively efficient in their use of the communication resources of power and bandwidth. The demodulators have been designed to yield minimum bit error probability for the given transmitted signal in AWGN.

Although many real-world communication channels are accurately modeled as stationary AWGN channels, there are other important channels which do not fit in this model. For example, jamming (continuous wave tone jamming or pulse jamming) in military communications, or the interference occurs when there are multiple propagation paths between the transmitter and the receiver called multipath reception, see Fig.1.1.

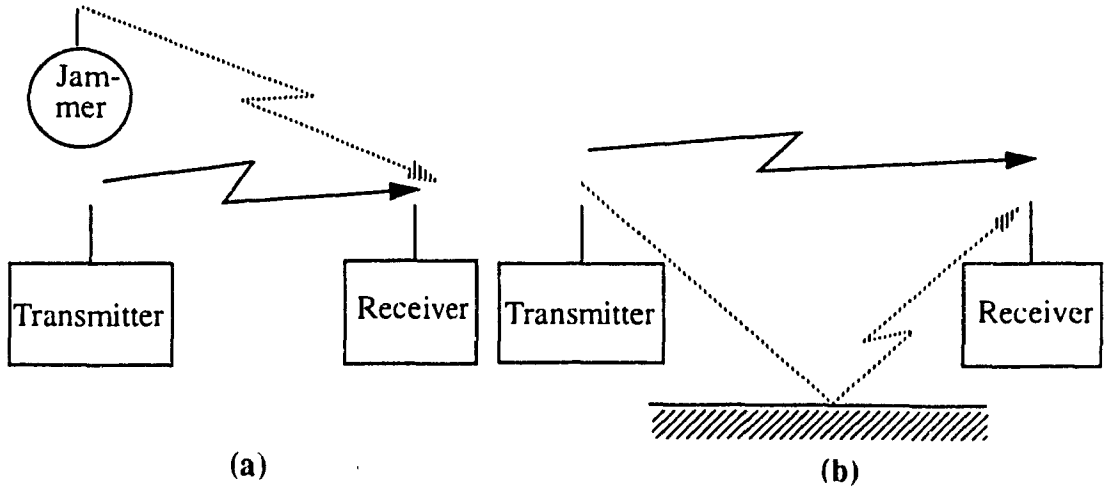

Fig. 1.1: Two examples of non AGWN channels [1], (a) Narrowband interference, (b) Multipath reception.

The spread spectrum is a modulation and demodulation technique that can be used as an aid in mitigating the effects of the types of interference described above [2]. It is called spread spectrum because the bandwidth occupied by the information signal is much larger than the minimum bandwidth required for transmitting the digital information. In other words, the information signal is spread in a very wide bandwidth by means of a code which is independent of data, called spreading code or sequence. At the receiver, the signal is despread to its normal bandwidth by applying the synchronized spreading code, see Fig.1.2 (page 7).

Fig.1.3 (page 7) shows the interference rejection capability of spread spectrum communications. As it is shown in Fig.1.3(a), at the receiver, the desired signal has the bandwidth much wider than interference. After despreading, applying the spreading code to the received signal (desired signal plus noise and interference), the bandwidth of the desired signal is reduced to B (bandwidth of signal before spreading), while the interference energy is spread over a bandwidth exceeding W (bandwidth of spread spectrum signal), Fig.1.3(b). The filtering action of the demodulator removes most of the interference spectrum that does not overlap the signal spectrum. Thus, most of the original interference energy is eliminated and does not affect the receiver performance [3]. The ratio W/B which is an approximate measure of the interference rejection is called *processing gain*:

$$G = \frac{W}{B} \tag{1.1}$$

The spread spectrum techniques fall into one of four general categories:

1- Direct Sequence (DS)

2- Frequency Hopping (FH)

3- Time Hopping (TH)

4- Chirp

Hybrid combinations of these might also be used to take advantage of some of the properties of the different categories.

1.2 Direct Sequence Systems

A direct sequence system spreads the transmitted spectrum by directly applying the baseband pulses (of normalized amplitudes equal to +1 or -1) representing the pseudorandom sequence, which is produced by a pseudorandom code generator (see chapter 3). The pseudorandom sequences are long binary sequences (of ones and zeros) at bit rates usually much higher than the bit rate of information sequence.

Fig.1.4 (page 8) shows the direct sequence system with binary phase modulation [3]. The processing gain in DS system is equal to the number of chips (the pulses of code sequence) in a symbol interval:

$$G = \frac{T_s}{T_c} \tag{1.2}$$

where T_s and T_c are the data symbol period and the chip period, respectively.

1.3 Frequency Hopping Systems

The desired wideband frequency spectrum is generated in a different manner in a frequency hopping system. It does just what its name implies. That is, it "hops" from frequency to frequency over a wide band. In other words, in frequency hopping system the frequency of the carrier is changed from time to time according to a pseudorandom code. In the receiver these hops are regenerated, by employing a frequency synthesizer controlled by pseudorandom code, in order to catch and detect the desired signal, Fig.1.5 (page 9).

A frequency hopping signal may be regarded as a sequence of modulated pulses with pseudorandom carrier frequencies. The set of possible carrier frequencies is called the *hopset*. Hopping occurs over a frequency band that includes a number of *frequency channels*. Each channel is defined as spectral region with a center frequency in the hopset and a bandwidth large enough to include most of the power in a pulse with corresponding carrier frequency. The bandwidth of a frequency channel is often called the *instantaneous bandwidth* denoted by B. The bandwidth of the frequency band over which the hopping occurs is called the *total hopping bandwidth* denoted by W. The time duration between hops is *hop duration* or the *hopping period* and is denoted by T_h.

Frequency hopping may be classified as fast or slow. Fast frequency hopping (FFH) occurs if there is one or more frequency hops for each transmitted symbol. Thus, fast frequency hopping implies that the hopping rate ($f_h = 1/T_h$) equals or exceeds the information symbol rate. Slow frequency hopping (SFH) occurs if two or more symbols are transmitted in the time interval between frequency hops.

The processing gain in frequency hopping spread spectrum system is equal to the total hopping bandwidth divided by instantaneous bandwidth, Eq. (1.1).

1.4 Time Hopping Systems

In time hopping systems, the spreading is achieved by compressing the information signal in the time domain. That is, the time hopping systems control their transmission time and period with a code sequence in the same way that frequency hoppers control their frequencies. A typical time hopping system is shown in Fig.1.6 (page 10).

In the time hopping system, the time axis is divided into intervals known as frames, and each one of these frames is subdivided into M time slots. During each frame, in only one time slot, the carrier will be modulated with a message by any modulation method.

The time slot is chosen for a given frame by means of PN (pseudonoise) code generator. High bandwidth efficiency and simpler implementation than FH are the advantages of the TH. The disadvantages are long acquisition time and the need for error correction [4].

1.5 Chirp Systems

Chirp systems are the only spread spectrum systems that do not normally employ a code sequence to control their output signal spectra. Instead, a chirp signal is generated by sliding the carrier over a given range of frequencies in a linear or some other known manner during a fixed pulse period.

The idea behind chirp signals is that the receiver can employ a matched filter of the relatively simple design to reassemble the time-dispersed carrier power in such a way it adds coherently and thus provides an improvement in signal to noise ratio [5].

1.6 Code Division Multiple Access (CDMA)

The Spread Spectrum Multiple Access (SSMA) systems, or more specifically Code Division Multiple Access (CDMA), have been studied as a powerful alternative to traditional multiple access schemes such as Frequency Division Multiple Access (FDMA) and Time Division Multiple Access (TDMA), for civil and commercial communications. In a CDMA system, all users transmit the data simultaneously on the same bandwidth. Each user is assigned with a specific spreading waveform called signature code, $s_k(t)$, which makes it possible for the receiver to distinguish and detect the data transmitted by the desired user. Fig.1.7 (page 11) shows a simple model for DS-CDMA system.

1.7 Thesis Outline

The thesis is organized as follows:

In chapter 2, multi-user detection for CDMA systems is introduced. The optimum multi-user detection and decorrelating receiver are briefly explained. Then a few different schemes for multi-user detection are explained in more details.

In chapter 3, the effects of choosing different kinds of codes as signature codes in multi-user detection scheme on signal to noise ratio and bit error rate are studied. Different kinds of codes are described in details and the results, obtained by simulations, of employing these codes as signature codes in multi-user detection are brought and compared with each other in this chapter.

In chapter 4, a new hybrid single user/multi-user detection scheme is introduced. Then the single user and multi-user detection are compared with each other for different cases. The rest of this chapter is devoted to the performance of the multi-user detection in voice transmission, when there is ON and OFF periods.

Finally, summary and some conclusion remarks are brought in chapter 5.

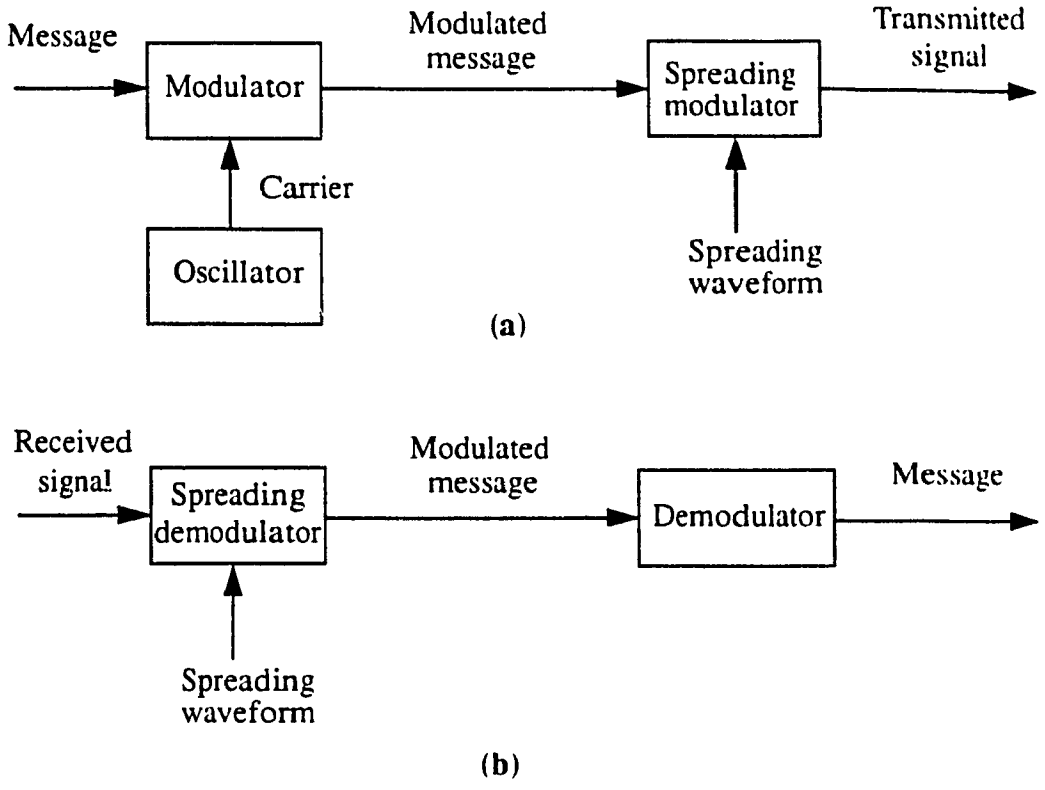

Fig. 1.2: Spread spectrum system: (a) transmitter, (b) receiver

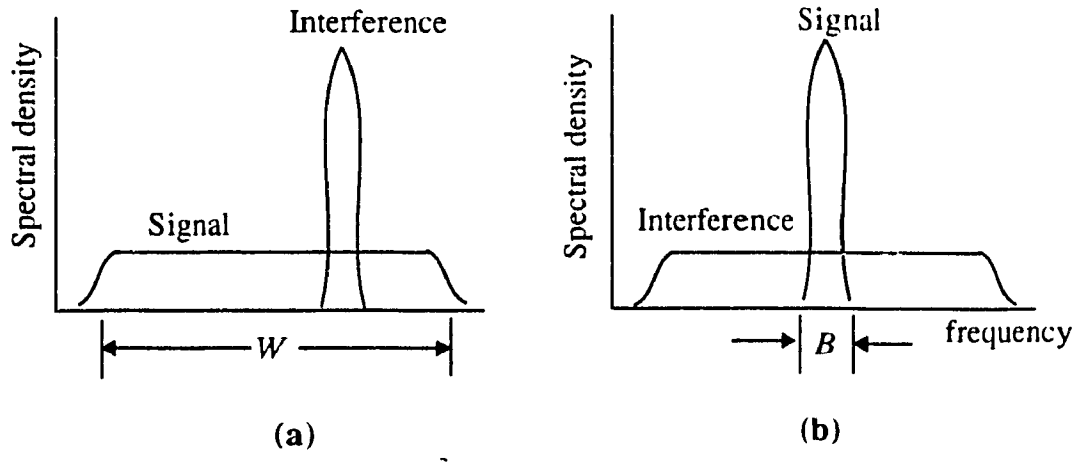

Fig. 1.3: Spectra of desired signal and interference: (a) before despreading, (b) after despreading

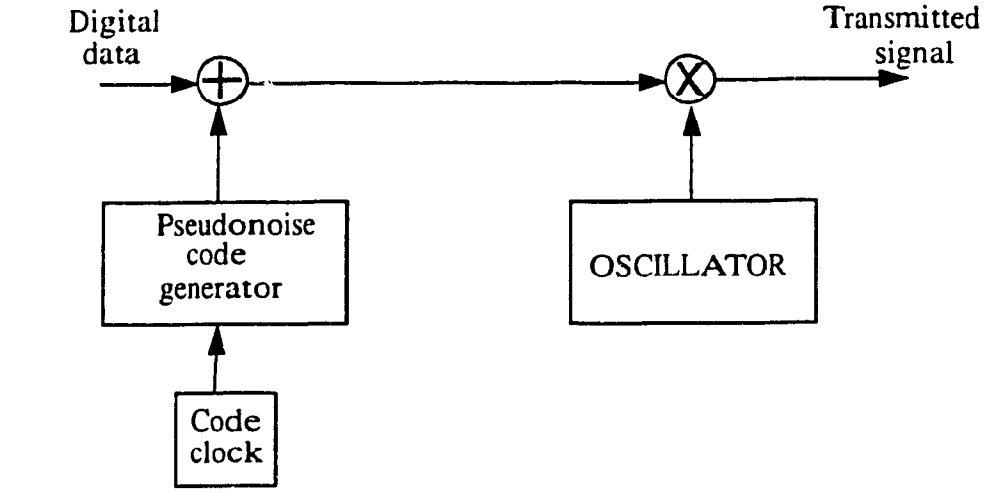

(a)

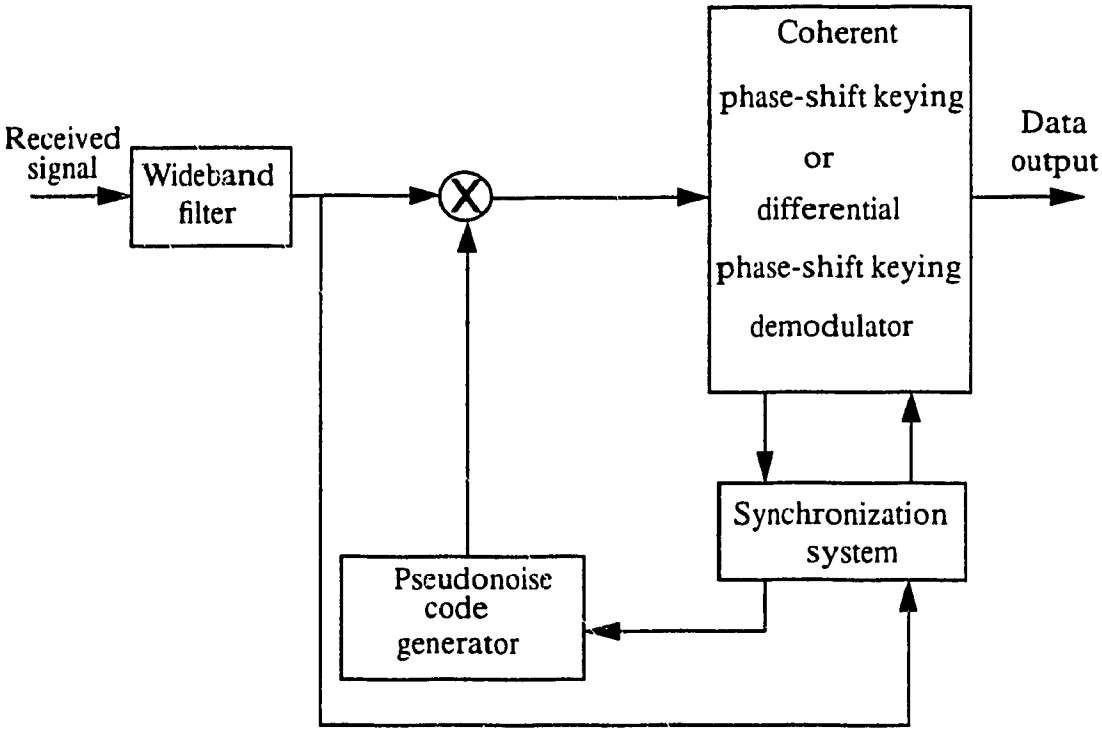

(b)

Fig. 1.4: Direct sequence system with binary phase modulation: (a) transmitter, (b) receiver

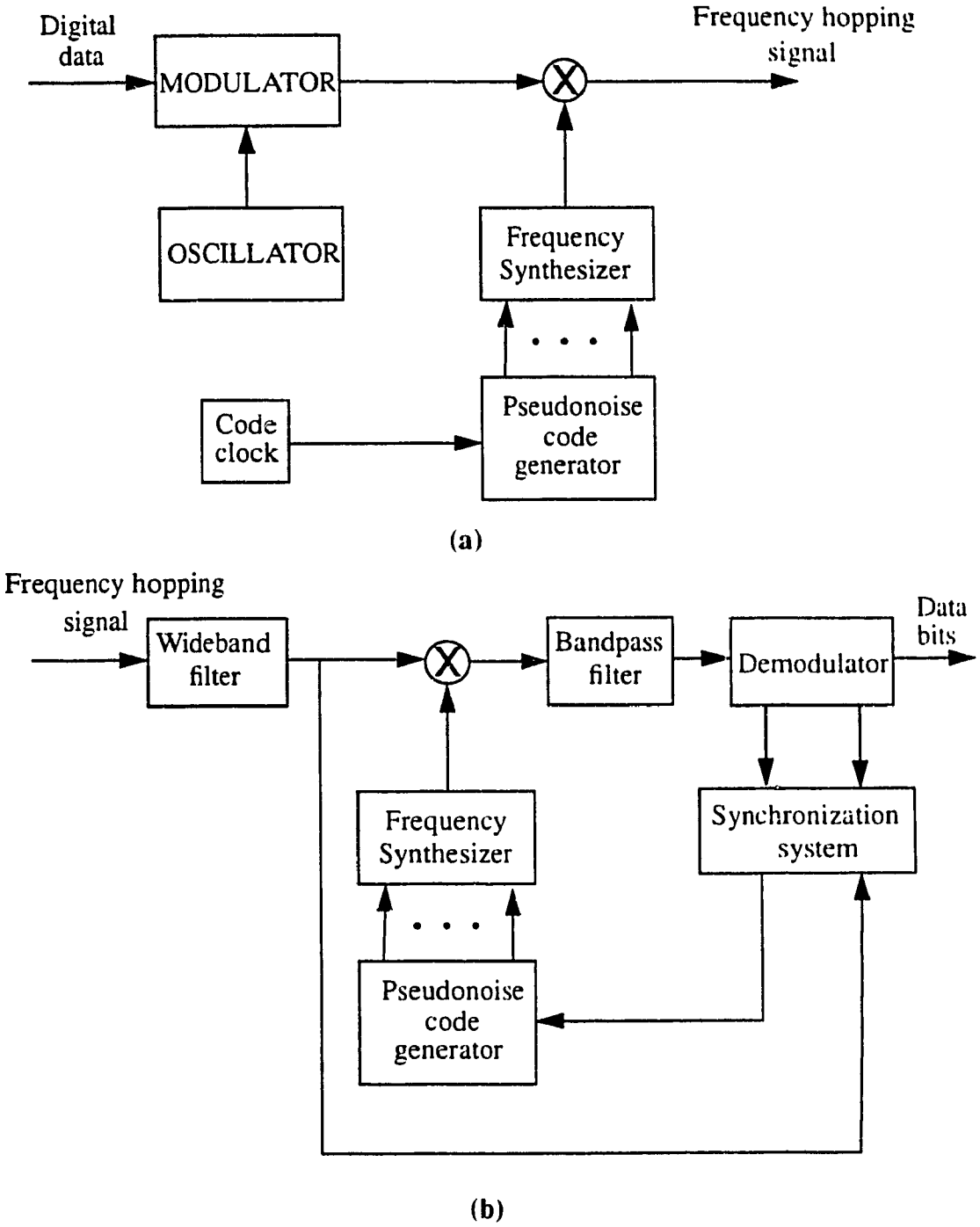

Fig. 1.5: General form of frequency hopping system: (a) transmitter, (b) receiver

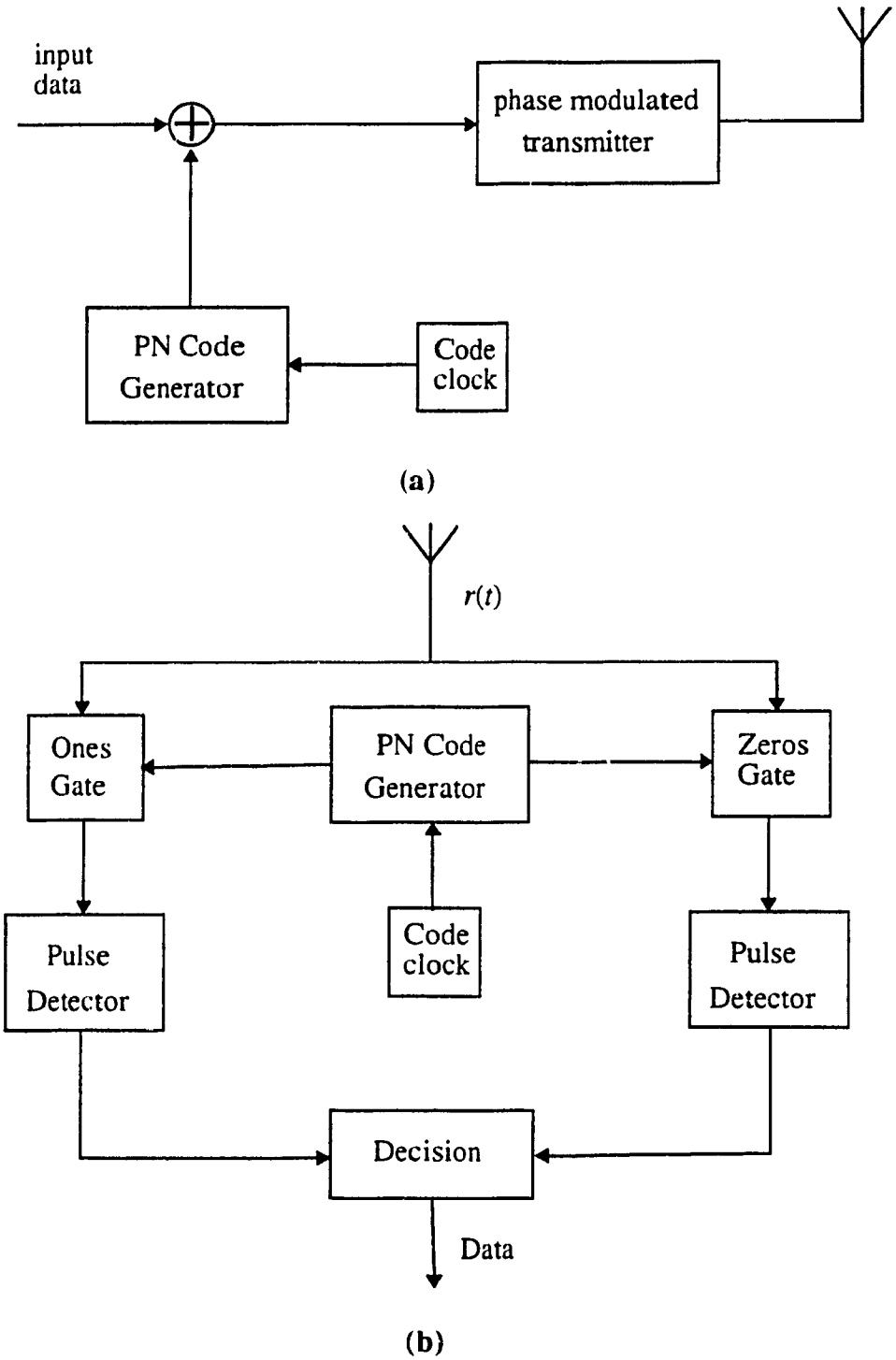

Fig. 1.6: Block diagram of Time Hopping system: (a) transmitter, (b) receiver

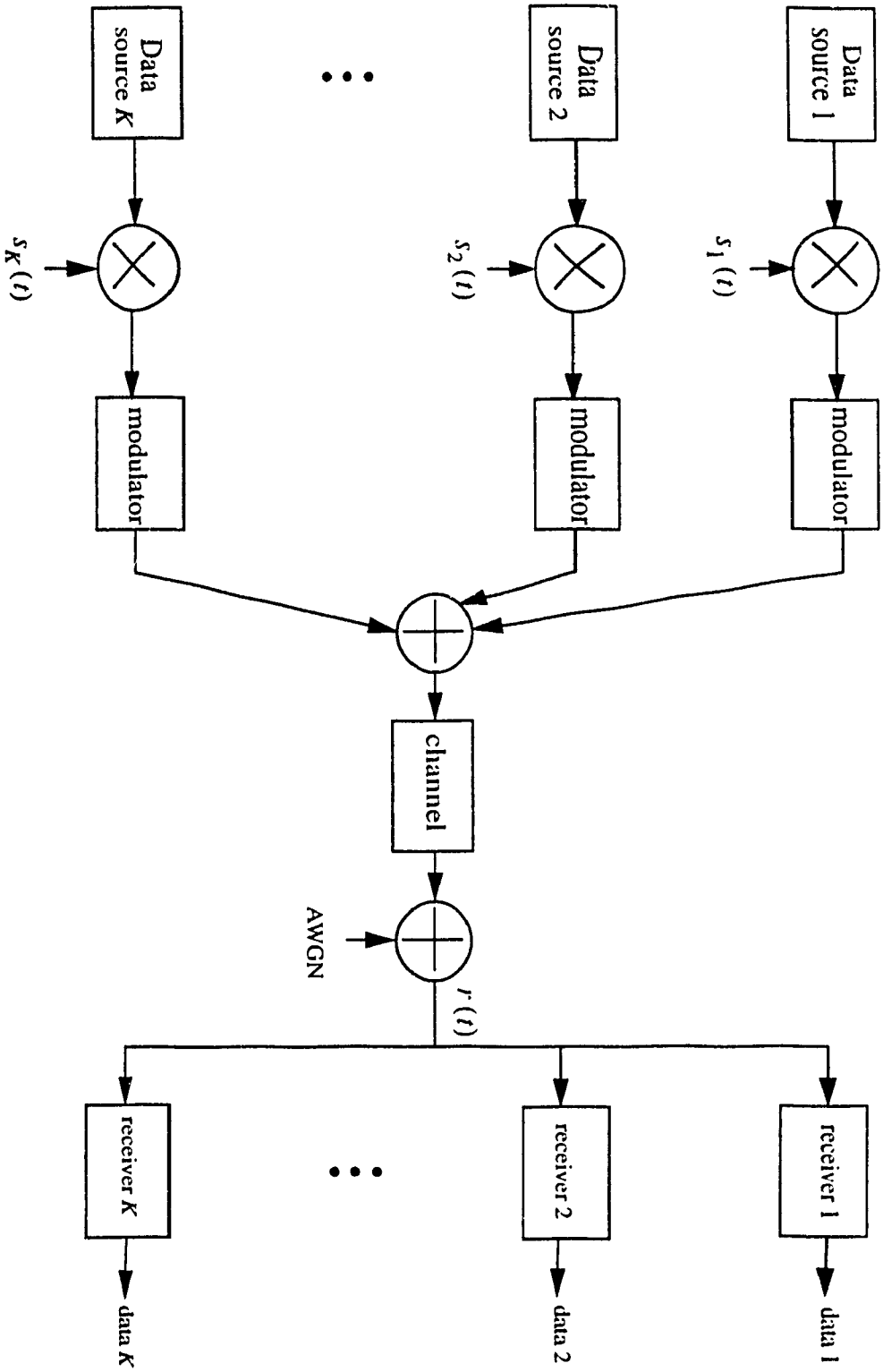

Fig. 1.7: Model of DS-CDMA system

CHAPTER 2

THE MULTI-USER DETECTION SCHEMES FOR CDMA SYSTEMS

2.1 Introduction

In conventional single user detector, Fig.2.1 (page 33), the signals from other users, co-channel interference, are considered as Gaussian noise, while detecting the signal of desired user. This detector (matched filter or correlator receiver) minimizes the probability of the error in a single user channel (in the absence of interfering users) corrupted by additive white Gaussian noise.

The performance of conventional single user detector is acceptable if the energies of the received signals from different users are not too different and the signature waveforms are designed so that their cross-correlations are low enough (this depends on the desired maximum number of simultaneous users) [6]. In practice, low cross-correlations are usually achieved by employing pseudonoise sequences of long periodicity (these sequences are described in details in chapter 3). If the received signal energies are very different, i.e., some users are very weak in comparison to others, then the conventional single user detector is unable to recover the messages of the weak users reliably, even if the signature waveforms have very low cross-correlations. This is known as the *near-far* problem and is the main shortcoming of currently operational Direct Sequence Spread Spectrum Multiple Access (DS-SSMA) systems. Power control and the design of signals with better cross-correlation properties are two possible ways to solve this problem.

Unfortunately, power control (i.e., the adaptive adjustment of transmitter power depending on its location and on the received powers of the other users) dictates signifi-

cant reductions in the transmitted powers of the strong users in order for the weaker users to achieve reliable communication. Thus, power control actually decreases the overall multiple access and antijamming capabilities of the system. Furthermore, more and more complex signature waveforms lead to rapid increase in system cost and bandwidth, and as it was noted, do not eliminate the near-far problem [6]. Multi-user detection is the possible solution for the near-far problem besides its capability of increasing the capacity of the system.

The multi-user detection did not develop until relatively recently because there was a belief that multiple access interference is accurately modeled as a white Gaussian random process, and thus the conventional detector is essentially optimum. But in recent years there has been a lot of effort to find and develop the optimum and sub-optimum multi-user detection schemes.

The optimum multi-user detector, which is a bank of matched filters followed by a decision system, Fig.2.2 (page 33), for general asynchronous Gaussian channels was derived and analyzed in [7]. Here we focus on the synchronous case, where the users maintain symbol synchronization, and explain the optimum receiver [8].

The received signal at the receiver is:

$$r(t) = \sum_{k=1}^{K} b_k(j)\, s_k(t - jT) + n(t), \qquad t \in [jT, jT + T] \tag{2.1}$$

where $n(t)$ is the Gaussian noise with power spectral density σ_n^2, $s_k(t)$, $t \in [0, T]$, is the finite energy signature waveform and, $b_k(j) \in \{-1, 1\}$ is the kth user information symbol in the symbol interval j. Assuming that all possible information sequences are equally likely, it suffices to restrict attention to a specific symbol interval in Eq. (2.1), e.g., $j = 0$.

It is easy to check that the likelihood function depends on the observations only

through the outputs of a bank of matched filters [8];

$$y_k = \int_0^T r(t)\, s_k(t)\, dt, \qquad k = 1, \ldots, K \tag{2.2}$$

and therefore $\boldsymbol{y} = (y_1, \ldots, y_K)$ are sufficient statistics, [9,10], for demodulating $\boldsymbol{b} = (b_1, \ldots, b_K)$. From Eq. (2.2) we have

$$\boldsymbol{y} = \boldsymbol{H}\boldsymbol{b} + \boldsymbol{n} \tag{2.3}$$

where $\boldsymbol{H}$ is the non negative definite matrix of cross-correlations between the assigned signature waveforms:

$$H_{ij} = \int_0^T s_i(t)\, s_j(t)\, dt \tag{2.4}$$

and $\boldsymbol{n}$ is a zero-mean Gaussian K-vector with covariance matrix equal to $\sigma_n^2 \boldsymbol{H}$.

Conventional single user is the simplest way to make decisions based on y_k yielding the following decisions for the kth user:

$$\hat{b}_k = \operatorname{sgn}[y_k] \tag{2.5}$$

On the other hand, the optimum multi-user detector selects the most likely hypothesis $\hat{\boldsymbol{b}}^* = (\hat{b}_1^*, \ldots, \hat{b}_k^*)$ given the observations, which corresponds to selecting the noise realization with minimum energy [6], i.e.,

$$\hat{\boldsymbol{b}}^* \in arg \min_{\boldsymbol{b} \in \{-1, 1\}^K} \int_0^T \left[r(t) - \sum_{k=1}^{K} b_k s_k(t) \right]^2 dt$$

$$= arg \max_{\boldsymbol{b} \in \{-1, 1\}^K} 2y^T\boldsymbol{b} - \boldsymbol{b}^T\boldsymbol{H}\boldsymbol{b} \tag{2.6}$$

The optimum detector affords important performance gain over the conventional single user detector, in particular, it solves the near-far problem. However, the price for this is exponential complexity in the number of users [7], since the combinational optimization problem of selecting the most likely transmitted bits given the matched filter outputs is inherently hard [11].

Consequently, considerable recent effort has been expected to develop multi-user detectors that are robust (i.e., show near-far resistance) without the exponential complexity of the optimum multi-user detector. An important class of such sub-optimal detectors with linear complexity (in the number of users) is the decorrelating detector originally proposed by [12] and comprehensively analyzed by [8]. In decorrelating detector the decision is done as following [8]:

$$\hat{\boldsymbol{b}} = \text{sgn}\,[\boldsymbol{H}^{-1}y] \tag{2.7}$$

This detector is not an optimum detector but it is near-far resistant with much less complexity than the optimum detector.

There is a large number of papers in recent years proposing different kinds of sub-optimal multi-user detection schemes. In the following sections a few of theses schemes will be explained. The system explained in Sec.2.2, is used as multi-user scheme in simulations for this thesis.

2.2 Adaptive Multi-User Detector for Synchronous CDMA [13]

In Direct Sequence Code Division Multiple Access (DS-CDMA) each user is

assigned with a specific code called signature code, $s_k(t)$, k=1,2,...,K.

The signature waveform is composed of a spreading sequence of L chips, i.e.,

$$s_k(t) = \sum_{m=1}^{L} a_m^k P_{T_c}[t-(m-1)T_c] \tag{2.8}$$

and

$$\int_0^T s_k^2(t)\,dt = 1 \tag{2.9}$$

where T is common symbol duration, P_{T_c} is the spreading pulse of duration $T_c = \frac{T}{L}$ and the chip symbols $a_m^k \in \{-1, 1\}$.

The received signal in additive white Gaussian noise (AWGN) $w(t)$ is then given by (refer to Eq. (2.8))

$$r(t) = \sum_{i} \sum_{k=1}^{K} \sqrt{E_k} b_k(i)\, s_k(t-iT) + w(t) \tag{2.10}$$

where $b_k(i) \in \{1, -1\}$ represents kth user's bit during the ith interval. If we consider synchronous transmission, Fig.2.3 (page 34), we may set $i = 0$ without loss of generality to obtain (dropping the superscript representing the bit interval for simplicity)

$$r(t) = \sum_{k=1}^{K} \sqrt{E_k} b_k s_k(t) + w(t) \tag{2.11}$$

where E_k is the received energy of the kth user's signal. Fig.2.4 (page 35) shows the adaptive multi-user detector for synchronous CDMA which is proposed in [13]. The received signal is sampled twice per spreading chip at $t = m\frac{T_c}{2}$ to yield the discrete-time model

$$r(m) = \sum_{k=1}^{K} \sqrt{E_k} b_k s_k(m) + w(m) \tag{2.12}$$

where $r(m) \equiv r(m\frac{T_c}{2})$ is the sample of the received signal, $r(t)$, with sampling rate $\frac{2}{T_c}$ (two samples per chip duration). $\hat{r}(m)$ denotes an estimate of $r(m)$ which is obtained as the output of a transversal filter with coefficients $c_k(m\text{-}1)$ at time m-1 as shown in Fig.2.4, (page 35):

$$\hat{r}(m) = \sum_{k=1}^{K} c_k(m-1)\, s_k(m) = \boldsymbol{C}^T(m-1)\, \boldsymbol{S}(m) \tag{2.13}$$

where

$$\boldsymbol{C}^T(j) = (\; c_1(j) \;\; c_2(j) \;\; \ldots \;\; c_K(j) \;) \tag{2.14}$$

$$\boldsymbol{S}^T(j) = (\; s_1(j) \;\; s_2(j) \;\; \ldots \;\; s_K(j) \;) \tag{2.15}$$

are K dimensional vectors. Note that $\hat{r}(m)$ requires knowledge of the spreading sequence $\{s_k(m)\}$ at the receiver.

The coefficients $\boldsymbol{C}(n)$ of the transversal filter are obtained as the solution to a Least Squares (LS) criterion

$$min_{\boldsymbol{C}(n)} \sum_{m=1}^{n} \lambda^{n-m} |r(m) - \hat{r}(m)|^2 \tag{2.16}$$

where $0 < \lambda \leq 1$ is a scaling factor. The optimum solution for LS filter coefficients $\boldsymbol{C}(n)$ at the nth iteration is well-known to be given by [14]:

$$\boldsymbol{C}(n) = \boldsymbol{R}^{-1}(n)\, \boldsymbol{D}(n) \tag{2.17}$$

$$\boldsymbol{R}(n) = \sum_{m=1}^{n} \lambda^{n-m} \boldsymbol{S}(m) \boldsymbol{S}^T(m) \tag{2.18}$$

$$\boldsymbol{D}(n) = \sum_{m=1}^{n} \lambda^{n-m} r(m) \boldsymbol{S}^T(m) \tag{2.19}$$

Using Eq. (2.12) for $r(m)$ in Eq. (2.19) and substituting in Eq. (2.17) yields

$$\boldsymbol{C}(n) = \boldsymbol{E}\boldsymbol{b} + \boldsymbol{R}^{-1}(n) \sum_{m=1}^{n} \lambda^{n-m} \boldsymbol{S}(m) w(m) \tag{2.20}$$

where $\boldsymbol{b}^T = (b_1, b_2, \ldots, b_K)$ is the vector of unknown symbols to be recovered, and $\boldsymbol{E} = diag \cdot (\sqrt{E_1}, \sqrt{E_2}, \ldots, \sqrt{E_K})$ is a K-dim. diagonal matrix containing the (unknown) symbol received energies at the receiver.

At the end of one symbol interval (during which a total of $2L$ samples are processed), the LS coefficients are given by (setting $\lambda = 1$ in Eq. (2.20))

$$\boldsymbol{C}_0 = \boldsymbol{C}(2L) = \boldsymbol{E}\boldsymbol{b} + \left[\sum_{m=1}^{2L} \boldsymbol{S}(m) \boldsymbol{S}^T(m) \right]^{-1} \sum_{m=1}^{2L} w(m) \boldsymbol{S}(m) = \boldsymbol{E}\boldsymbol{b} + \boldsymbol{R}^{-1}\Gamma \tag{2.21}$$

where $\Gamma = \sum_{m=1}^{2L} w(m) \boldsymbol{S}(m)$ is a Gaussian random variable. From Eq. (2.20), it follows that the symbol detection rule is simply

$$\hat{\boldsymbol{b}} = \text{sgn}\,[\boldsymbol{C}(2L)] \tag{2.22}$$

Now, the output of the decorrelating detector is known to be given by [8,15]:

$$\boldsymbol{Z} = \boldsymbol{E}\boldsymbol{b} + \boldsymbol{H}^{-1}\eta \tag{2.23}$$

where the elements of $\boldsymbol{H}$, η are obtained from

$$\boldsymbol{H}_{ij} = \int_0^T s_i(t)\, s_j(t)\, dt \tag{2.24}$$

$$\eta_i = \int_0^T s_i(t)\, w(t)\, dt \tag{2.25}$$

Note that η is a (zero-mean) Gaussian K-dimensional vector with covariance matrix equal to $\sigma_w^2 \boldsymbol{H}$, σ_w^2 being the variance of the AWGN $w(t)$.

Note that in Eq. (2.21)

$$\boldsymbol{R} = \sum_{m=1}^{2L} \boldsymbol{S}(m)\, \boldsymbol{S}^T(m) \tag{2.26}$$

implying

$$\boldsymbol{R}_{ij} = \frac{2}{T_c} \sum_{m=1}^{2L} \frac{T_c}{2} s_i(m)\, s_j(m) = \frac{2}{T_c} \boldsymbol{H}_{ij} \tag{2.27}$$

Using $\boldsymbol{R} = \frac{2}{Tc}\boldsymbol{H}$ in Eq. (2.21) yields

$$\boldsymbol{C}_0 = \boldsymbol{E}\boldsymbol{b} + \frac{T_c}{2}\boldsymbol{H}^{-1}\Gamma \tag{2.28}$$

The covariance of the (zero-mean) elements of Γ is now obtained as

$$E[\Gamma_i \Gamma_j] = E \sum_{m=1}^{2L} \sum_{k=1}^{2L} w(m)\, s_i(m)\, w(k)\, s_j(k)$$

$$= E\frac{4}{T_c^2}\sum_{m=1}^{2L}\sum_{k=1}^{2L}\frac{T_c}{2}w(m)\,s_i(m)\,\frac{T_c}{2}w(k)\,s_j(k)$$

$$= \frac{4}{T_c^2}E\sum_{m=1}^{2L}\sum_{k=1}^{2L}\int_{(m-1)\frac{Tc}{2}}^{m\frac{Tc}{2}} w(m)\,s_i(t)\,dt\int_{(k-1)\frac{Tc}{2}}^{k\frac{Tc}{2}} w(k)\,s_j(\tau)\,d\tau$$

$$= \frac{4}{T_c^2}\sum_{m=1}^{2L}\sum_{k=1}^{2L}\int_{(m-1)\frac{Tc}{2}}^{m\frac{Tc}{2}}\int_{(k-1)\frac{Tc}{2}}^{k\frac{Tc}{2}} E\left[w(m)\,w(k)\right]s_i(t)\,s_j(\tau)\,dtd\tau$$

$$= \frac{4}{T_c^2}\sum_{m=1}^{2L}\sum_{k=1}^{2L}\int_{(m-1)\frac{Tc}{2}}^{m\frac{Tc}{2}}\int_{(k-1)\frac{Tc}{2}}^{k\frac{Tc}{2}} E\left[w(t)\,w(\tau)\right]s_i(t)\,s_j(\tau)\,dtd\tau$$

$$= \frac{4}{T_c^2}E\left[\int_0^T w(t)\,s_i(t)\,dt\int_0^T w(\tau)\,s_j(\tau)\,d\tau\right] = \frac{4\sigma_w^2}{T_c^2}H_{ij} \qquad (2.29)$$

resulting in

$$E\Gamma\Gamma^T = \frac{4\sigma_w^2}{T_c^2}\boldsymbol{H} \qquad (2.30)$$

Using Eq. (2.30) in Eq. (2.21), Eq. (2.23), it follows that $\boldsymbol{H}^{-1}\eta$ and $\boldsymbol{R}^{-1}\Gamma = \frac{T_c}{2}\boldsymbol{H}^{-1}\Gamma$ have the same covariance matrix $\sigma_w^2\boldsymbol{H}^{-1}$. As a result, the equivalence of this adaptive receiver (at convergence) to the decorrelating detector [8] is established. The *SNR* of the

kth user for the decorrelating detector in AWGN is well-known [8] and can be analytically computed from:

$$(SNR)_k = \frac{E_k}{\sigma_n^2 [R^{-1}]_{kk}} \tag{2.31}$$

where E_k and σ_n^2 are energy of the kth user's signal and the variance of the noise respectively. $[R^{-1}]_{kk}$ is the kth diagonal element of the inverse matrix of R which is the matrix of normalized cross-correlations, i.e.

$$H = E^{1/2} R E^{1/2} \tag{2.32}$$

where H is the matrix of cross-correlations and $E=diag\{E_1,...,E_k\}$.

2.3 The Successive Interference Cancellation Scheme in DS/CDMA System [16]

The block diagram of a simple successive interference cancellation [16] is shown in Fig.2.5 (page 36). The received signal is:

$$r(t) = \sum_{k=1}^{K} A_k b_k (t+\tau_k) s_k (t+\tau_k) \cos(\omega_c t + \phi_k) + n(t) \tag{2.33}$$

where:

K : total number of active users

A_k : amplitude of kth user

$b_k(t)$: bit sequence of the kth user at bit-rate R_b and period T

$s_k(t)$: spreading chip sequence (signature code) of the kth user at chip-rate R_c and period T_c

$n(t)$: additive white gaussian noise (two sided power spectral density = $N_0/2$)

τ_k and ϕ_k are the time delay and phase of the kth user, which are assumed to be known, i.e., tracked accurately.

The bits and chips are assumed to be rectangular with the values of ±1 with probability of 0.5. The τ_k and ϕ_k are i.i.d. uniform random variables in $[0,T]$ and $[0,2\pi]$, respectively, for the asynchronous case.

Knowledge of the spread sequences of all users (signature codes) is assumed, but no knowledge of the energies of the individual users is needed. As shown in Fig.2.5, the basic idea is decoding the strongest users (whichever they may be) and then cancelling their effects from the received signal. Here the strongest user is not known beforehand, but is detected from the strength of the correlations of each of the users' signature code with the received signal. The correlation values (obtained from the conventional bank of correlators) are passed on to a selector which determines the strongest correlation value and selects the corresponding user for decoding and cancellation. These correlation values (as opposed to separate power estimates) form the basis for not only estimating the amplitude but also for maintaining the order of cancellation.

The cancellation scheme does not cancel all the cross-correlations among the users (it is not an optimal scheme). The error involved in using correlations as the estimate of the amplitude of a bit will limit the performance of the Interference Cancellation (IC) scheme. The reason for not considering the cross-correlations is to keep the IC scheme as simple as possible and yet be able to perform as needed in the presence of a degree of power variations.

The correlation values obtained are then passed on to decision block (selector), which identifies the maximum correlation (and hence the estimated strongest user). This user signal is then decoded (hard decision) and its effect is cancelled from the received signal

using the correlation value. The process is repeated until the weakest user is detected. The flow chart of the process is shown in Fig.2.6 (page 37). Detailed analysis of the IC scheme for coherent BPSK system (after low-pass filtering) can be found in [17]. The results of the analysis are as follows:

After j cancellations, the decision variable for the $(j+1)$'st user is given by:

$$\hat{Z}_{j+1} = \frac{1}{2}A_{j+1}b_{j+1} + \frac{1}{2}C_{j+1} \tag{2.34}$$

and C_{j+1} is given by:

$$C_{j+1} = \sum_{k=j+2}^{K} A_k I_{k,j+1}(\tau_{k,j+1}, \phi_{k,j+1}) + (n_{j+1}^{I} + n_{j+1}^{Q}) - \sum_{i=1}^{j} C_i I_{i,i+1}(\tau_{i,i+1}, \phi_{i,i+1}) \tag{2.35}$$

In the above expression, the first term is the multiple access interference of the uncancelled users, the second term is due to the Gaussian noise, and the third term is the cumulative noise due to imperfect cancellation. The cross-correlation between the ith user and the kth user is defined as:

$$I_{k,i}(\tau_{k,i}) = \frac{1}{T}\int_{0}^{T} s_k(t-\tau_{k,i}) \cdot s_i(t)\, dt \tag{2.36}$$

and

$$I_{k,i}(\tau_{k,i}, \phi_{k,i}) = I_{k,i}(\tau_{k,i}) \cdot \cos(\phi_k - \phi_i) \tag{2.37}$$

where $\tau_{k,i}$, and $\phi_{k,i}$ are time delay and phase of the kth user relative to the ith user.

Since the decision on the bit sign is made using $\hat{Z}_{j+1}$, we are concerned with obtaining the mean square value of the noise C_{j+1}. The variance of C_{j+1} conditioned on A_k is

defined as follows (considering the fact that the mean value of C_{j+1} is zero and all random variables in Eq. (2.35) are independent):

$$\eta_{j+1} = Var[C_{j+1}|A_k] = \sum_{k=j+2}^{K} A_k^2 \cdot Var[I_{k,j+1}(\tau_{k,j+1}, \phi_{k,j+1})] +$$

$$Var[(n_{j+1}^I + n_{j+1}^Q)] + \sum_{i=1}^{j} \eta_i \cdot Var[I_{i,i+1}(\tau_{i,i+1}, \phi_{i,i+1})] \quad (2.38)$$

For the purely synchronous case, where τ_k and ϕ_k are zero for all k's, the cross-correlation term, Eq. (2.37), is given by ($L=T/T_c$):

$$\sigma_{k,i}^2 = Var[I_{k,i}(\tau_{k,i}, \phi_{k,i})] = \frac{1}{L} \quad (2.39)$$

while for the asynchronous case, where τ_k and ϕ_k are uniformly distributed over $[0,T]$ and $[0, 2\pi]$ respectively, the variance of the cross-correlation is given by [17],

$$\sigma_{k,i}^2 = Var[I_{k,i}(\tau_{k,i}, \phi_{k,i})] = \frac{1}{3L} \quad (2.40)$$

The variance of the Gaussian noise n_j^I is given by:

$$Var[n_j^I] = Var\left[\frac{1}{T}\int_0^T n_c(t)\, s_j(t-\tau_j)\cos(\phi_j)\, dt\right]$$

$$= \frac{1}{2T^2} Var\left[\int_0^T n_c(t)\, s_j(t-\tau_j)\, dt\right] \approx \frac{N_0}{2T} \quad (2.41)$$

Hence n_j^I and n_j^Q are uncorrelated Gaussian random variables with zero mean and variance $\frac{N_0}{2T}$. So the variance of the noise in the decision variable, conditioned on A_k, is given by:

$$\eta_{j+1} = \begin{cases} \frac{1}{L}\sum_{k=j+2}^{K} A_k^2 + \frac{N_0}{T} + \frac{1}{L}\sum_{i=1}^{j}\eta_i & ;Synchronous \\ \frac{1}{3L}\sum_{k=j+2}^{K} A_k^2 + \frac{N_0}{T} + \frac{1}{3L}\sum_{i=1}^{j}\eta_i & ;Asynchronous \end{cases} \tag{2.42}$$

The signal to noise ratio (SNR) conditioned on A_k, using Eq. (2.34) and Eq. (2.42), is then given by (for asynchronous case):

$$\gamma_{j+1} = \frac{\frac{1}{4}A_{j+1}^2}{\frac{1}{4}\eta_{j+1}} = \frac{A_{j+1}^2}{\frac{1}{3L}\sum_{k=j+2}^{K} A_k^2 + \frac{N_0}{T} + \frac{1}{3L}\sum_{i=1}^{j}\eta_i} \tag{2.43}$$

To calculate the bit error rate (BER), the Gaussian approximation [18,19] shall be used, i.e., the noise C_{j+1} shall be assumed Gaussian with zero mean and variance η_{j+1}. The probability of bit error after the jth cancellation, conditioned on the amplitude A_k, is then given by:

$$P_e^{j+1} = P\{\hat{Z}_{j+1} < 0 \,|\, \hat{b}_{j+1} = 1\} = P\{C_{j+1} < -A_{j+1}\}$$

$$= Q\left(\frac{A_{j+1}}{\sqrt{\eta_{j+1}}}\right) = Q(\sqrt{\gamma_{j+1}}) \tag{2.44}$$

2.3.1 BER Performance of the IC Scheme under Rayleigh Fading

Equations Eq. (2.42), Eq. (2.43), and Eq. (2.44) are the expressions of the noise, signal to noise ratio, and the error probability resulting after j cancellations. These expressions are conditioned on A_k, which are the ordered set of amplitudes of K users (assumed A_1 is the strongest and A_K is the weakest amplitude). The amplitudes are assumed to be Rayleigh distributed with unit mean square value, i.e., its probability density function

(pdf) is given by,

$$f(x) = 2xe^{-x^2} \tag{2.45}$$

and its cumulative density function (cdf) is given by:

$$F(x) = 1 - e^{-x^2} \tag{2.46}$$

To find the probability density functions of the ordered A_k (where A_1 is the strongest and A_K is the weakest) denoted by $f_{A_k}(x)$, the generalization of Bernoulli trials [20] can be used as follows:

$$P_n(k_1, \ldots, k_r) = \frac{n!}{k_1! \ldots k_r!} p_1^{k_1} \ldots p_r^{k_r} \tag{2.47}$$

where, $k_1 + \ldots + k_r = n$.

$f_{A_k}(x)$ is the probability that the user with amplitude x is the kth strongest user. It means that (k-1) users are stronger and (K-k) users are weaker than this user, so from Eq. (2.47) the $f_{A_k}(x)$ is obtained as follows:

$$f_{A_k}(x) = \frac{K!}{(K-k)!\,(k-1)!} F^{K-k}(x)\,[1 - F(x)]^{k-1} f(x) \tag{2.48}$$

The expected values of the ordered A_k are then obtained as $E[A_k^2] = \int_0^\infty x^2 f_{A_k}(x)\,dx$. The dominator of Eq. (2.43) is approximated Gaussian because the dominating terms for both small and large j are sums of random variables. We have that

$$E_{A_k}[\eta_{j+1}] = \begin{cases} \frac{1}{L} \sum_{k=j+2}^{K} E[A_k^2] + \frac{N_0}{T} + \frac{1}{L} \sum_{i=1}^{j} \eta_i & ;Synchronous \\ \frac{1}{3L} \sum_{k=j+2}^{K} E[A_k^2] + \frac{N_0}{T} + \frac{1}{3L} \sum_{i=1}^{j} \eta_i & ;Asynchronous \end{cases} \tag{2.49}$$

The error probability expression after jth cancellation, Eq. (2.44), is then unconditioned using the probability density function of the $(j+1)$st strongest amplitude as follows:

$$\hat{P}_e^{j+1} = \int_0^{\infty} Q\left(\frac{A_{j+1}}{\sqrt{E_{A_k}[\eta_{j+1}]}}\right) f_{A_{j+1}}(x)\,dx \tag{2.50}$$

The average probability of error is then obtained as the average of the BER resulting from all stages of cancellation.

2.4 Hybrid C / TDMA Mobile Radio System Applying Joint Detection and Coherent Receiver Antenna Diversity [21]

In [21], a hybrid system termed JD-C/TDMA system using a combination of TDMA (Time Division Multiple Access) and CDMA (Code Division Multiple Access) with JD (Joint Detection) and coherent receiver antenna diversity (CRAD) at the base station (BS) receiver is presented. JD (or multi-user detection) means the simultaneous detection of all users' signals using the knowledge about ISI (Inter Symbol Interference) and MAI (Multiple Access Interference). In this system only the uplink transmission, from mobile stations (MS) to base station (BS) is considered.

In a TDMA system, the users transmit in bursts and the bursts of different users, spread in duration due to multipath reception, are separated by setting time windows at the receiver. This requires channel estimation, guard intervals, and synchronization.

The basic structure of the uplink is shown in Fig.2.7 (page 38). A number of K users, i.e., mobile stations (MS), which are only separated by their different user specific signature sequence, are simultaneously active in the same frequency band of width B. Each mobile station is assumed to have a single transmitter antenna. The transmitted signals are received at the uplink receiver, base station, over K_a receiver antennas. Therefore, the

transmission of the K user signals takes place over $K \cdot K_a$ different radio channels with time variant complex impulse responses $\underline{h}^{(k,k_a)}(\tau, t)$, $k = 1, \ldots, K$, $k_a = 1, \ldots, K_a$, where the radio channel with the impulse response $\underline{h}^{(k,k_a)}(\tau, t)$ refers to the connection of mobile k with receiver antenna k_a. The parameter τ denotes the delay time referring to time spreading of the transmitted signals due to multipath reception and t denotes the real time referring to the time variance of each radio channel.

Each of the K users transmits in bursts. The duration T_{bu} of each burst is chosen such that during the transmission of one burst, the radio channel can be assumed to be time invariant. The burst structure is shown in Fig.2.8 (page 39). Each burst consists of two data blocks, a user-specific midamble, i.e., a training sequence used for channel estimation, and a guard interval to prevent subsequent bursts from overlapping at the receiver. Each data block contains a number N of data symbols of duration T_s and each data symbol consists of L chips of duration $T_c = T_s / L$ denoting the user specific signature sequence. The midamble consists of L_{mid} chips and the duration of the guard interval is T_g. The bursts of the K users which are simultaneously active in the same frequency band are assumed to be synchronized at the receiver except for a timing error in the order of a fraction of the symbol duration T_s. By allocating a time slot to each K-tuple of bursts, the TDMA component is introduced in the JD-C/TDMA system.

The transmitter and receiver structures, see Fig.2.7, shall be discussed in more detail. In Fig.2.9 (page 39), the block structure of transmitter K is shown. A bit stream representing voice or data information is convolutionally encoded and interleaved to avoid burst errors. More significant bits may be protected by stronger coding than less significant bits. The encoded binary data stream is mapped onto a symbol stream consisting in general of complex data symbols. Each data symbol is spread by a user-specific signature sequence. Bursts as shown in Fig.2.8 are generated by linking together two data blocks and the user-

specific midamble. After linear modulation and D/A (Digital to Analog) conversion, the signal is passed through a transmitter filter for lowpass filtering, and an amplifier.

The block structure of the uplink receiver is illustrated in Fig.2.10 (page 40). The amplified signal received at receiver antenna k_a is the sum of K user signals. This sum is filtered for band limitation and noise suppression, and A/D (Analog to Digital) converted. The sampling frequency is the inverse of the chip duration T_c. A synchronization unit in the receiver has to compensate for the slightly different delay times of K_a received signals resulting from the different propagation paths to the K_a antennas.

The set of samples resulting from K user bursts is separated into a subset of samples corresponding to the K midambles of the K users and two subsets of samples corresponding the $K \cdot N$ data symbols of the K user bursts transmitted before and after the midamble, respectively. A subset of samples corresponding to the K midambles of the K users exists if the K_a receiver antennas are not too far apart from each other since the K bursts are assumed to arrive synchronously at the receiver. Distances of the K_a receiver antennas of a few wavelengths are sufficient to generate independent fading processes at the K_a antennas [21].

From the subset of samples corresponding to the K midambles, estimates of the K channel impulse responses $\underline{h}^{(k, k_a)}(\tau, t)$, $k = 1, \ldots, K$, bandlimited to the user bandwidth B, are determined by channel estimator K_a. A data estimator applying a JD algorithm with CRAD determines continuous valued estimates of the $K \cdot N$ data symbols transmitted before and after the midamble, respectively, using the knowledge about the estimates of the $K \cdot K_a$ channel impulse responses $\underline{h}^{(k, k_a)}(\tau, t)$, $k = 1, \ldots, K$, $k_a = 1, \ldots, K_a$, the K user-specific signature sequences and the K_a subsets of samples corresponding to the $K \cdot N$ data symbols transmitted before or after the midamble, respectively.

The user-specific signature sequences are known at the uplink receiver, as they are allocated to each mobile by the base station during the first access or handover. The $2 \cdot N$ complex, continuous valued estimates of the data symbols transmitted by user k, $k = 1, \ldots, K$, are mapped onto a real-valued data stream. This data stream is deinterleaved and convolutionally decoded in a soft input decoder.

In Fig.2.11 (page 41), a discrete-time lowpass representation of the uplink of the JD-C/TDMA mobile radio system with CRAD, representing the blocks between the data to symbol mapper in Fig.2.9 and the symbol to data mapper in Fig.2.10, is shown.

The K users which are simultaneously active in the same frequency band are transmitting finite data symbol sequences:

$$\underline{d}^{(k)} = (\underline{d}_1^{(k)}, \underline{d}_2^{(k)}, \ldots, \underline{d}_N^{(k)})^T \tag{2.51}$$

Each of the data symbols $\underline{d}_n^{(k)}$, $n = 1, \ldots, N$, of mobile k is spread by the user specific signature sequence,

$$\underline{s}^{(k)} = (\underline{s}_1^{(k)}, \underline{s}_2^{(k)}, \ldots, \underline{s}_L^{(k)})^T \tag{2.52}$$

consisting of L complex chips $\underline{s}_l^{(k)}$ of duration T_c. The influence of modulator in Fig.2.9, the analog components in Fig.2.9 and Fig.2.10 and the mobile radio channel with impulse response $\underline{h}^{(k, k_a)}(\tau, t)$ is represented by the discrete time channel impulse response,

$$\underline{\boldsymbol{h}}^{(k, k_a)} = (\underline{h}_1^{(k, k_a)}, \underline{h}_2^{(k, k_a)}, \ldots, \underline{h}_W^{(k, k_a)})^T \tag{2.53}$$

consisting of W complex samples $\underline{h}_w^{(k, k_a)}$ taken at the chip rate $1/T_c$. The combined channel responses are defined as:

$$\underline{b}^{(k,k_a)} = (b_1^{(k,k_a)}, b_2^{(k,k_a)}, \ldots, b_{L+W-1}^{(k,k_a)})^T = \underline{h}^{(k,k_a)} * \underline{s}^{(k)} \tag{2.54}$$

As shown in Fig.2.11, each received sequence $\underline{e}^{(k_a)}$ consists of a sum of K sequences, each of length $(N \cdot L + W - 1)$ [21], which are perturbed by an additive stationary noise sequence

$$\underline{n}^{(k_a)} = (\underline{n}_1^{(k_a)}, \underline{n}_2^{(k_a)}, \ldots, \underline{n}_{N\,L+W-1}^{(k_a)})^T \tag{2.55}$$

with zero mean and covariance matrix [20,22]:

$$\underline{R}_n^{(k_a)\,(k_a)} = E[\underline{n}^{(k_a)} \underline{n}^{(k_a)^{*}\,T}] \tag{2.56}$$

where the symbols (.)* and (.)^T designate complex conjugation and transposition, respectively.

The matrix $\underline{A}$ is defined as following [21]:

$\underline{A}^{(k_a)} = (\underline{A}_{i,j}^{(k_a)})$ where,

$$\underline{A}_{L\,(n-1)+q,\,N\cdot(k-1)+n}^{(k_a)} = \begin{cases} \underline{b}_q^{(k,k_a)} & for \quad k=1\ldots K,\ k_a=1\ldots K_a \\ & \quad q=1\ldots Q+W-1,\ n=1\ldots N \\ 0 & else \end{cases} \tag{2.57}$$

and,

$$\underline{A} = (\underline{A}^{(1)T}, \underline{A}^{(2)T}, \ldots, \underline{A}^{(K_a)T})^T \tag{2.58}$$

The combined noise vector is defined as:

$$\underline{n} = (\underline{n}^{(1)T}, \underline{n}^{(2)T}, \ldots, \underline{n}^{(K_a)T})^T \tag{2.59}$$

having the covariance matrix:

$$\underline{\underline{R}}_n = E[\underline{n}\ \underline{n}^{*T}] = \begin{bmatrix} \underline{\underline{R}}_n^{(1)(1)} & \underline{\underline{R}}_n^{(1)(2)} & \cdots & \underline{\underline{R}}_n^{(1)(K_a)} \\ \underline{\underline{R}}_n^{(2)(1)} & \underline{\underline{R}}_n^{(2)(2)} & \cdots & \underline{\underline{R}}_n^{(2)(K_a)} \\ \vdots & \vdots & & \vdots \\ \underline{\underline{R}}_n^{(K_a)(1)} & \underline{\underline{R}}_n^{(K_a)(2)} & \cdots & \underline{\underline{R}}_n^{(K_a)(K_a)} \end{bmatrix} \tag{2.60}$$

The combined received vector is given by [21]:

$$\underline{e} = (\underline{e}^{(1)T}, \underline{e}^{(2)T}, \ldots, \underline{e}^{(K_a)T})^T = \underline{\underline{A}}\,\underline{d} + \underline{n} \tag{2.61}$$

where $\underline{d}$ is the data vector:

$$\underline{d} = (\underline{d}^{(1)T}, \underline{d}^{(2)T}, \ldots, \underline{d}^{(K)T})^T \tag{2.62}$$

The combined received vector $\underline{e}$, Eq. (2.61), is processed in a JD data estimator with CRAD in order to determine continuous valued estimates:

$$\hat{\underline{d}} = (\hat{\underline{d}}^{(1)T}, \hat{\underline{d}}^{(2)T}, \ldots, \hat{\underline{d}}^{(K)T})^T = \underline{\underline{M}}\,\underline{e} \tag{2.63}$$

The choice of the matrix $\underline{\underline{M}}$ determines the equalizer type. In [21], it is proved that by employing the zero forcing block linear equalizer, ZF-BLE, [22,23] the SNR per symbol at the output of the ZF-BLE is equal to:

$$\gamma(k,n) = \frac{E\left[\left|d_n^{(k)}\right|^2\right]}{\left[\left(\underline{\underline{A}}^{*T}\underline{\underline{R}}_n^{-1}\underline{\underline{A}}\right)^{-1}\right]_{n+N(k-1),\,n+N(k-1)}}, \qquad k=1\ldots K, \quad n=1\ldots N \tag{2.64}$$

The $[\underline{\underline{X}}]_{i,i}$ means the element in the ith row and ith column of the matrix $\underline{\underline{X}}$.

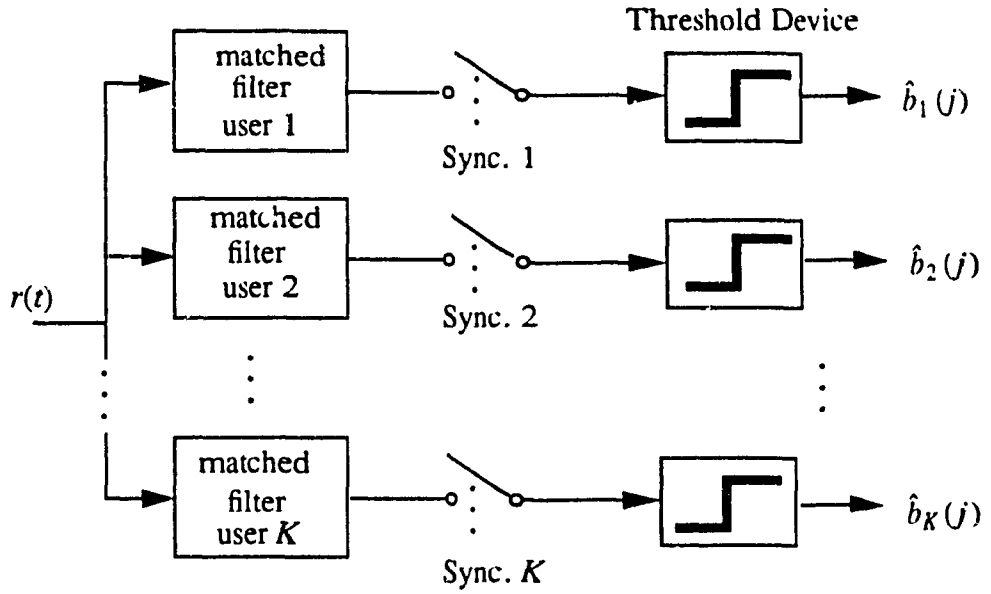

Fig. 2.1: Conventional single user detector

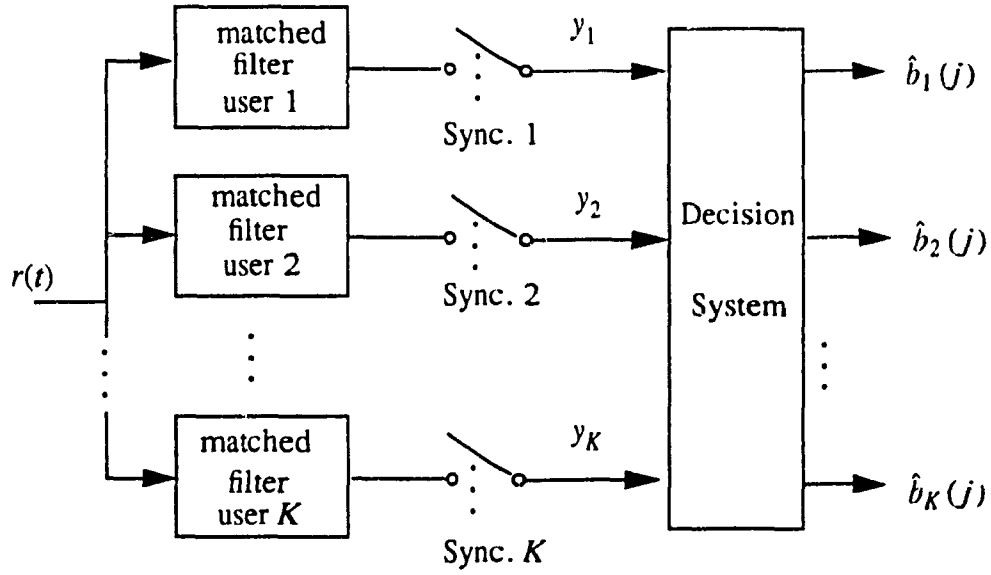

Fig. 2.2: Optimum multi-user detector

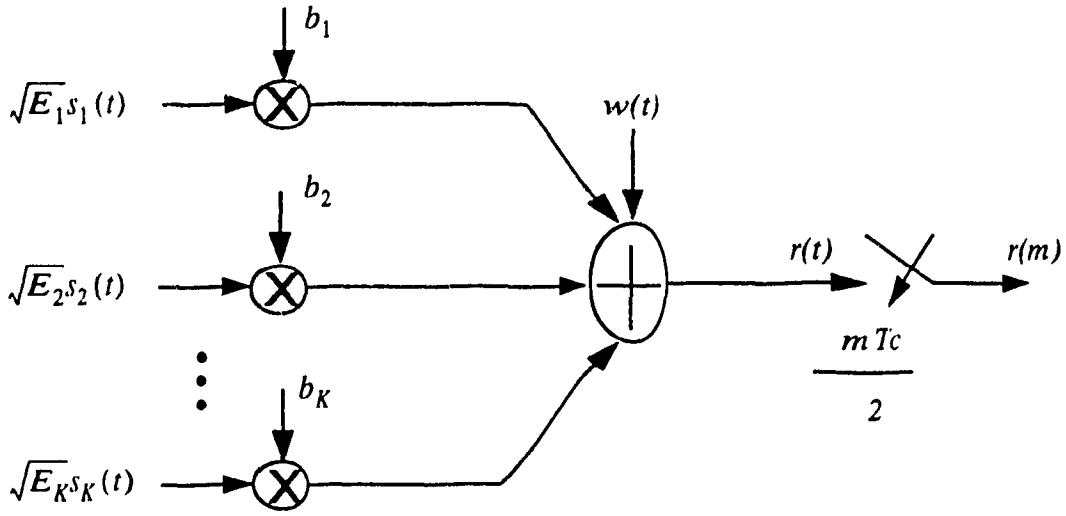

Fig. 2.3: Synchronous CDMA system model

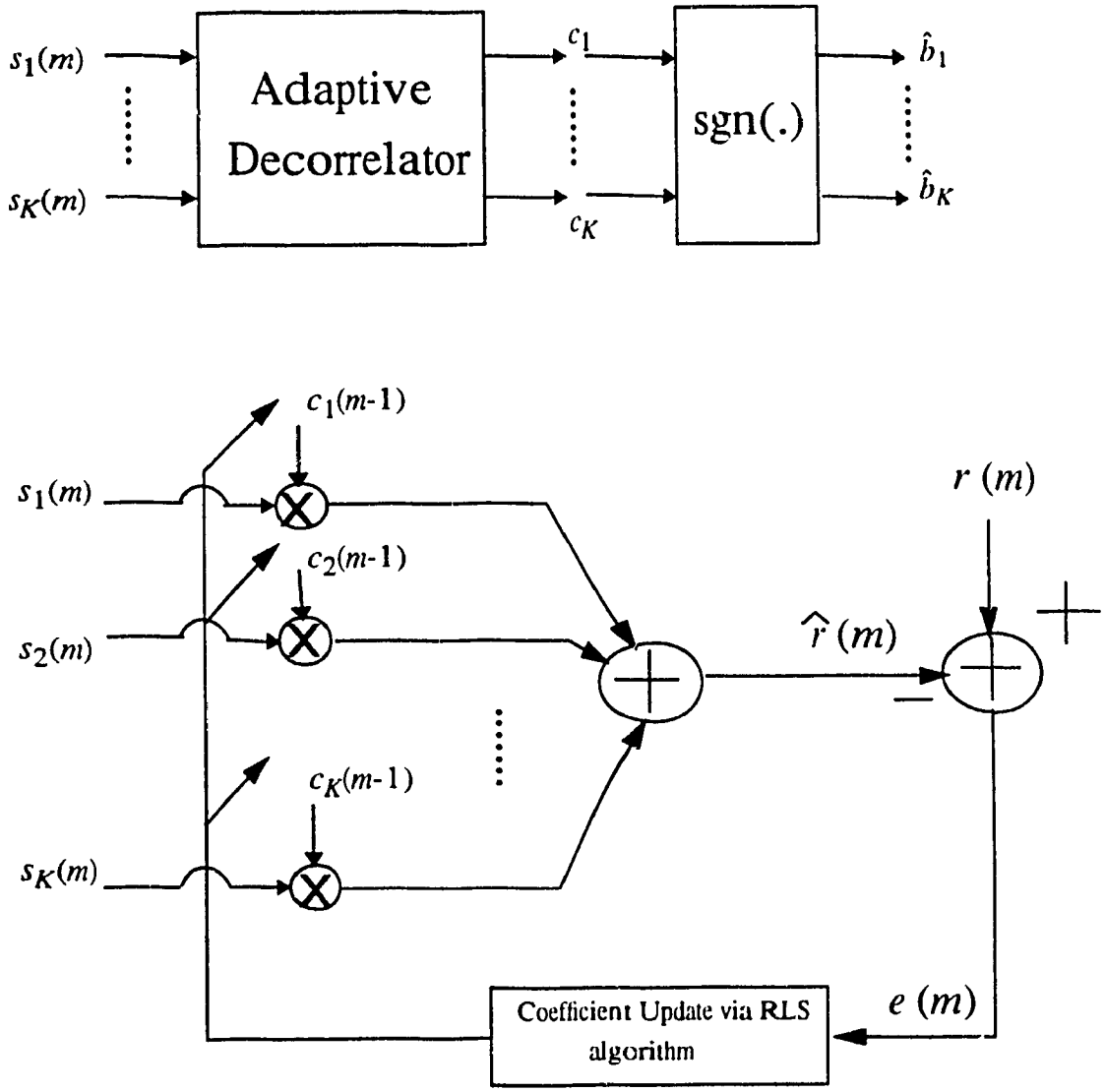

Fig. 2.4: Adaptive multi-user decorrelating detector

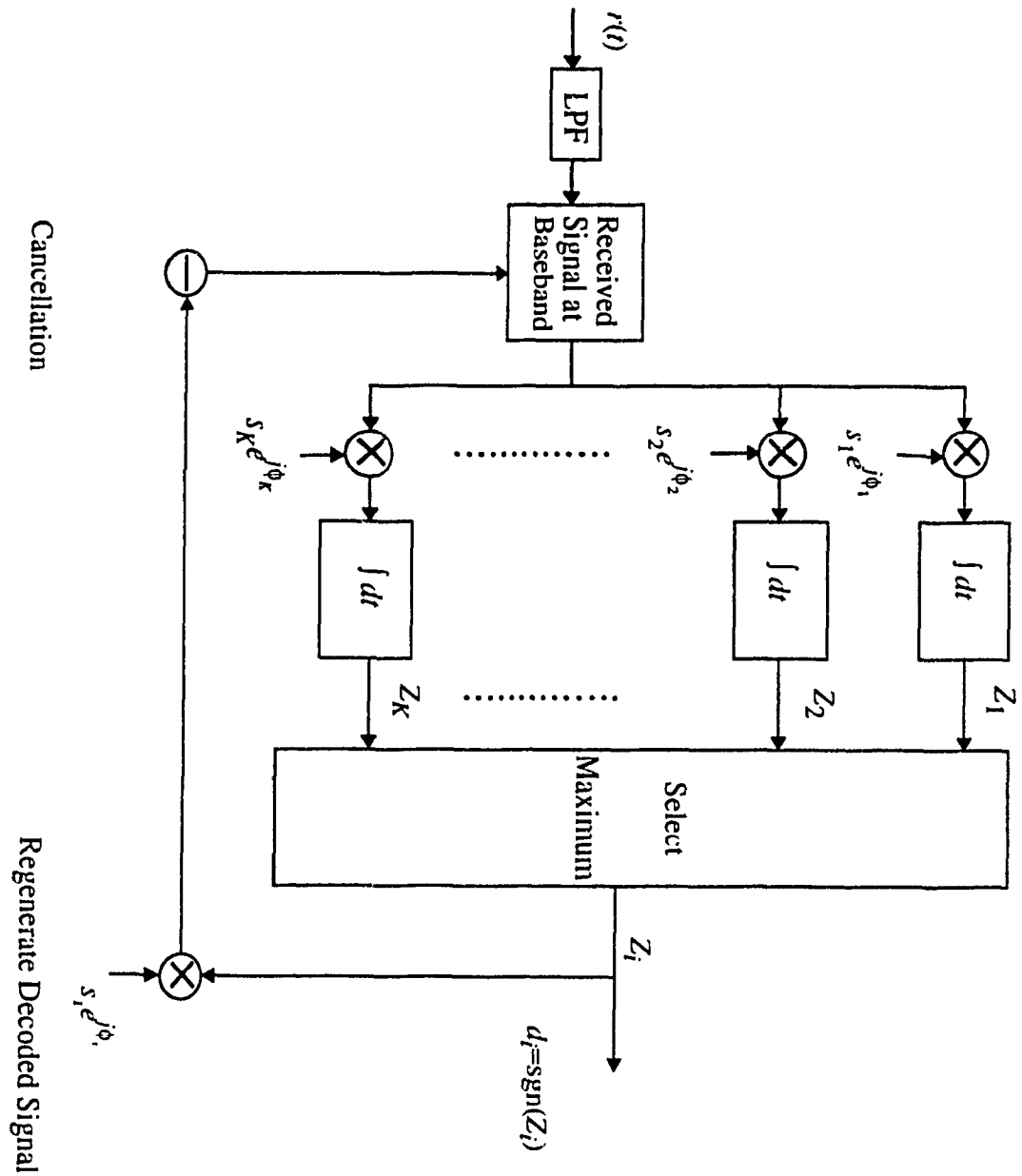

Fig. 2.5: Successive Interference Cancellation in DS/CDMA System

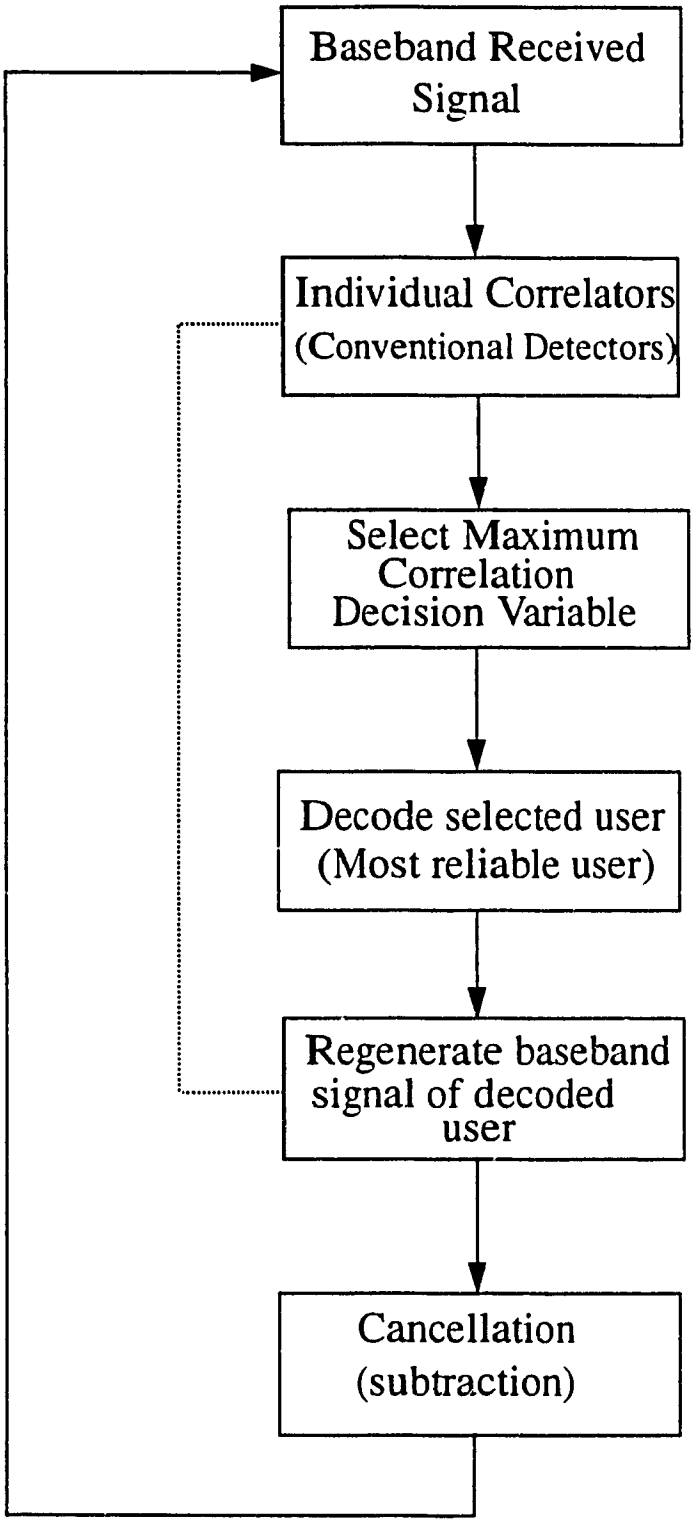

Fig. 2.6: Flow diagram of interference cancellation scheme

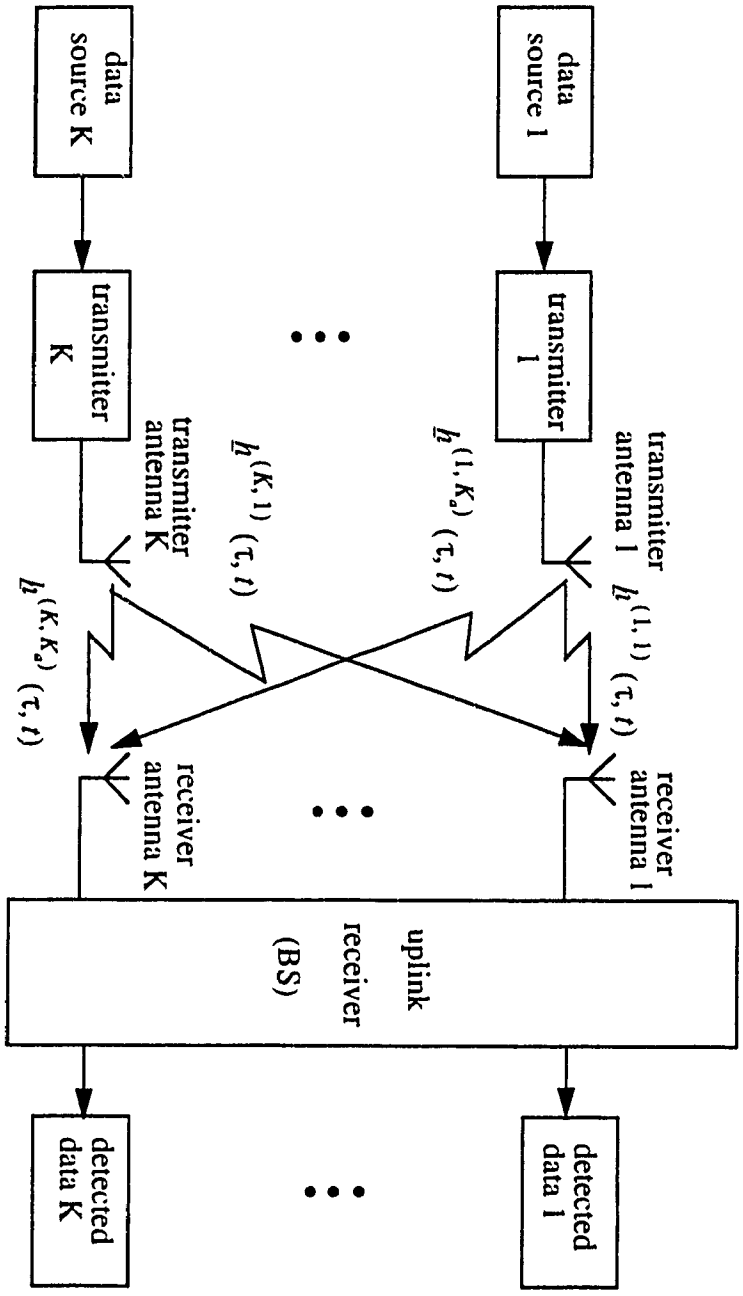

Fig. 2.7: System model of the uplink of the JD-C/TDMA system with CRAD [21]

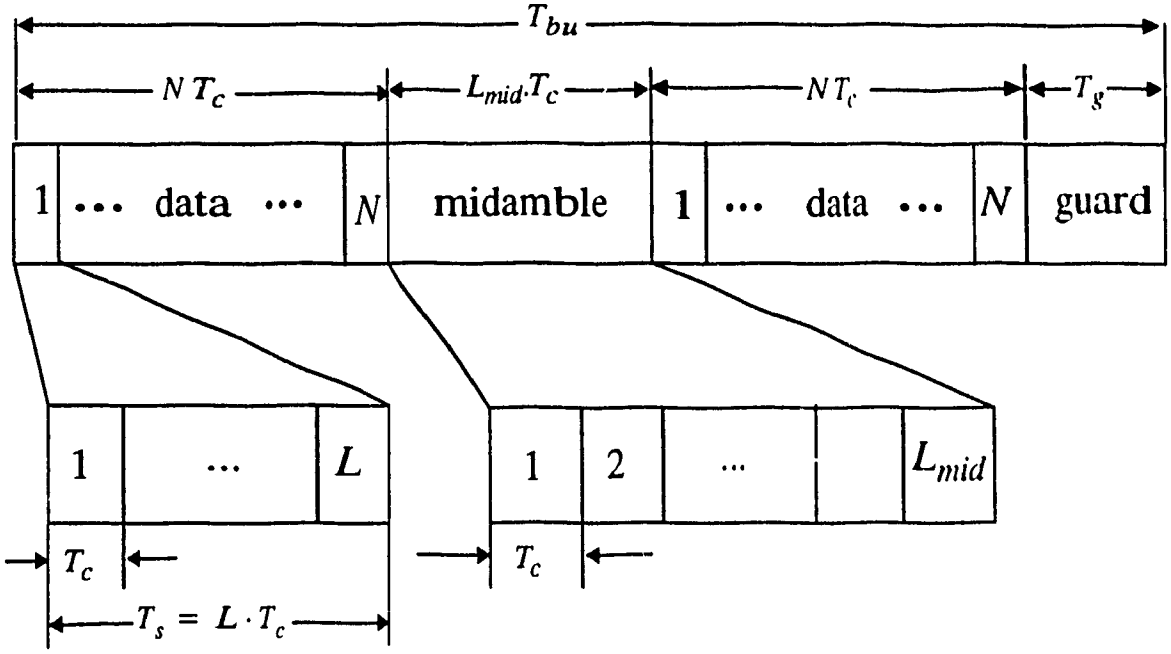

Fig. 2.8: Burst Structure

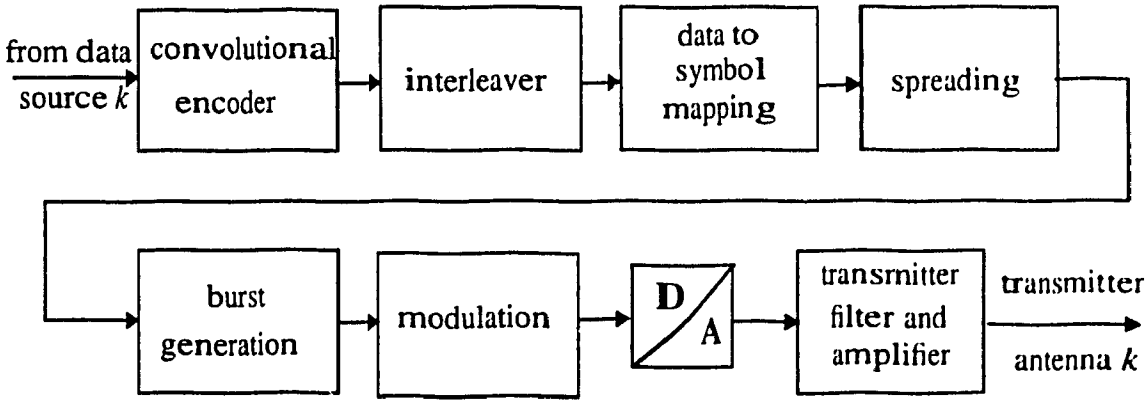

Fig. 2.9: Block structure of transmitter k

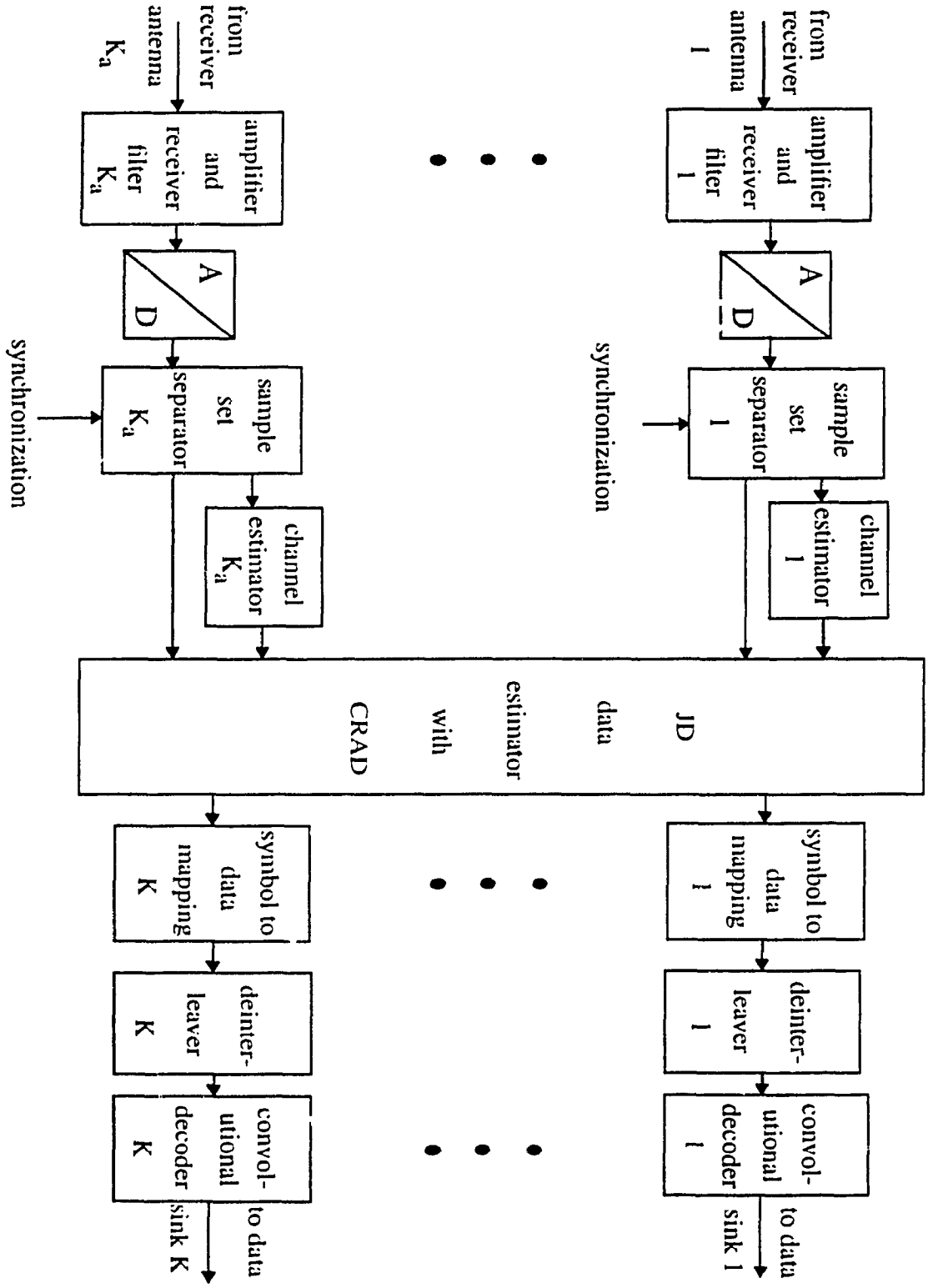

Fig. 2.10: Block structure of the uplink receiver

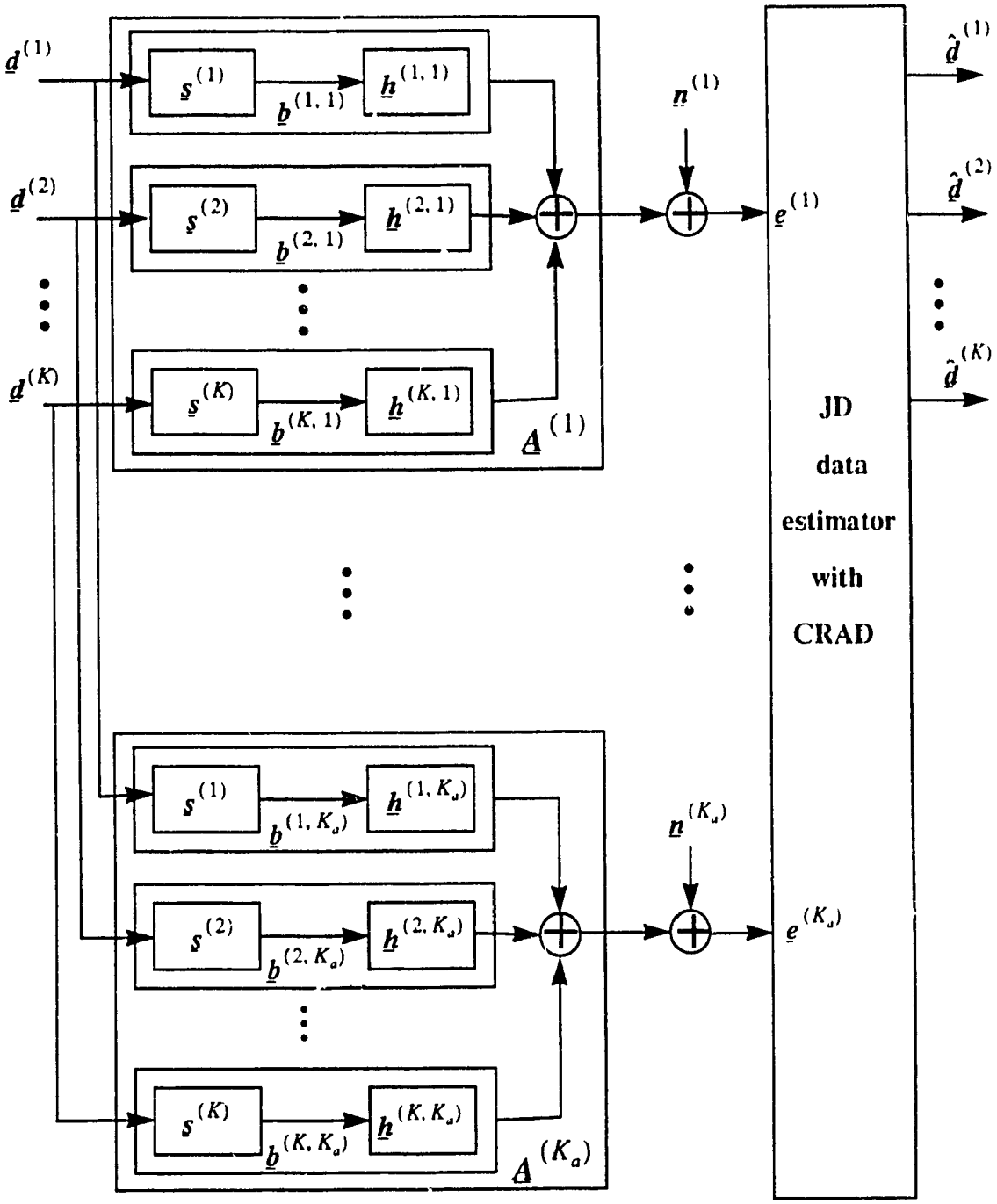

Fig. 2.11: Discrete-time lowpass representation of the uplink of the JD-C/TDMA system with CRAD [21]

CHAPTER 3

SIGNATURE CODE SELECTION FOR MULTI-USER DETECTION IN CDMA SYSTEMS

3.1 Introduction

In the previous chapter, it was mentioned that the conventional single user receivers, due to the fact that multiple access interference is considered as AWGN in this kind of receivers, have a poor performance when the number of users and consequently the multiple access interference increases. The multi-user detection was introduced (in previous chapter) as a possible solution to eliminate the interference.

Besides the receiver, the choice of appropriate codes plays an important role to eliminate the interference of other users in the system. It is clear, in conventional receivers, that employing codes with less cross-correlations gives better SNR [14]. In [24], it is shown that better SNR can be achieved by using orthogonal functions combined by short linear codes, in conventional receivers.

The main point in this chapter is to determine the effects of choosing different kinds of signature codes on SNR in multi-user detection. The multi-user receiver, for different cases of employing different kinds of codes as signature codes, has been simulated and the SNR and BER (Bit Error Rate) have been found for each case.

This chapter is organized as follows [25]. Sec.3.2 is a brief description of different well-known codes and their cross-correlation properties. The simulations procedures are described in Sec.3.3 and the results are reported in Sec.3.4.

3.2 Signature Codes

To determine the behavior of the system we need to know the users' signature codes and their properties. The important factor in signature codes which we are interested to know is the cross-correlation between two different codes. Different kinds of codes can be used as signature codes which some of them are briefly explained in this section [2,3].

3.2.1 Maximal Pseudonoise Sequences

In direct sequence spread spectrum systems for spreading and despreading the transmitted spectrum, a pseudonoise (PN) sequence is directly applied to the data signal. A pseudonoise or pseudorandom sequence is a periodic binary sequence with an autocorrelation that resembles, over one period, the autocorrelation of a random binary sequence, which roughly resembles the autocorrelation of bandlimited white noise. Although it is deterministic, a pseudonoise sequence has many characteristics, such as a nearly even balance of digits 0 and 1, similar to those of a random binary sequence.

In practice, It is desired to generate PN sequences which satisfy the following properties [26]. They

1) are easy to generate

2) have randomness properties

3) have long periods

4) are difficult to reconstruct from a short segment

PN sequences can be simply generated by a linear feedback shift register as shown in Fig.3.1. The sequences generated by linear feedback shift registers posses properties 1) and 3), most of property 2), but not property 4).

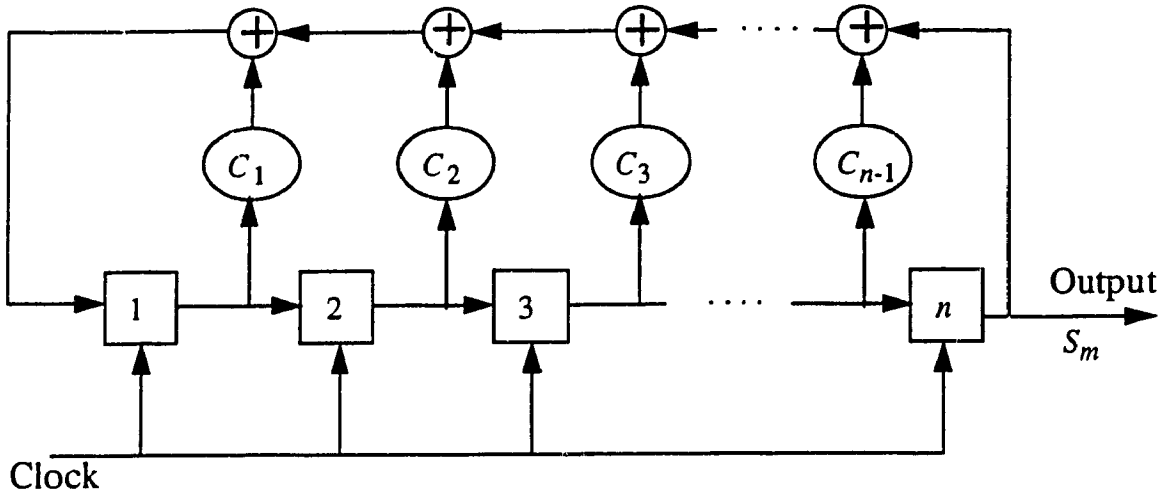

Fig. 3.1: Linear feedback shift register where $C_i \in \{0, 1\}$, i=1,...,n-1 (C_i=1 means connection).

A linear feedback shift register consists of consecutive two-state memory or storage stages and modulo-2 adders. Binary sequences are shifted through the shift register in response to clock pulses. The contents of the stages are linearly combined with the binary (0, 1) coefficients C_i's to produce the input to the first stage. The binary (code) sequence S_m for $m \geq n$ clearly satisfies the recursion (C_n=1):

$$S_m = \sum_{i=1}^{n} C_i \, S_{m-i} \, , \quad (mod \ 2) \tag{3.1}$$

The periodic cycle of the states (also output) depends on the initial state and on the coefficients (feedback taps) C_i's. The feedback taps (C_i's) can be chosen in the way that the period of the generated PN sequence to be $L=2^n-1$ (maximum period). Such kind of PN sequences are called *maximal sequence* codes. If a linear feedback shift register generates a maximal sequence, then all of its nonzero output sequences are maximal, regardless of the initial states. A maximal sequence contains exactly $2^{n-1}-1$ *zeros* and 2^{n-1} *ones* per period.

The *characteristic polynomial* associated with a linear feedback shift register of n stages is defined as:

$$f(x) = 1 + \sum_{i=1}^{n} C_i \; x^i \tag{3.2}$$

A polynomial $f(x)$ over $GF(2)$ (Galois field of two elements) of degree n is called *irreducible* if $f(x)$ is not divisible by any polynomial over $GF(2)$ of degree less than n but greater than zero. An irreducible polynomial over $GF(2)$ of degree n is called *primitive* if the smallest positive integer m for which $f(x)$ divides $1+x^m$ is $m=2^n-1$.

In order to have maximal sequence code, C_i's must be chosen in the way that the characteristic polynomial, $f(x)$, is a primitive polynomial over $GF(2)$.

It can be shown that the autocorrelation function of a maximal sequence code ($R_C(\tau)$) over one period is as following [3]:

$$R_C(\tau) = \begin{cases} 1 - (\dfrac{L+1}{L}\dfrac{|\tau|}{T_C}) & |\tau| \le T_C \\ -\dfrac{1}{L} & T_C < |\tau| \le \dfrac{LT_C}{2} \end{cases} \tag{3.3}$$

where T_c is the chip duration (clock timing in linear feedback shift register) and L is the code length ($L=2^n-1$). $R_C(\tau)$ is plotted in Fig.3.2.

The power spectral density of maximal sequence which is defined as the Fourier transform of $R_C(\tau)$, is as following [3]:

$$S_C(f) = \frac{L+1}{L^2} \sum_{i=-\infty}^{\infty} \mathrm{sinc}^2(\frac{i}{L})\,\delta(f - \frac{i}{LT_C}) + \frac{1}{L^2}\delta(f) \tag{3.4}$$

This function for L=7 (n=3) is plotted in Fig.3.3.

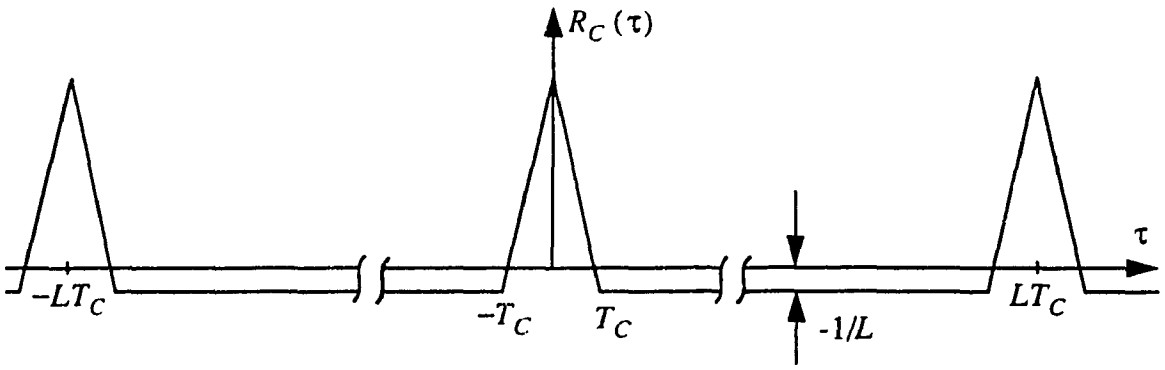

Fig. 3.2: Autocorrelation of maximal sequence

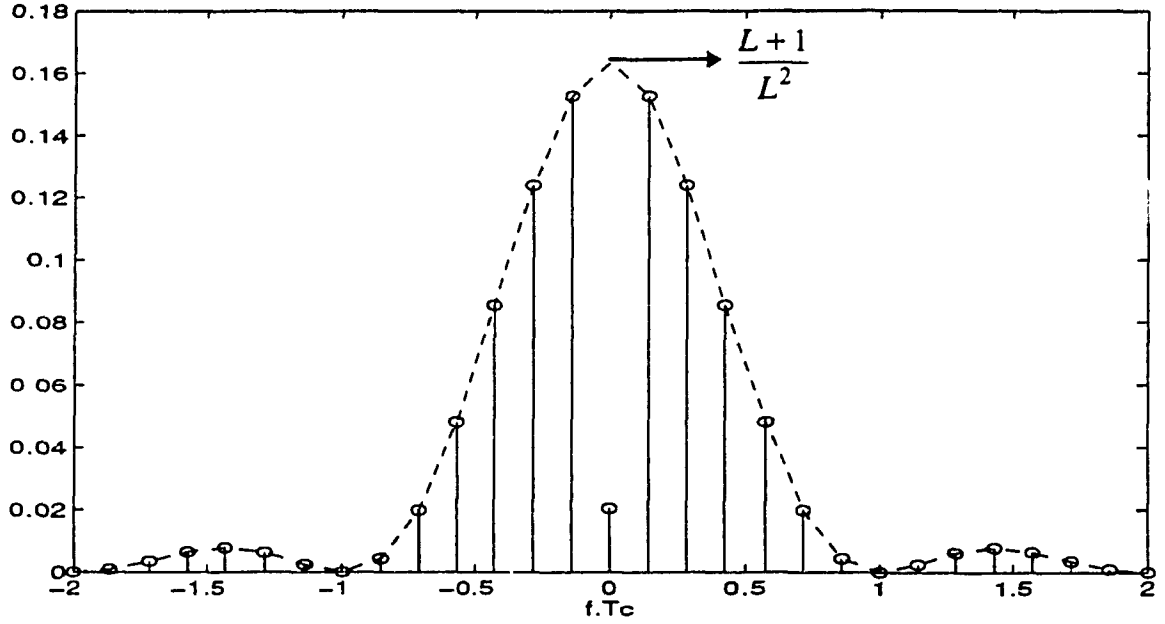

Fig. 3.3: Power spectral density of maximal sequence

If linear maximal sequence codes generated by one feedback shift register but with different initial states (different phases of one maximal sequence code) are used as signature codes in CDMA system, from Eq. (3.3) we can see that the cross-correlation between two signature codes will be $-1/L$ ($|\tau| > T_C$).

3.2.2 Gold Codes

Since the users in a CDMA system in general are not synchronized, if different phases of a linear m_sequence code are used as signature codes it may happen that for two codes we have $|\tau| < T_C$ and in this case there is a large cross-correlation between two codes and even they might be confused with each other at the receiver. So we should use different m_sequences (generated by different feedback shift registers) as signature codes. In general there is no closed form for describing the cross-correlation spectrum of pairs of m_sequences a. d it can be three-valued, four-valued, or possibly many-valued.

Certain special pairs of m_sequences whose cross-correlation spectrums are three-valued, are called *preferred pairs* of m_sequences. By using two feedback shift register which generate a preferred pair of m_sequences (of length $L=2^n-1$) and adding the output of them together for different initial states, as shown in Fig.3.4, we can achieve to a family of nonmaximal codes called *Gold* codes.

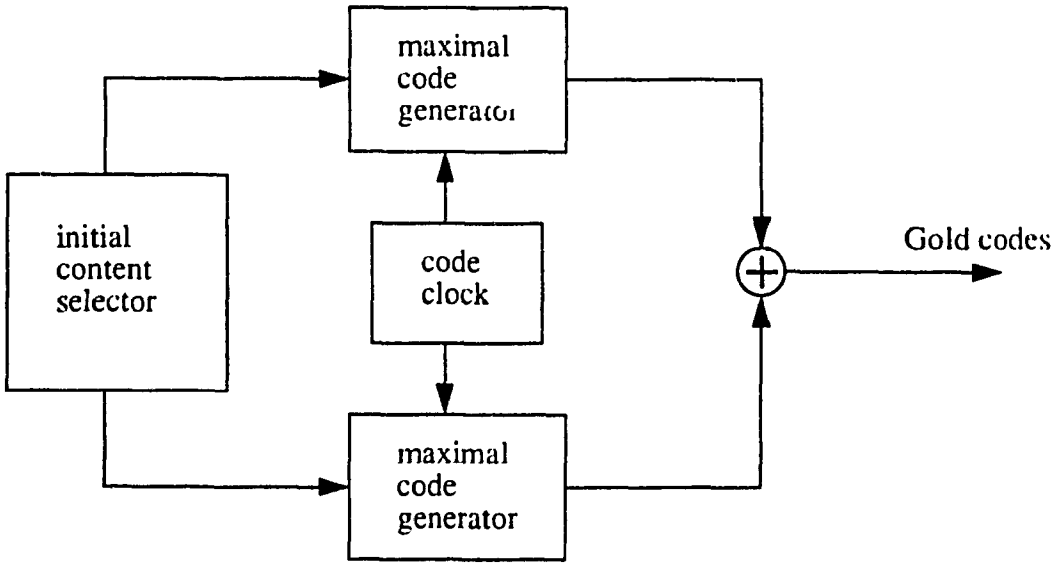

Fig. 3.4: Gold code generator

There are 2^n+1 different codes with a period of $L=2^n-1$ in each family of Gold codes.

The cross-correlation between any two Gold codes can only take three values with different probabilities as it is shown in Table 3.1, [27].

	Normalized Cross-Correlation Level	Probability of Level
n odd	$-[2^{(n+1)/2}+1]/L$	0.25
	$-1/L$	0.5
	$[2^{(n+1)/2}-1]/L$	0.25
n even and $n \neq 4k$	$-[2^{(n+2)/2}+1]/L$	0.125
	$-1/L$	0.75
	$[2^{(n+2)/2}-1]/L$	0.125

TABLE 3.1: Cross-Correlation Properties of Gold Codes

The Gold codes were invented in 1967 at the Magnavox Corporation specifically for multiple-access applications of spread spectrum. These codes are important since they have been selected by NASA for use on the Tracking and Data Relay Satellite Systems (TDRSS). The particular set of Gold codes employed in TDRSS are defined in STDN 108 by Goddard Space Flight Center [2].

3.2.3 Walsh Functions

One way to eliminate multiple access interference for specific delays is to use orthogonal functions like Walsh functions. Walsh functions form an ordered set of rectangular waveforms taking only two amplitude values +1 and -1. One way to show a Walsh function is to use symbol $WAL(n,T)$, where T is the period of Walsh function and n is the sequence order or the number of zero crossings in one period. The first 32 Walsh functions based on this ordering scheme are shown in Fig.3.5.

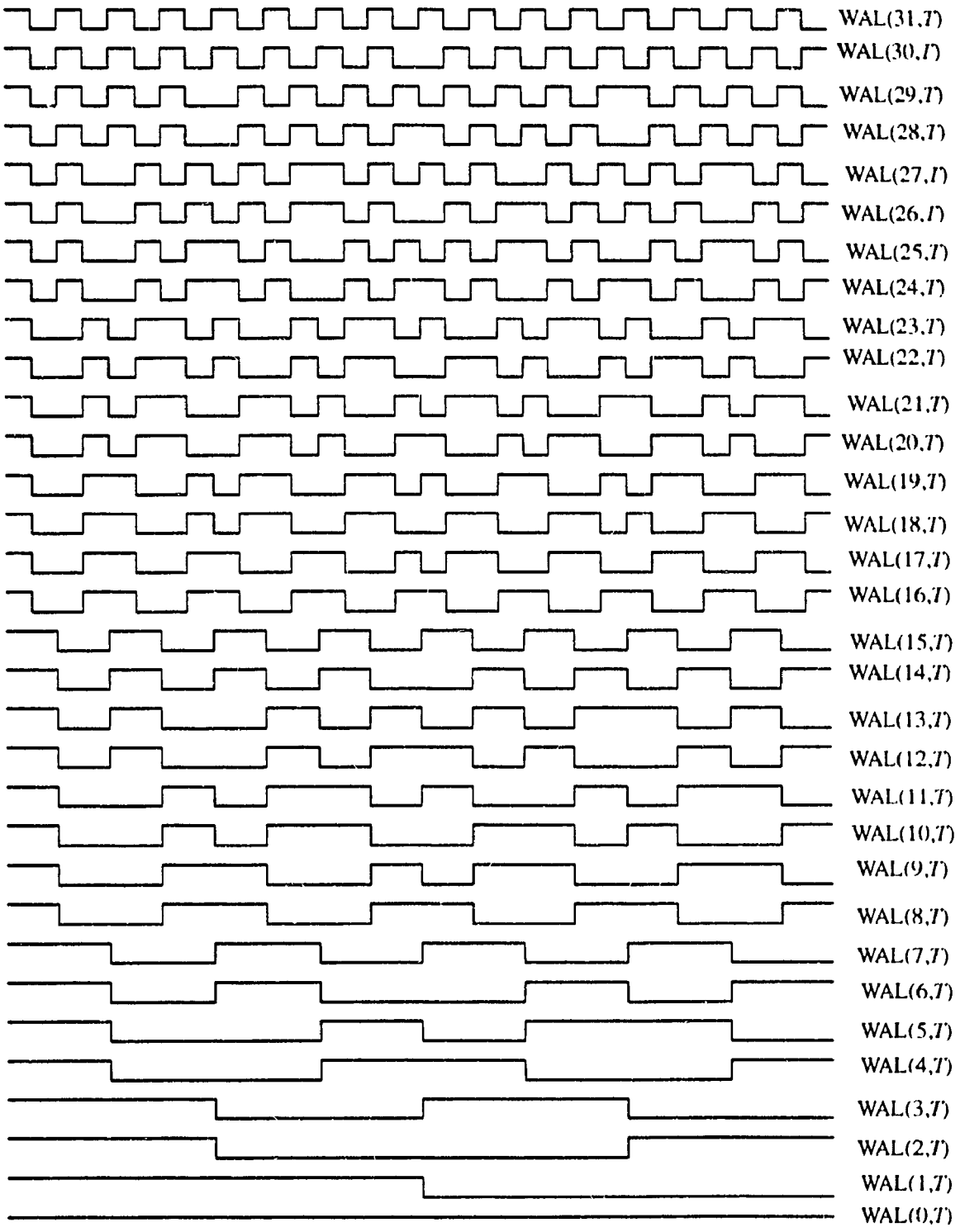

Fig. 3.5: A set of 32 Walsh functions

An alternative way to derive and show a set of Walsh functions is using *Hadamard* Matrices. The *Hadamard* matrix ($\boldsymbol{H}_N$) is a symmetric $(N \times N)$ matrix with +1, or -1 elements and N is a power of 2. The rows (columns) of $\boldsymbol{H}_N$ compose an orthogonal set of vectors. It means that the inner product of two different rows (columns) is equal zero. So each row (column) of $\boldsymbol{H}_N$ shows one of the first N Walsh functions.

The lowest order Hadamard matrix is of order two (N=2):

$$\boldsymbol{H}_2 = \begin{bmatrix} 1 & 1 \\ 1 & -1 \end{bmatrix} \tag{3.5}$$

Higher order matrices (power of 2), can be obtained from the recursive relation:

$$\boldsymbol{H}_N = \boldsymbol{H}_{N/2} \otimes \boldsymbol{H}_2 \tag{3.6}$$

where $\otimes$ denotes the direct *Kronecker* product.

The Kronecker product means replacing each element in the matrix, in this case $\boldsymbol{H}_{N/2}$, by the matrix $\boldsymbol{H}_2$ (instead each 1 and -1 in $\boldsymbol{H}_{N/2}$ we replace $\boldsymbol{H}_2$ and $-\boldsymbol{H}_2$). Thus for $\boldsymbol{H}_4$:

$$\boldsymbol{H}_4 = \boldsymbol{H}_2 \otimes \boldsymbol{H}_2 = \begin{bmatrix} 1 & 1 \\ 1 & -1 \end{bmatrix} \otimes \begin{bmatrix} 1 & 1 \\ 1 & -1 \end{bmatrix} = \begin{bmatrix} 1 & 1 & 1 & 1 \\ 1 & -1 & 1 & -1 \\ 1 & 1 & -1 & -1 \\ 1 & -1 & -1 & 1 \end{bmatrix} \tag{3.7}$$

Furthermore, if we now replace each element in the matrix $\boldsymbol{H}_4$ by $\boldsymbol{H}_2$ we obtain the *Hadamard* matrix of the order 8, $\boldsymbol{H}_8$.

$\boldsymbol{H}_8$ and the Walsh function corresponding to each row are shown in Fig.3.6

$$H_8 = \begin{bmatrix} 1 & 1 & 1 & 1 & 1 & 1 & 1 & 1 \\ 1 & -1 & 1 & -1 & 1 & -1 & 1 & -1 \\ 1 & 1 & -1 & -1 & 1 & 1 & -1 & -1 \\ 1 & -1 & -1 & 1 & 1 & -1 & -1 & 1 \\ 1 & 1 & 1 & 1 & -1 & -1 & -1 & -1 \\ 1 & -1 & 1 & -1 & -1 & 1 & -1 & 1 \\ 1 & 1 & -1 & -1 & -1 & -1 & 1 & 1 \\ 1 & -1 & -1 & 1 & -1 & 1 & 1 & -1 \end{bmatrix} \Leftrightarrow \begin{matrix} WAL(0,T) \\ WAL(7,T) \\ WAL(3,T) \\ WAL(4,T) \\ WAL(1,T) \\ WAL(6,T) \\ WAL(2,T) \\ WAL(5,T) \end{matrix}$$

Fig. 3.6: *Hadamard* matrix of the order 8 and the Walsh functions corresponding to its rows

3.3 Simulations Procedures

When the users' signature codes are not orthogonal, their non-zero cross-correlations create co-channel interference. In conventional single-user receivers (correlator or matched filter receivers), this interference makes the Signal to Noise Ratio (SNR) of each user decreases very fast when the number of users increases. The SNR in matched filter receiver is given by [14]:

$$SNR = \frac{E}{\sigma_n^2 + \frac{(K-1)E}{G}} \tag{3.8}$$

where E, σ_n^2, K, and G are signal power, noise power, number of users and processing gain, respectively.

In Fig.3.14, the SNR and BER for K=1,2,...,64 is shown where E, σ_n^2, and G are considered as 1, 0.1 and 127, respectively.

As we mentioned before, in multi-users detection scheme [13] the main goal is to cancel part of the co-channel interference. By doing this we expect that the behavior of the receiver will be much better than the single-user receiver when the number of users

increases. Besides the detection scheme, the choice of appropriate users' signature codes plays an important role to eliminate the interference. In this section we are trying to see the effects of choosing different well known codes on average Signal to Noise Ratio (SNR) and average Bit Error Rate (BER) in multi-user detection scheme. We will use the following relation to find average SNR:

$$(SNR)_k = \frac{[\boldsymbol{H}]_{kk}}{\sigma_n^2 [\boldsymbol{R}^{-1}]_{kk}} \tag{3.9}$$

$$average(SNR) = \frac{1}{K} \sum_{k=1}^{K} (SNR)_k \tag{3.10}$$

where:

$[\boldsymbol{H}]_{kk}$: the kth diagonal element of cross-correlation matrix $\boldsymbol{H}$ (the power of user k, E_k)

$[\boldsymbol{R}^{-1}]_{kk}$: the kth diagonal element of the inverse matrix of $\boldsymbol{R}$, matrix of normalized cross-correlations (represents the effects of non-zero cross-correlations of interference).

σ_n^2 : power of noise (in our simulations we considered arbitrary number 0.1 for this parameter).

K : number of users.

and [8,13]:

$$BER = \frac{1}{2} erfc\left(\sqrt{SNR/2}\right) \tag{3.11}$$

$$erfc(x) = \frac{2}{\sqrt{\pi}} \int_x^{\infty} e^{-t^2} dt \tag{3.12}$$

In our simulations we assumed that all users have the same power at the receiver (perfect power control situation). So in Eq. (3.9) all users have the same power which can be considered 1.

Since the cross-correlation between two signature codes depends on the delay and delay is random, we randomly choose the elements of $\boldsymbol{H}$ and find SNR. For having a general idea of SNR for different kinds of signature codes, for each of them we should do the process of choosing $\boldsymbol{H}$ and finding SNR for several times (in some cases we have done it more than 10000 times) and take the average over all the results. In our simulations we considered at most 64 users in the system (k = 1,2,....64).

If all users use the same linear maximal sequence codes with different delays as signature codes, the cross-correlation between two users' signature codes will be $-1/L$ where L is the code length ($L=2^n-1$, n is the number of delay units in the code generating circuit). In our case for K=64 users, we chose L=127 (n=7).

In the case of Gold codes, the cross-correlation between two Gold codes have three values with different probabilities for each of those values (Table 3.1). For 64 users we chose Gold codes of length L=127, (n=7), which have the normalized cross-correlation levels -17/127, -1/127, and 15/127 with probabilities 0.25, 0.5, and 0.25 respectively. We also considered the case of employing Gold codes of length L=2047, (n=11), with the cross-correlation levels found from Table 3.1. This case is needed to be compared with the case of employing combination if Walsh functions and Gold codes (will be discussed later in this section).

For each H_{ij}, the element of the cross-correlation matrix $\boldsymbol{H}$ (the cross-correlation between the signature codes of user i and j), we should choose one of these values by considering the probabilities. So, to substitute the cross-correlations of Gold codes of length 127 and 2047 (n=7 and n=11, respectively) in matrix $\boldsymbol{H}$, we use a random number in the

interval (0, 1) and assign each H_{ij} $(i \neq j)$ as following (we should keep in our mind that $H_{ij}=H_{ji}$):

m: random number in (0, 1)

$$H_{ij} = \begin{cases} \frac{-17}{127} & 0 < m \leq 0.25 \\ \frac{-1}{127} & 0.25 < m < 0.75 \\ \frac{15}{127} & 0.75 \leq m < 1 \end{cases} \qquad (n= 7) \tag{3.13}$$

and,

$$H_{ij} = \begin{cases} \frac{-65}{2047} & 0 < m \leq 0.25 \\ \frac{-1}{2047} & 0.25 < m < 0.75 \\ \frac{63}{2047} & 0.75 \leq m < 1 \end{cases} \qquad (n= 11) \tag{3.14}$$

If the signature codes are orthogonal there is no interference and we can get the best results. So it seems that using orthogonal functions like Walsh functions as signature codes can completely eliminate interference. But the problem is that most of these functions are orthogonal only for specific delays and when the delay is randomly changing they may have non-zero cross-correlations. Even for some delays the normalized cross-correlation between two Walsh functions can be one (the worst case when the two signature codes look exactly alike at the receiver and receiver cannot distinguish each of them).

For this reason Walsh functions by themselves cannot be used as signature codes and for using their orthogonality property we should use them in combination with other codes. It means that the data of each user first are multiplied by a linear code (maximal sequence or Gold codes) and then by a Walsh function as it is shown Fig.3.7:

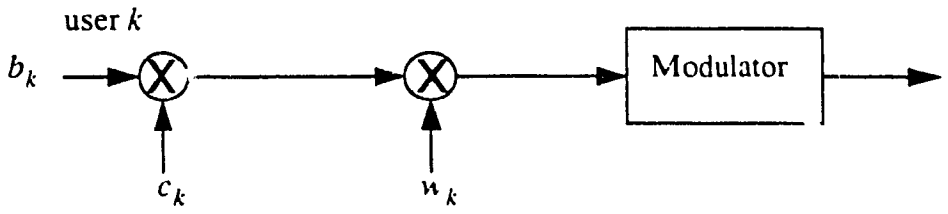

Fig. 3.7: Employing the combination of Walsh functions and linear codes as signature code

b_k : binary data,

c_k : linear code (maximal sequence or Gold code)

w_k : Walsh function k,

We can assign one Walsh function to each user or divide users into some groups and assign one Walsh function to each group. In the case of 64 users we can divide them into 16 groups and use 16 Walsh functions. Here instead of using a long linear code (n=11), we use a repetitive short one (n=7) repeated for each pulse of Walsh function, i.e., the data bit period is split over 16 subcode periods, each having a repetitive short linear code. In this situation, the cross-correlation between two signature codes (combination of Walsh functions and linear codes) is equal to multiplication of cross-correlation between two Walsh function and cross-correlation between two linear codes [24].

The problem for Walsh functions is that we don't have their cross-correlations for different delays. The first step for simulation is to find the cross-correlation between two Walsh functions. In our case we have 16 Walsh functions that we can use Hadamard matrix ($\boldsymbol{H}_{16}$) to show them,

$$
\boldsymbol{H}_{16} = \begin{bmatrix}
1 & 1 & 1 & 1 & 1 & 1 & 1 & 1 & 1 & 1 & 1 & 1 & 1 & 1 & 1 & 1 \\
1 & -1 & 1 & -1 & 1 & -1 & 1 & -1 & 1 & -1 & 1 & -1 & 1 & -1 & 1 & -1 \\
1 & 1 & -1 & -1 & 1 & 1 & -1 & -1 & 1 & 1 & -1 & -1 & 1 & 1 & -1 & -1 \\
1 & -1 & -1 & 1 & 1 & -1 & -1 & 1 & 1 & -1 & -1 & 1 & 1 & -1 & -1 & 1 \\
1 & 1 & 1 & 1 & -1 & -1 & -1 & -1 & 1 & 1 & 1 & 1 & -1 & -1 & -1 & -1 \\
1 & -1 & 1 & -1 & -1 & 1 & -1 & 1 & 1 & -1 & 1 & -1 & -1 & 1 & -1 & 1 \\
1 & 1 & -1 & -1 & -1 & -1 & 1 & 1 & 1 & 1 & -1 & -1 & -1 & -1 & 1 & 1 \\
1 & -1 & -1 & 1 & -1 & 1 & 1 & -1 & 1 & -1 & -1 & 1 & -1 & 1 & 1 & -1 \\
1 & 1 & 1 & 1 & 1 & 1 & 1 & 1 & -1 & -1 & -1 & -1 & -1 & -1 & -1 & -1 \\
1 & -1 & 1 & -1 & 1 & -1 & 1 & -1 & -1 & 1 & -1 & 1 & -1 & 1 & -1 & 1 \\
1 & 1 & -1 & -1 & 1 & 1 & -1 & -1 & -1 & -1 & 1 & 1 & -1 & -1 & 1 & 1 \\
1 & -1 & -1 & 1 & 1 & -1 & -1 & 1 & -1 & 1 & 1 & -1 & -1 & 1 & 1 & -1 \\
1 & 1 & 1 & 1 & -1 & -1 & -1 & -1 & -1 & -1 & -1 & -1 & 1 & 1 & 1 & 1 \\
1 & -1 & 1 & -1 & -1 & 1 & -1 & 1 & -1 & 1 & -1 & 1 & 1 & -1 & 1 & -1 \\
1 & 1 & -1 & -1 & -1 & -1 & 1 & 1 & -1 & -1 & 1 & 1 & 1 & 1 & -1 & -1 \\
1 & -1 & -1 & 1 & -1 & 1 & 1 & -1 & -1 & 1 & 1 & -1 & 1 & -1 & -1 & 1
\end{bmatrix} \tag{3.15}
$$

Each row of this matrix is one Walsh function. For finding the cross-correlation between two Walsh functions (two rows of the matrix), we just need to find the inner product of the two vectors made by this two rows and then normalized it. In other words the cross-correlation between two rows i and j (vectors V_i and V_j) is:

$$
C_{ij} = \frac{1}{N}(V_i^T \cdot V_j) = \frac{1}{N}\sum_{k=1}^{N} V_{ik} \cdot V_{jk} \tag{3.16}
$$

where N is the length of these two vectors.

To find the cross-correlation between these two vectors for different delays we just need to make a circular shift in one of them (because Walsh functions are periodic and we are finding the cross-correlations over one period). If we need to have delays less than one chip of Walsh functions, for instance $C/4$, (in Hadamard matrix each element in each row represents one chip) we just can make another matrix from $\boldsymbol{H}_{16}$ by repeating each of elements in its rows four times and repeat the explained procedure to find the cross-correlation between two rows of the new matrix for different delays (circular shifts). In our case

we used H_{16} (16 Walsh functions) and found the cross-correlations for 64 delays (delays of $C/4$) and stored them. The non-zero cross-correlations between two Walsh functions are shown in Fig.3.8 to Fig.3.13 (the cross-correlations which are not shown in these figures, are zero for all delays).

The 64 users are divided into16 groups and for each group there is one Walsh function. The group and Walsh function related to each user are chosen randomly but independent of the data. In addition to Walsh function, each user has a linear code which can be maximal sequence codes (generated by one linear circuit with different phases) or Gold codes.

Another approach for employing Walsh functions is QUALCOMM reverse link approach [28], in which the Walsh functions are chosen according to the data. In this case, the information bits are grouped to, for instance, four bit symbol groups and these symbol groups are used to select one of the 16 different orthogonal Walsh functions for transmission. So in this case, during transmission the Walsh function assigned to each user is changed according to the transmitted data and it may happen that two or more (even all) users have the same Walsh functions at a moment. Since data are assumed to be random, the assigned Walsh function to each user changed randomly during transmission. Here also each user, besides Walsh function, has a linear code (maximal sequence or Gold codes).

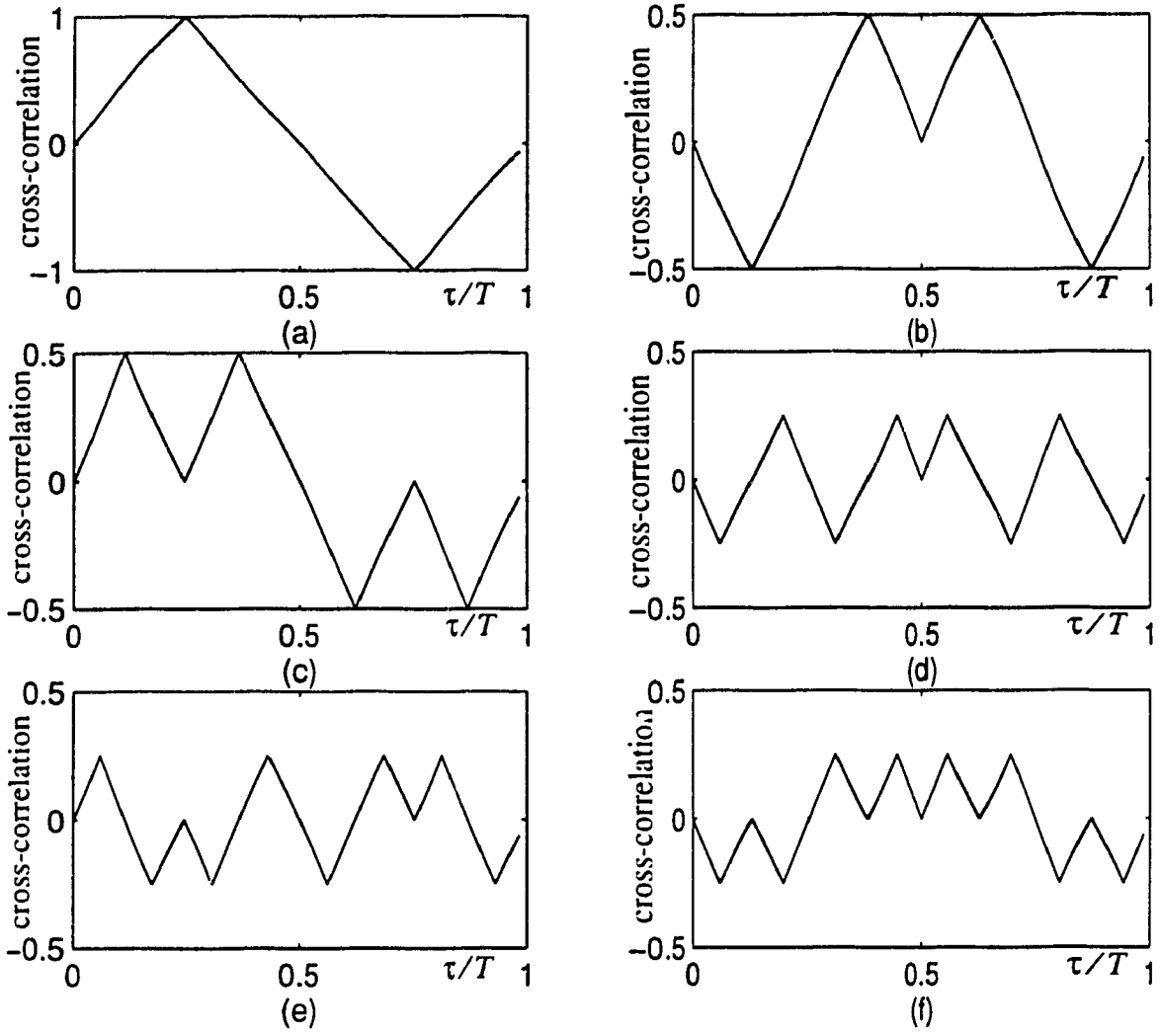

Fig. 3.8: The non-zero cross-correlations between Walsh functions (n_1,n_2): ($WAL(n_1,T)$ and $WAL(n_2,T)$), (a): (1,2), (b): (1,5), (c): (1,6), (d): (1,9), (e): (1,10), (f): (1,13).

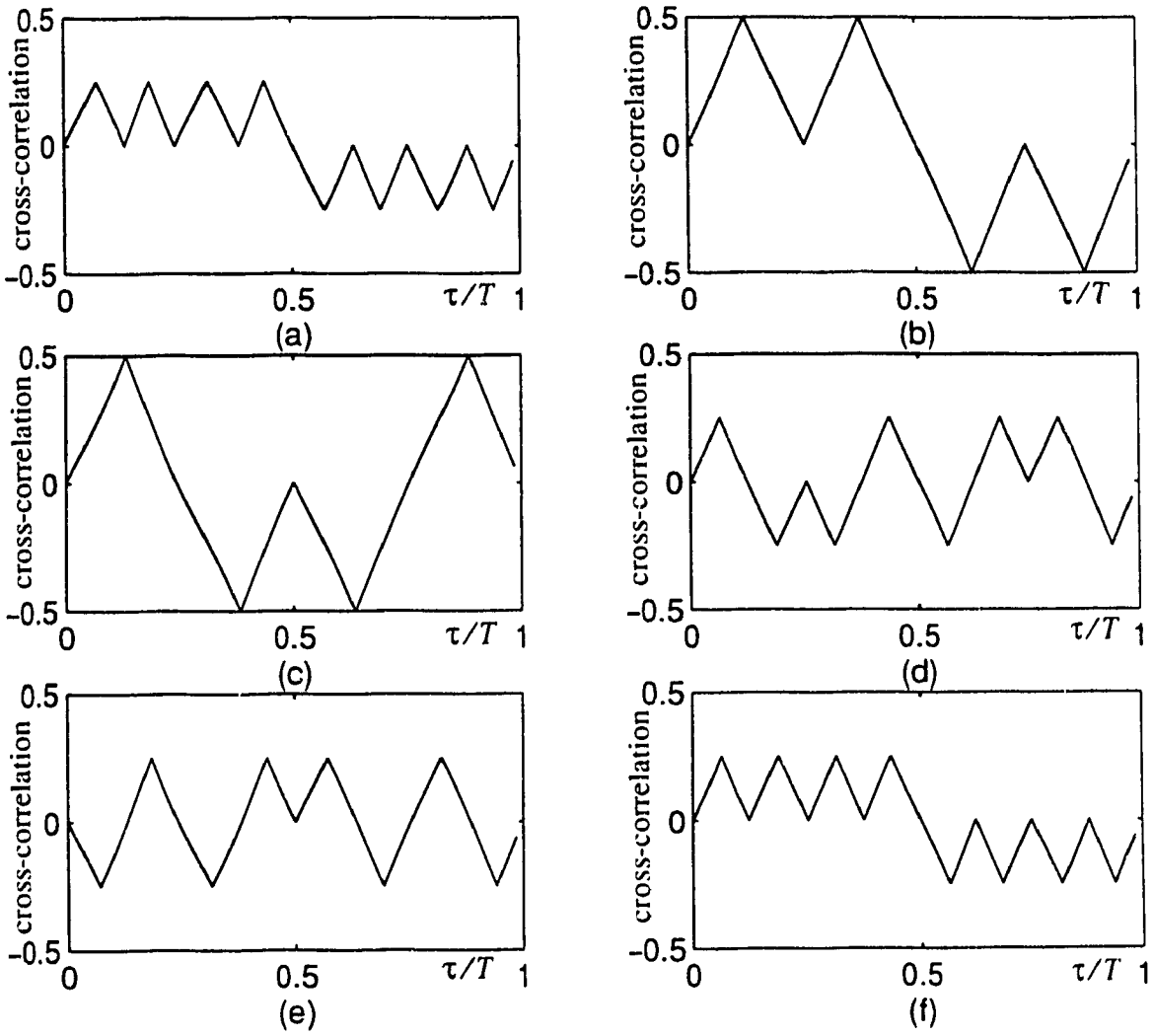

Fig. 3.9: The non-zero cross-correlations between Walsh functions (n_1,n_2): ($WAL(n_1,T)$ and $WAL(n_2,T)$), (a): (1,14), (b): (2,5), (c): (2,6), (d): (2,9), (e): (2,10), (f): (2,13).

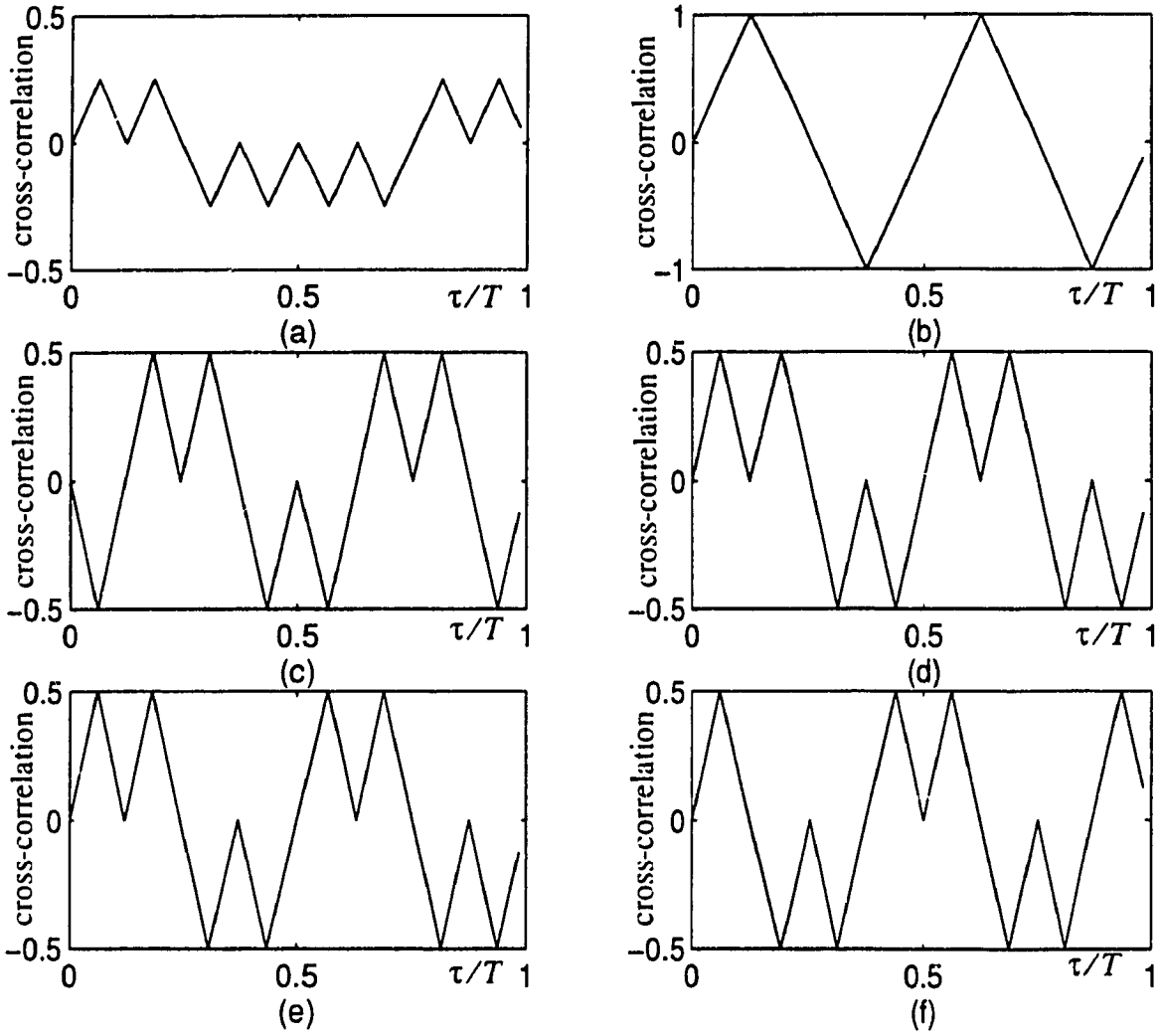

Fig. 3.10: The non-zero cross-correlations between Walsh functions (n_1,n_2): ($WAL(n_1,T)$ and $WAL(n_2,T)$), (a): (2,14), (b): (3,4), (c): (3,11), (d): (3,12), (e): (4,11), (f): (4,12).

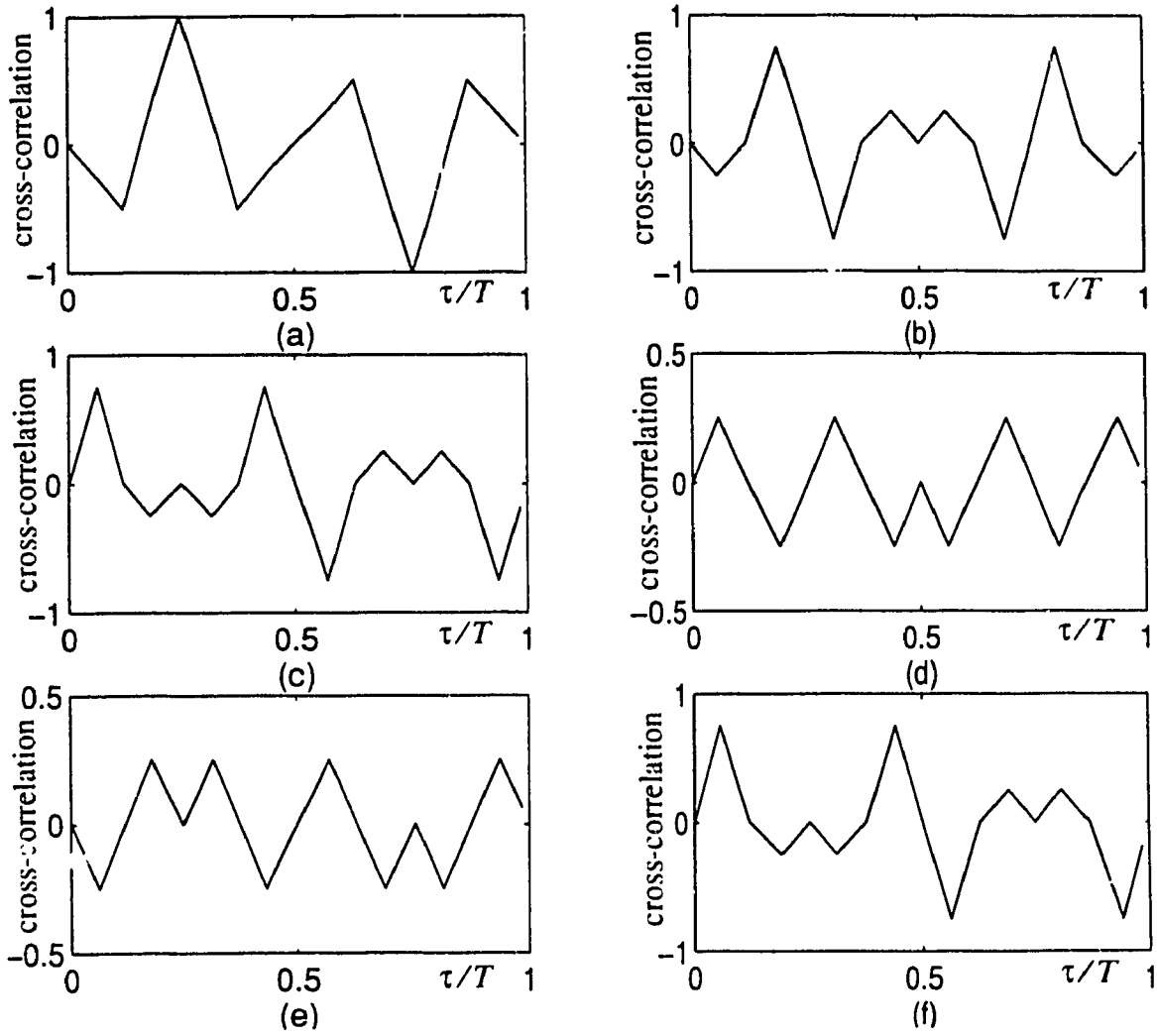

Fig. 3.11: The non-zero cross-correlations between Walsh functions (n_1,n_2): ($WAL(n_1,T)$ and $WAL(n_2,T)$), (a): (5,6), (b): (5,9), (c): (5,10), (d): (5,13), (e): (5,14), (f): (6,9).

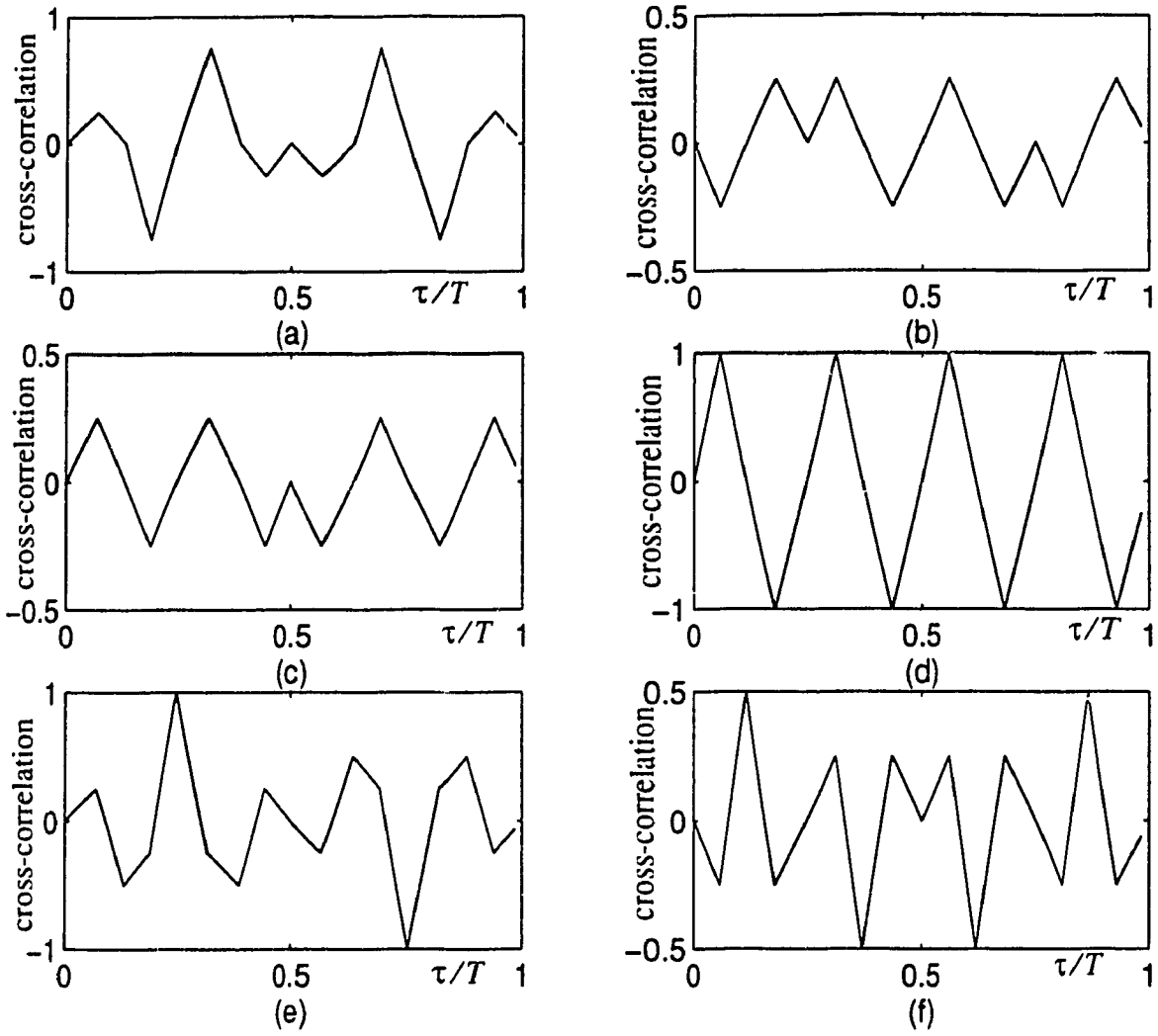

Fig. 3.12: The non-zero cross-correlations between Walsh functions (n_1,n_2): ($WAL(n_1,T)$ and $WAL(n_2,T)$), (a): (6,10), (b): (6,13), (c): (6,14), (d): (7,8), (e): (9,10), (f): (9,13).

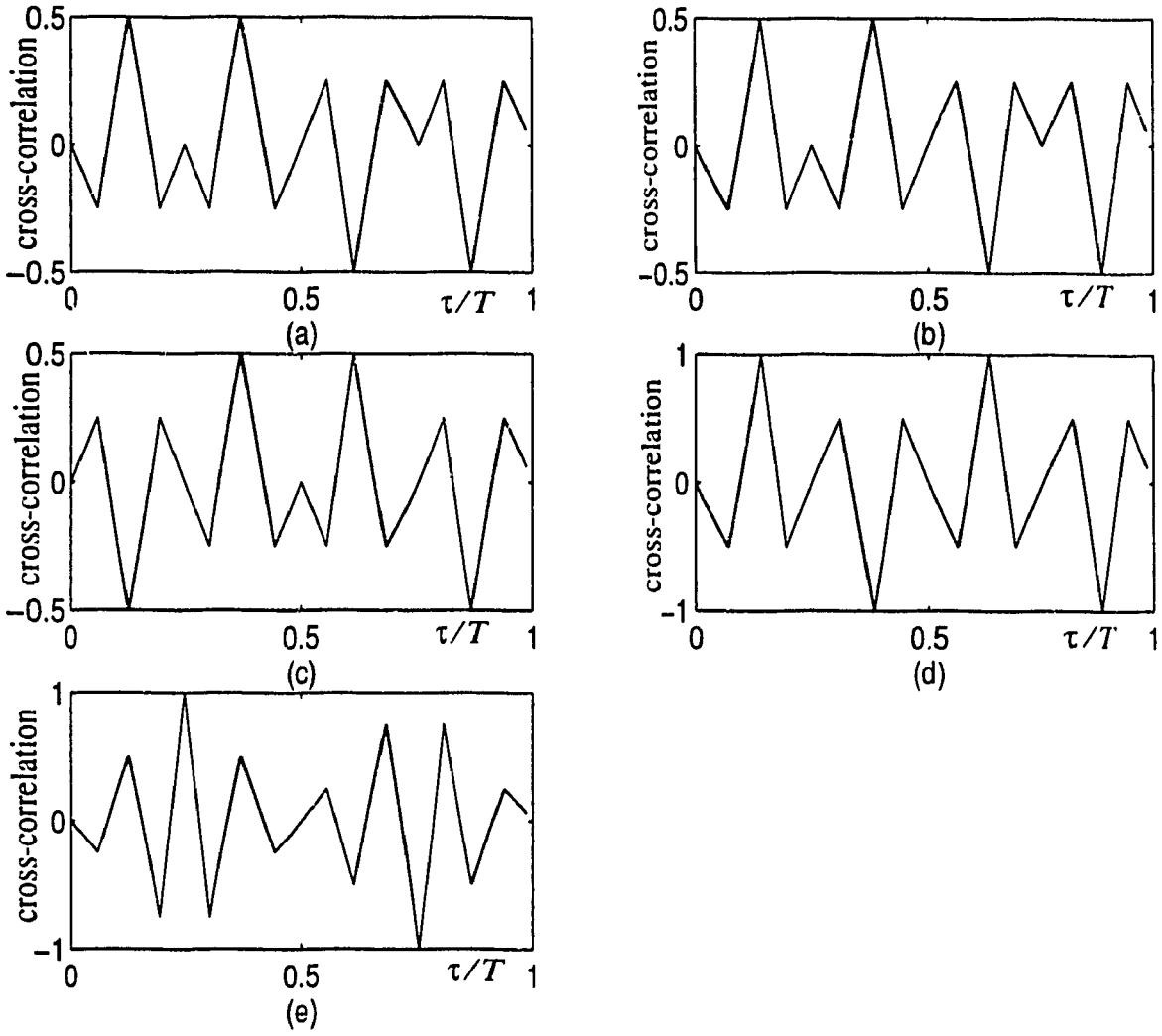

Fig. 3.13: The **non-zero cross-correlations between Walsh functions** (n_1,n_2): ($WAL(n_1,T)$ and $WAL(n_2,T)$), (a): **(9,14)**, (b): **(10,13)**, (c): **(10,14)**, **(d)**: (11,12), **(e)**: (13,14).

3.4 Simulations Results

In Fig.3.15 the average SNRs for 1 to 64 users when they use maximal sequence codes, Gold codes (for two cases n=7 and n=11), Walsh-maximal sequence (Walsh functions independent of data), and Walsh-Gold codes, respectively, are shown. Fig.3.16 is the average Bit Error Rates (BER) which are found from the above SNRs. It is easy to see that there is improvement when we use the combination of Walsh functions and short Gold codes.

In Fig.3.15 we assumed that 64 users are divided into 16 groups and in each group there are 4 users which have the same Walsh functions. To demonstrate the effect of using less number of Walsh functions, simulations have been done for when the users are divided into 8 groups and 8 Walsh functions are used. The result is shown in Fig.3.17 for combination of Walsh and Gold codes (n=7). It is clear from Fig.3.17 that using more Walsh functions gives better results, as it was expected.

Finally, in Fig.3.18 and Fig.3.19 the comparison of the performance of two different approaches for employing Walsh functions, are shown. Again, as it was expected, when Walsh functions are assigned independent of data we have better results.

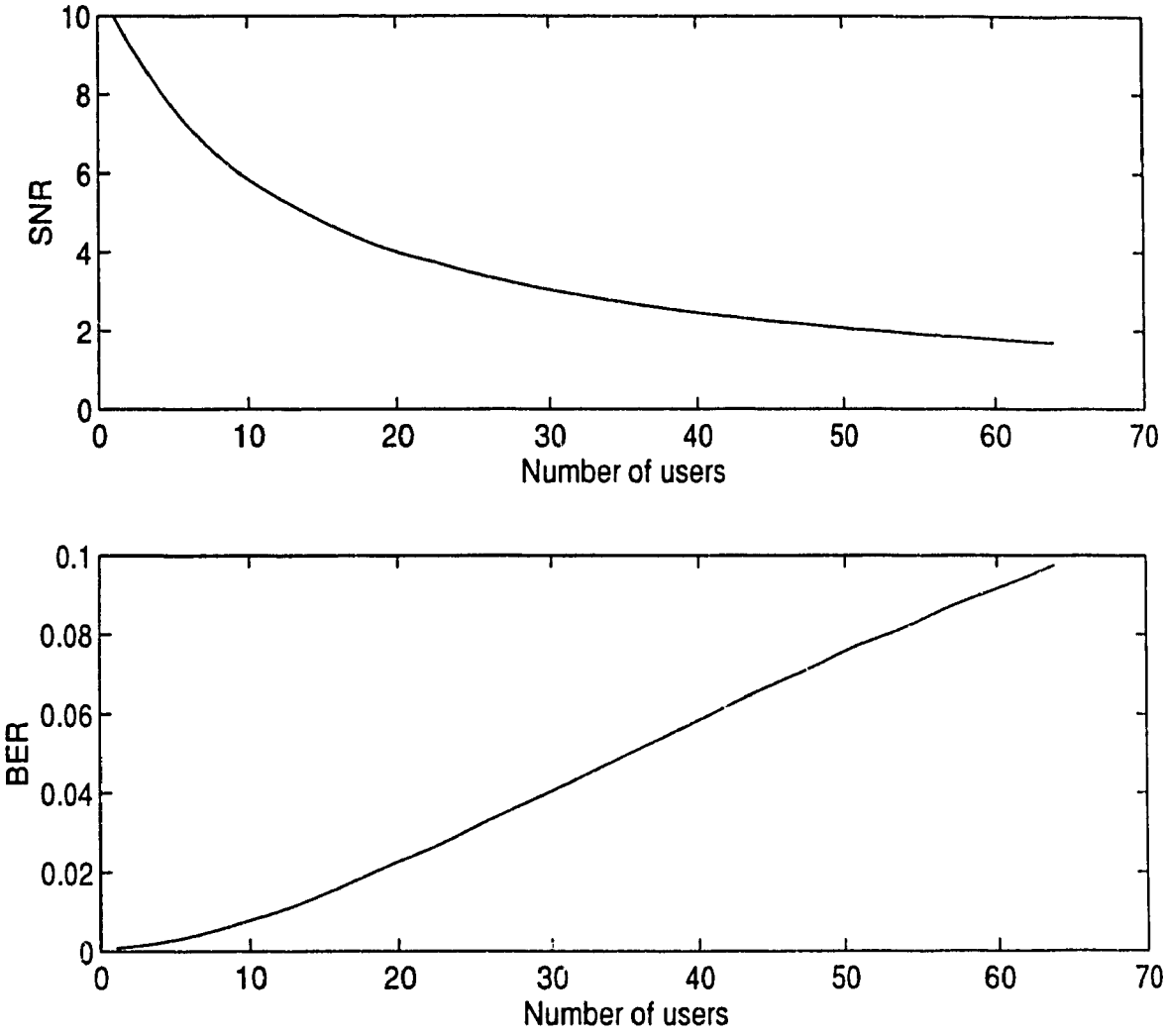

Fig. 3.14: The SNR and BER for single user detection, Eq. (3.8)

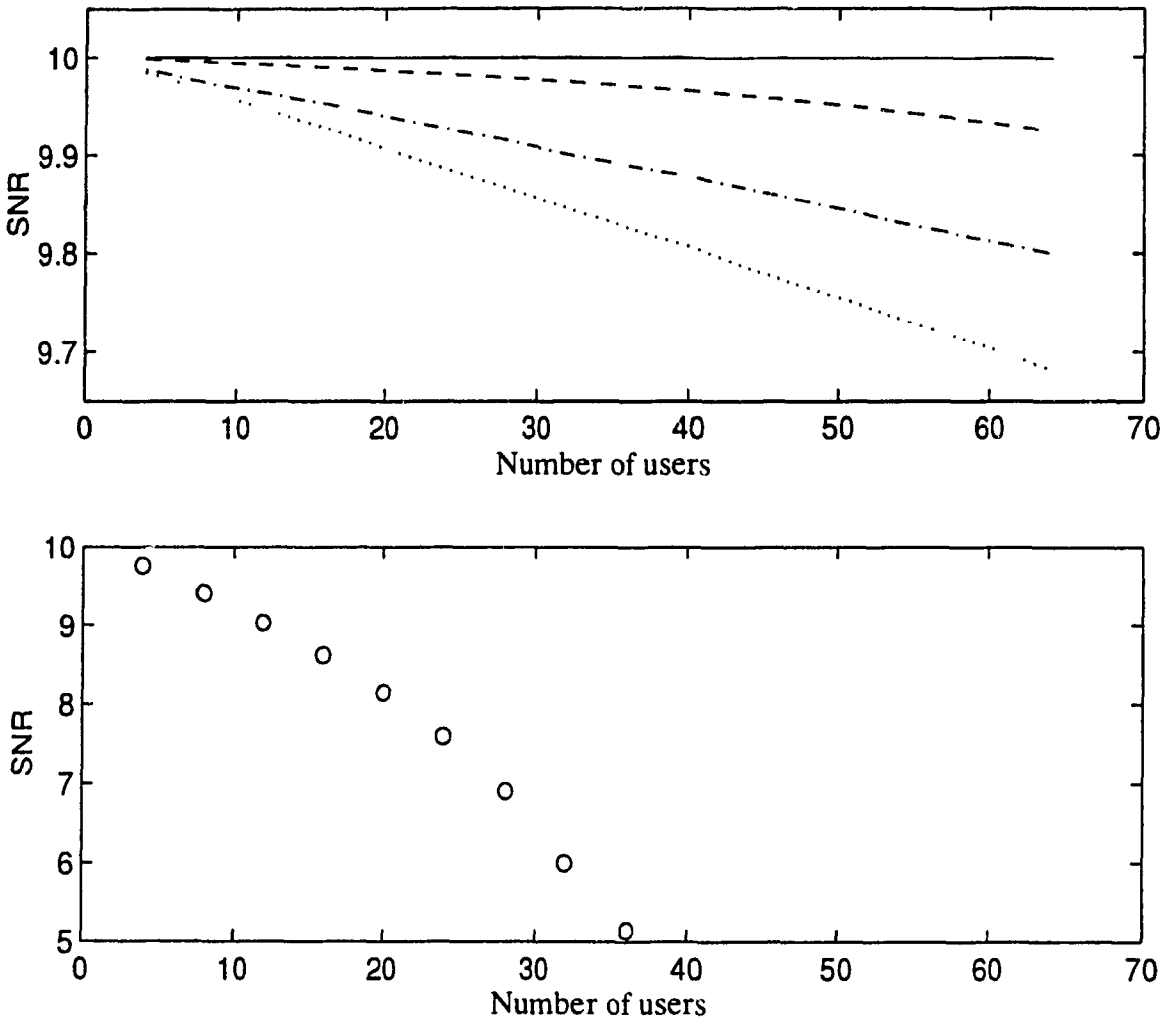

Fig. 3.15: SNR for 1 to 64 users, using different kinds of signature codes, '__': M_seq.-Walsh (n=7), '--' : M_seq. (n=7), '-.-' : Gold-Walsh (n=7), '...' : Gold Codes (n=11), 'o' : Gold Codes (n=7)

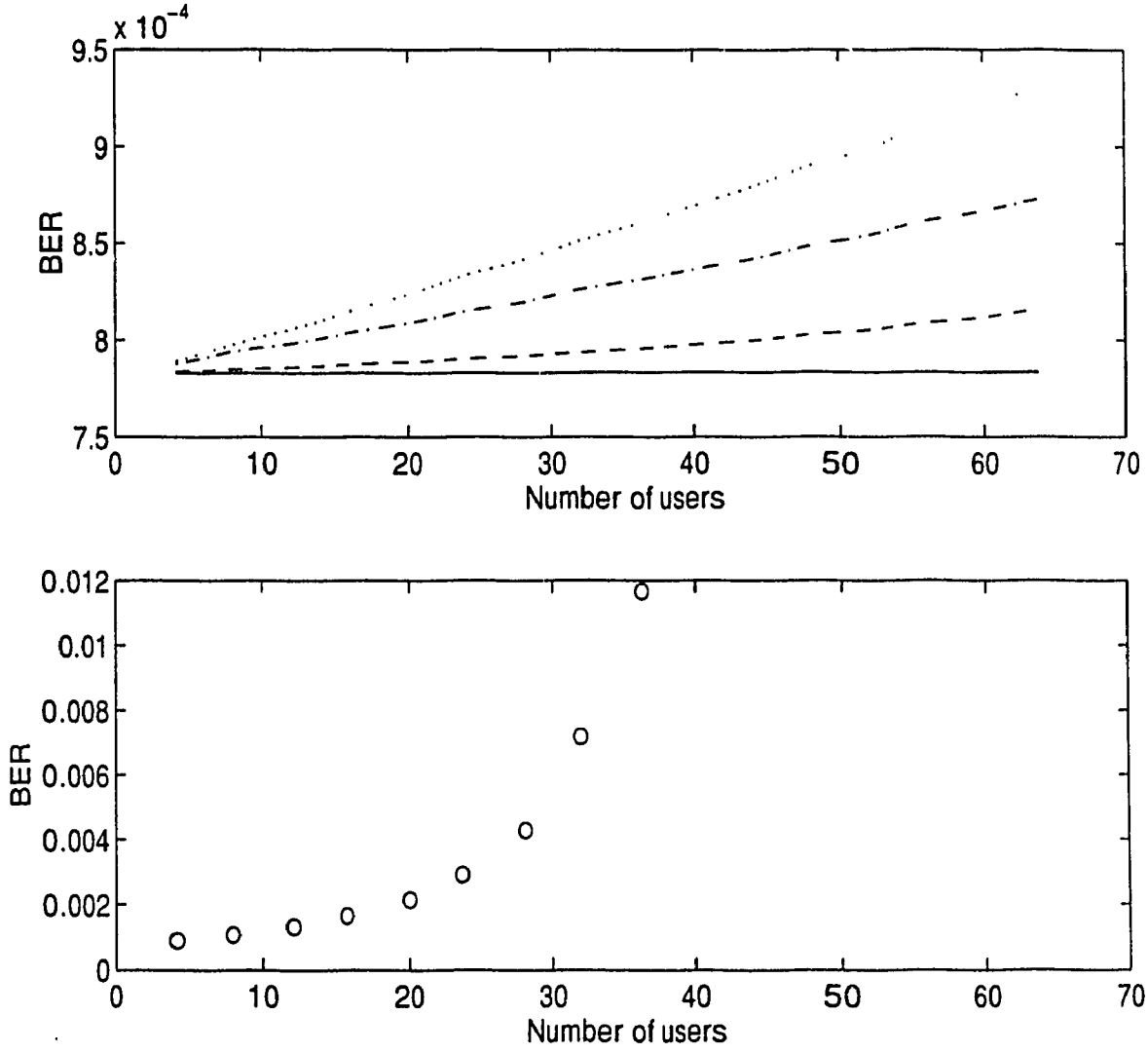

Fig. 3.16: BER for 1 to 64 users, using different kinds of signature codes, '__': M_seq.-Walsh (n=7), '--' : M_seq. (n=7), '-.-' : Gold-Walsh (n=7), '...' : Gold Codes (n=11), 'o' : Gold Codes (n=7)

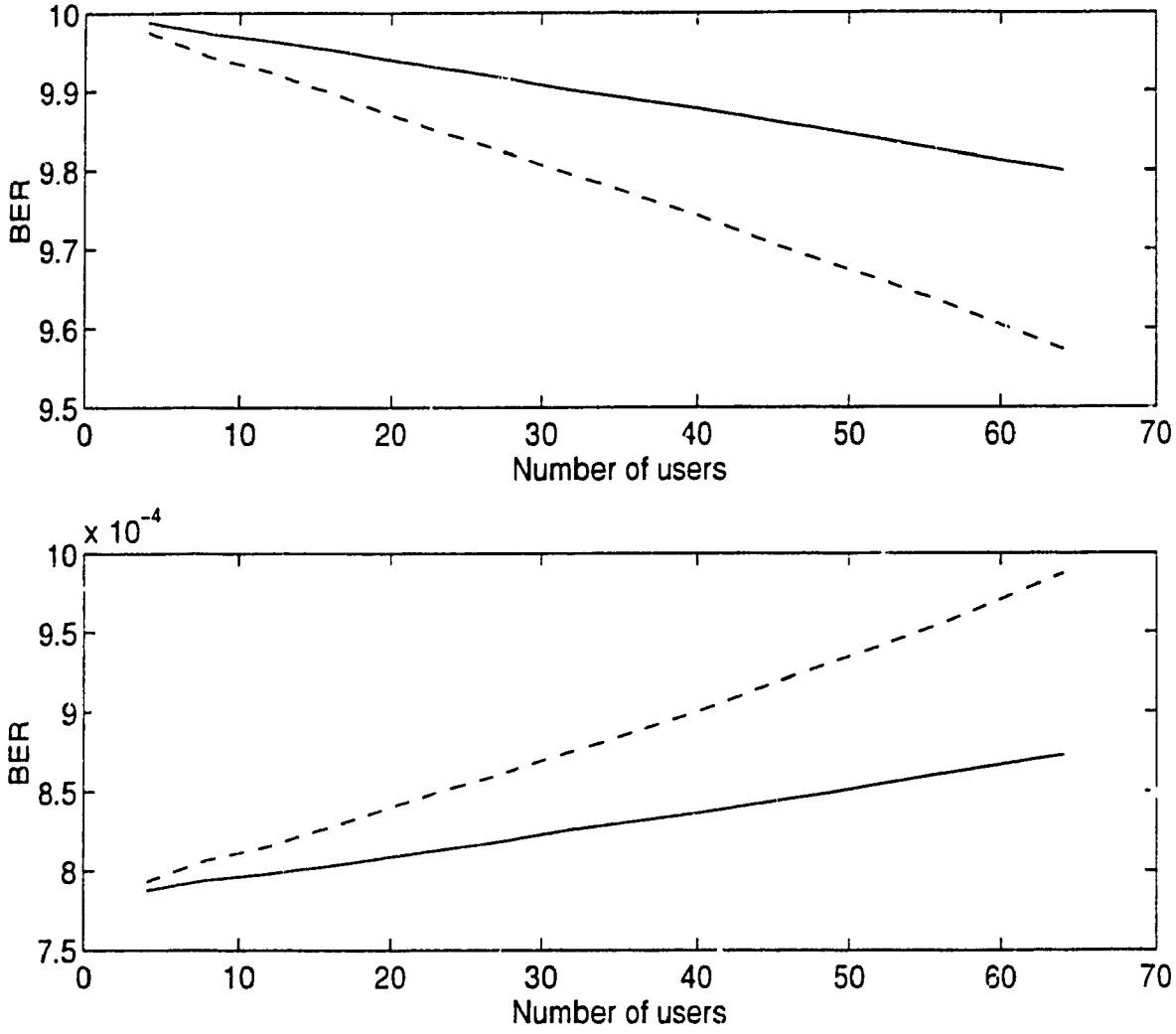

Fig. 3.17: The effect of using different number of Walsh functions (groups of users) in combination with Gold (n=7), on SNR and BER, '__' : 16 Walsh functions (4 users in each group), '--' : 8 Walsh functions (8 users in each group).

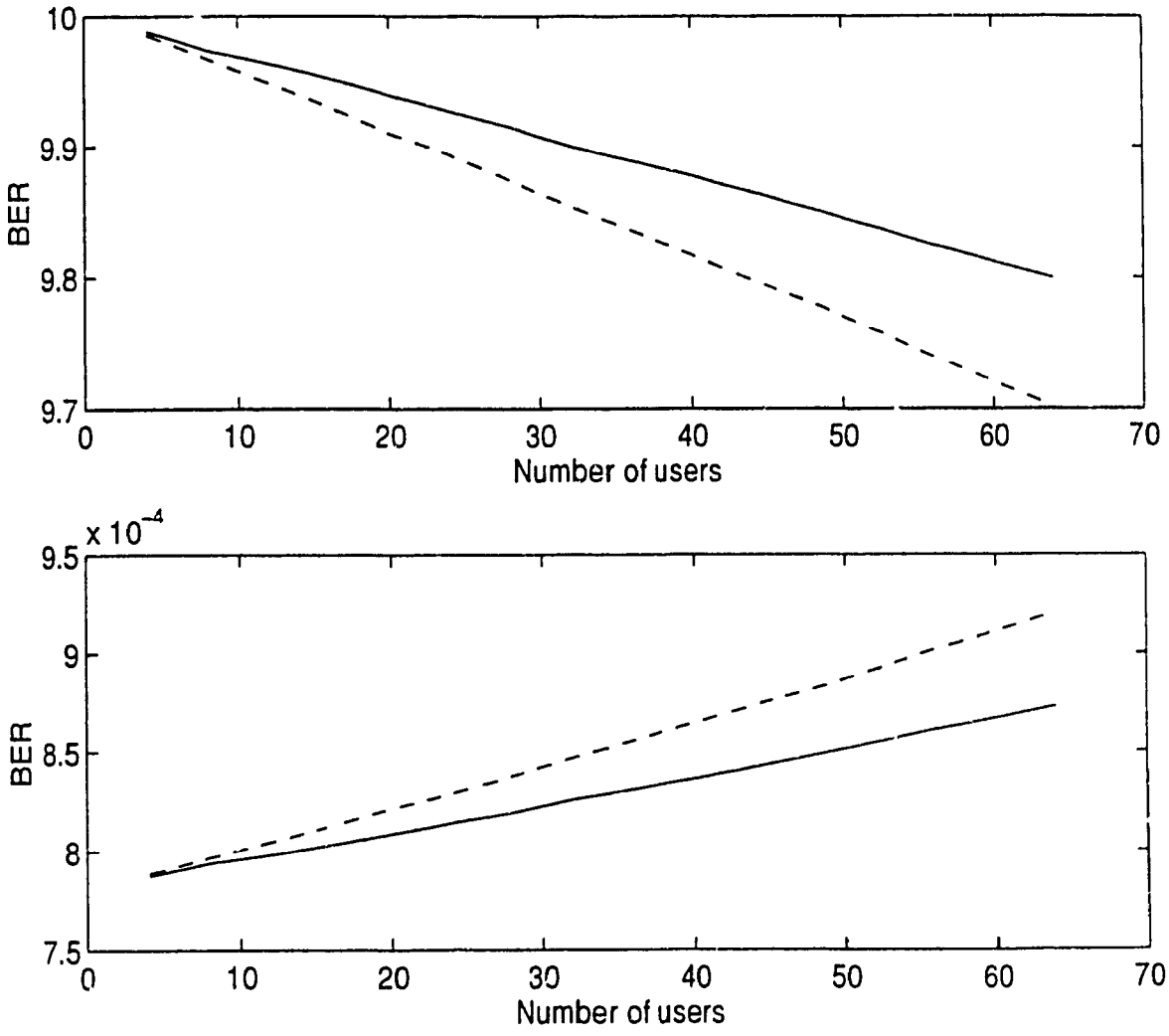

Fig. 3.18: The average SNR and BER for M_seq.-Walsh with two different methods of employing Walsh functions, '__' : Walsh functions are chosen independent of data, '--' : Walsh functions are chosen according to the data symbols [28].

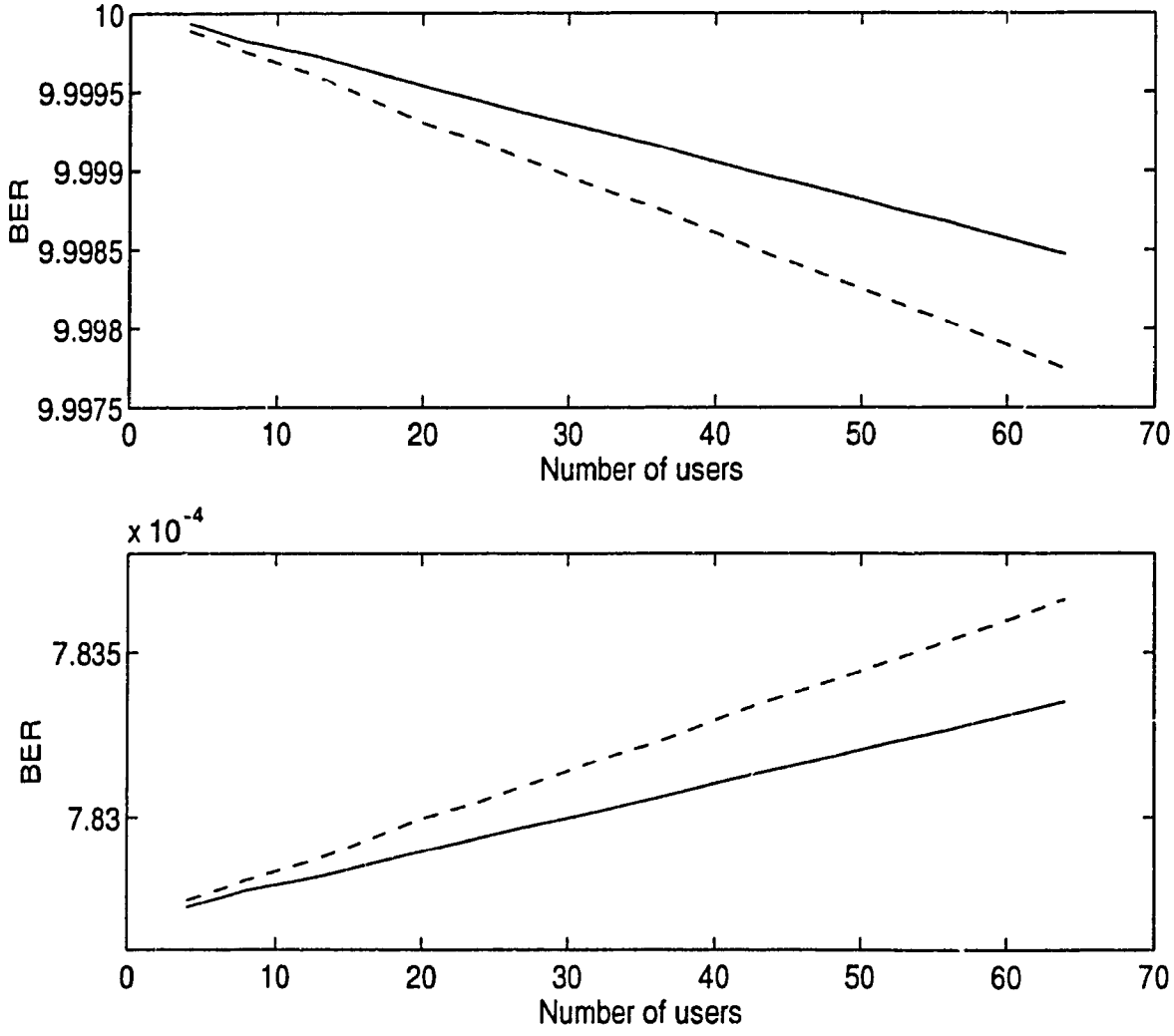

Fig. 3.19: The average SNR and BER for Gold-Walsh with two different methods of employing Walsh functions, '__' : Walsh functions are chosen independent of data, '--' : Walsh functions are chosen according to the data symbols [28].

CHAPTER 4

A HYBRID SINGLE USER / MULTI-USER DETECTION SCHEME FOR CDMA SYSTEMS

4.1 Introduction

There has been a growing interest lately in analyzing the performance of a Spread Spectrum receiver that cancels the multi-user interference of the simultaneously transmitting users in a CDMA network and detects all bits of all users at the same time [29]. These systems contrast with the single user receiver case where the multiple-access interference is treated as noise. The multi-user receiver treats those interferences as signals to be estimated and then subtracted from the received signal so as to provide less interference in this signal and better detection of desired signals.

In [13], an efficient adaptive decorrelating detector for synchronous multi-user CDMA was presented and evaluated via computer simulation in both noise and slow frequency-selective Rayleigh fading channels. Fig.2.4, (page 35), shows the basic building blocks of this receiver [13]. Synchronism or very small delay between users with no or relaxed power control, was assumed for this multi-user receiver.

In [16], a successive interference cancellation scheme for synchronous CDMA was proposed, as in Fig.4.1, the strongest signal is first detected and then subtracted from the received signal to gain a signal with less multiple-access interference. The process of detecting and subtracting the strongest signal continues successively to obtain the weakest signal. No knowledge of the energies of the individual users is needed and the strongest user is found by using a bank of correlators.

An adaptive linear receiver for coherent demodulation in asynchronous CDMA sys-

tems, as shown in Fig.4.2, was proposed in [30]. No knowledge of the signature waveforms and timing (delays) of other users for this adaptive receiver was assumed. The receiver is trained by a known training sequence prior to data transmission and continuously adjusted by an adaptive algorithm during data transmission.

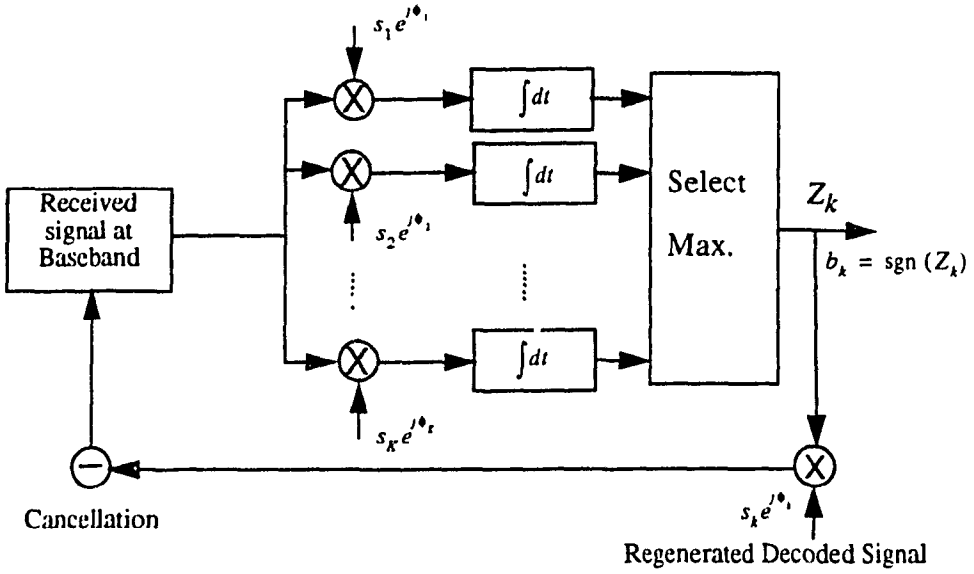

Fig. 4.1: Successive Interference Cancellation in DS/CDMA System [16].

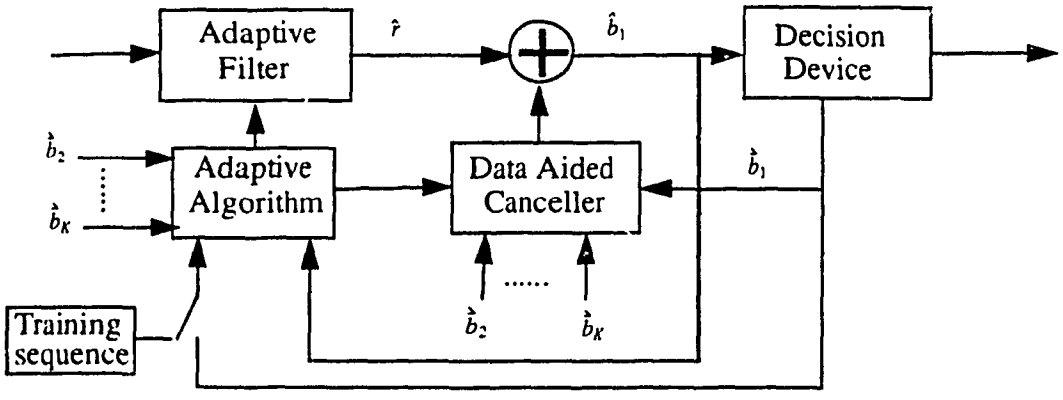

Fig. 4.2: Adaptive receiver [30]

Iltis and Mailaender, in [31], presented a new multi-user receiver based on the structure of a symbol-by-symbol detector. In this detector the delays and amplitudes of incoming waveforms are estimated recursively by using a set of extended Kalman filters. The resulting algorithm for this receiver is quite complex, due to the large number of possible composite symbol corresponding to the multiple users.

In [21], the uplink JD-C/TDMA mobile radio system applying a combination of TDMA (time division multiple access) and CDMA using joint detection (JD) with coherent receiver antenna diversity at the base station receiver was proposed.

Some attractive features of JD-C/TDMA are the possibility to flexibly offer voice and data services with different bit rates, soft capacity, inherent frequency and interferer diversity and high system capacity due to joint detection. In this receiver, channel estimation is provided by detecting known data bits (midamble) for each users.

In this chapter, a new receiver for CDMA systems, employing both single user and multi-user, (sub-optimum), detection in a hybrid manner, is proposed. The multi-user detector is a modification of the adaptive receiver in [13] for asynchronous case. The single user detection is used to not only provide an estimation of data bits (to be compared with the data detected by multi-user detector), but also yield the information (each user delay) replacement of the multi-user detector in asynchronous case.

In Sec.4.2 a description of the new system is provided. In Sec.4.3 and Sec.4.4 the simulations procedure and the results, obtained by simulations, of the performance of single user and sub-optimum multi-user detection as the main parts of the hybrid detection are presented.

4.2 The New Hybrid Single User/Multi-User Detection for CDMA Systems

Fig.4.4, (page 76), and Fig.4.5, (page 77), show the block diagrams of the transmitter and the receiver of the proposed hybrid system. While Fig.4.4 is the typical Direct Sequence system found in the literature, Fig.4.5 shows the way the bit detection results from single detection and multi-detection are combined to yield better results in the hybrid system. The receiver assumes the knowledge of the numbers, identities and codes of the K active users. Such information is usually provided from the call signaling channel which is not discussed here.

In Fig.4.5, the K banks of single user receivers (detecting single user bits at a time) also provide the adaptive multi-user receiver with such precious information as the code epoch, the data bit delay, τ_k, of each user signal. This will greatly facilitate and simplify the multi-receiver structure as opposed to the works of [31] and [30] which evaluate the different spread spectrum signals delays by different versions of Kalman filtering.

To obtain such delay information, independent carrier recovery loops and code epochs finding circuits (code acquisition) are assumed to exist for each active user. If data bits starting edges are aligned with chip edges (data and code are in synchronism) for each user, knowledge of code epochs translates into knowledge of timing offsets of users data bits from a certain local bit time, i.e., $\tau_1, \tau_2, \ldots, \tau_K$.

As will follow shortly, knowledge of $\tau_1, \tau_2, \ldots, \tau_K$ means that no code correlation loss will exist (in the single receiver or multi-user receiver) but for the multi receiver case it is recommended to have $\tau_1 = \tau_2 = \ldots = \tau_K = 0$, i.e., to force all users data bits to be in synchronism at the base station, or multi-user quality will degrade. In this chapter we assume the existence of necessary feedback communication channels between the data user and BS so as to force $\tau_1, \tau_2, \ldots, \tau_K$ to have diminishing values.

However, the simulations take into effect the random variations of τ_k values in a certain small range, i.e., τ_k, k=1,...,K are random variables uniformly distributed between 0 and τ_{max}. Due to presence of occasional high AWGN and/or fading and/or the τ_k non-zero values above (due to bit timing feedback loop imperfections), the multi-user receiver may degrade and bit error results of the single user detection may outperform those of multi-user receiver results. Fig.4.5 shows that final detected bit for each user is the one coming from single receiver or multi-receiver depending on the results of a midamble detection. The midamble is a 2 byte length known pattern of bits that is inserted by the user at the transmitter in the middle of each data packet, as in Fig.4.3. The receiver of Fig.4.5 compares the detected midamble bits coming from single and multi user receiver and picks the one that has minimum number of difference from the known midamble bit pattern.

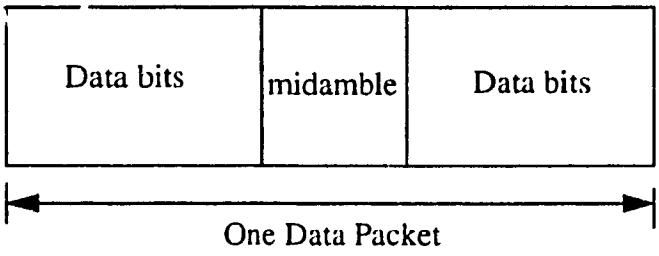

Fig. 4.3: A transmitted data packet

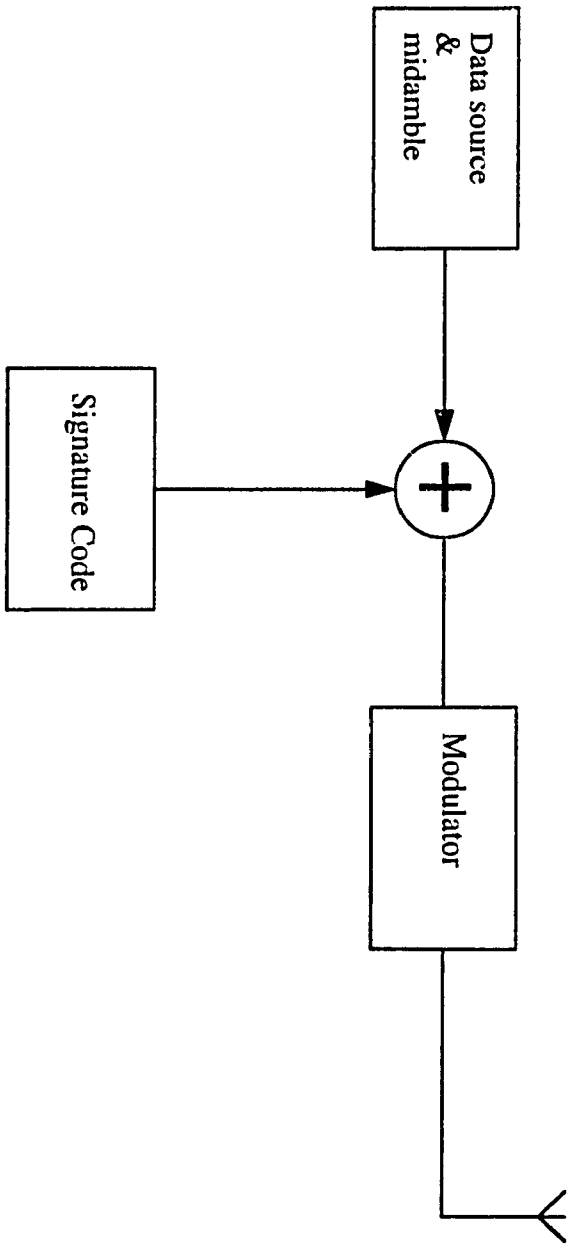

Fig. 4.4: The typical transmitter for CDMA system

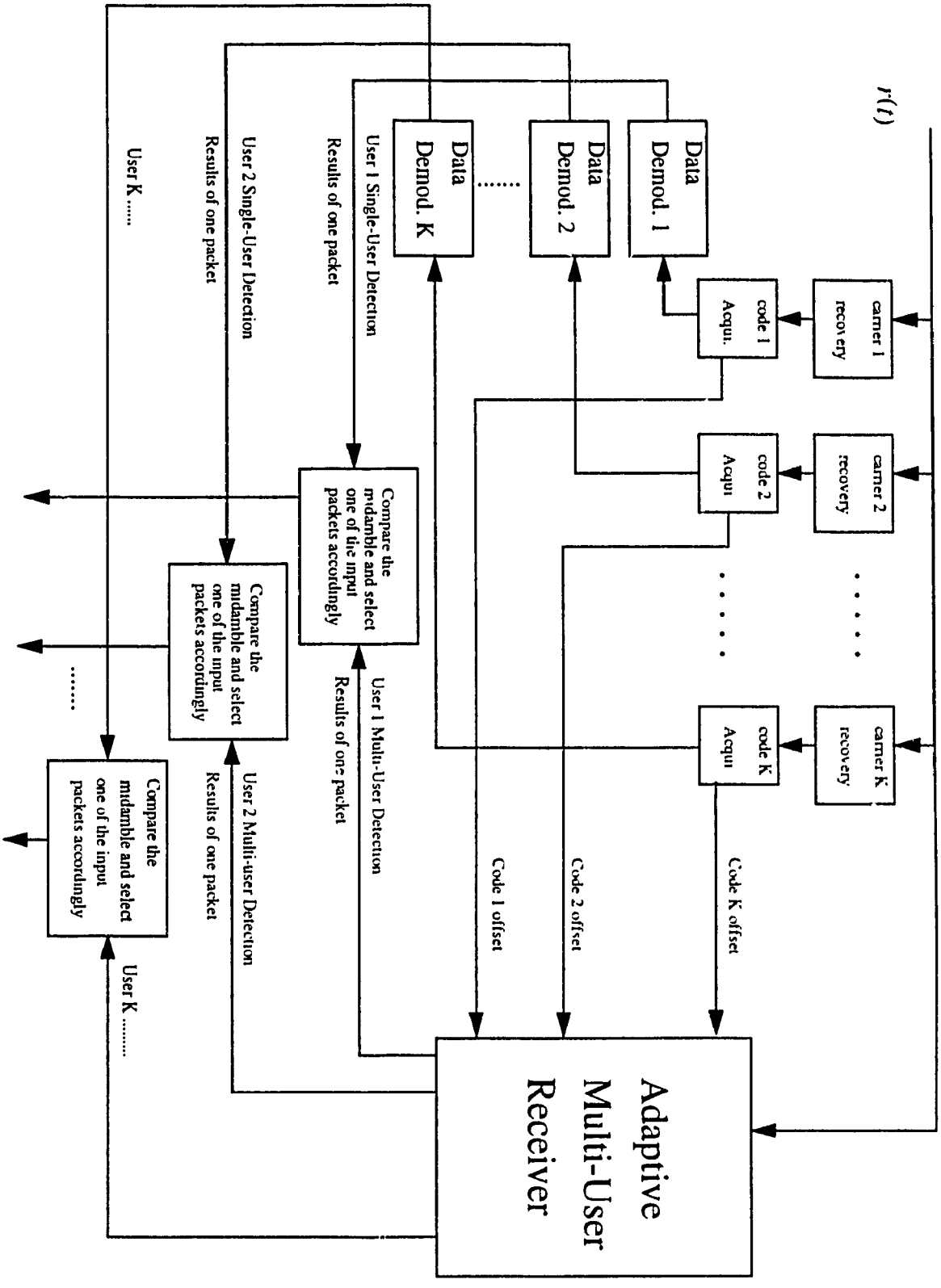

Fig. 4.5: Proposed multi-user detection scheme

4.3 Simulations Procedures and Performance of Multi-User Detection in Voice Transmission

As shown in Fig.4.5, in the proposed receiver, both multi-user (Adaptive Multi-user receiver [2]) and single user (Bank of Matched-Filters) detection are employed. The received signal has the form:

$$r(t) = \sum_{k=1}^{K} A_k b_k(t+\tau_k)\, s_k(t+\tau_k) \cos(\omega_c t + \phi_k) + n(t) \tag{4.1}$$

where:

K : total number of active users

A_k : amplitude of kth user

$b_k(t)$: bit sequence of the kth user at bit-rate R_b

$s_k(t)$: spreading chip sequence (signature code) of the kth user at chip-rate R_c

$n(t)$: additive white gaussian noise

τ_k and ϕ_k are the time delay and phase of the kth user. The knowledge of each user's phase, ϕ_k , and consequently accurate carrier recovery is assumed. After carrier recovery, the received signal can be expressed as:

$$r(t) = \sum_{k=1}^{K} A_k b_k(t+\tau_k)\, s_k(t+\tau_k) + n(t) \tag{4.2}$$

During the code acquisition process for each user (which is a requirement for the single user detection) the code offset of each user or equally the time delay of each user, τ_k, is found in the process. The code offsets, τ_k, are applied to the multi-user detector [13], shown in Fig.4.6, and used accordingly to fix the offset of signature codes

$s_1(m), s_2(m), \ldots, s_K(m)$ in adaptive receiver.

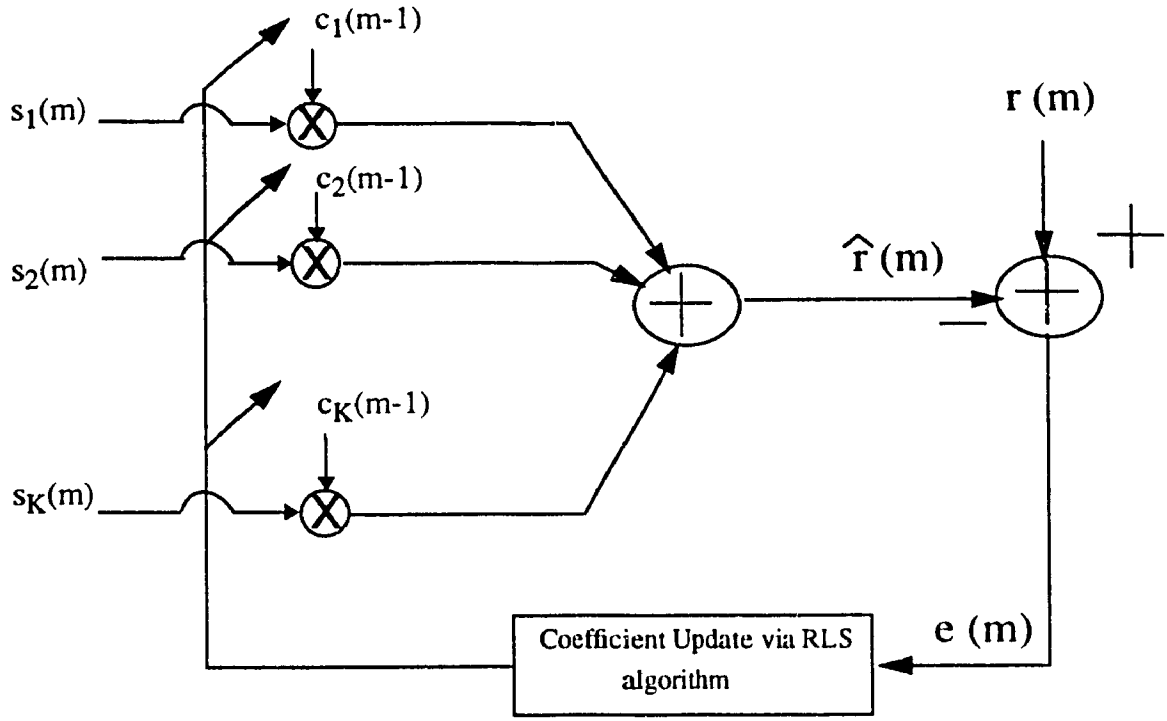

Fig. 4.6: Adaptive Multi-User Detector

The optimum solution for the LS filter coefficients at the nth iteration is [14]:

$$\boldsymbol{C}(n, \hat{\tau}) = \boldsymbol{R}^{-1}(n, \hat{\tau})\, \boldsymbol{D}(n, \hat{\tau}) \tag{4.3}$$

where:

$$\hat{\tau} = (\tau_1, \tau_2, \tau_3, \ldots, \tau_K) \tag{4.4}$$

$$\boldsymbol{R}(n, \hat{\tau}) = \sum_{m=1}^{n} \lambda^{n-m} \boldsymbol{S}(m, \hat{\tau})\, \boldsymbol{S}^T(m, \hat{\tau}) \tag{4.5}$$

$$\boldsymbol{D}(n, \hat{\tau}) = \sum_{m=1}^{n} \lambda^{n-m} r(m)\, \boldsymbol{S}^T(m, \hat{\tau}) \tag{4.6}$$

$$\boldsymbol{C}^T(j,\hat{\tau}) = (\ c_1(j,\hat{\tau})\ \ c_2(j,\hat{\tau})\ \ \ldots\ \ c_K(j,\hat{\tau})\ ) \tag{4.7}$$

$$\boldsymbol{S}^T(j,\hat{\tau}) = (\ s_1(j,\tau_1)\ \ s_2(j,\tau_2)\ \ \ldots\ \ s_K(j,\tau_K)\ ) \tag{4.8}$$

and $0 < \lambda \leq 1$ is a scaling factor. The parameter $\hat{\tau}$ in above equations shows the dependence of all parameters in adaptive receiver on relative delays of users.

The estimation of data symbols is [13]:

$$\hat{b} = \text{sgn}[\boldsymbol{C}(2L)] = \text{sgn}[\boldsymbol{R}^{-1}(2L)\,\boldsymbol{D}(2L)] \tag{4.9}$$

where L is the code length (in multi-user receiver procedure the received signal and signature codes are sampled twice per spreading chip)

The difference between this adaptive filter and *Kalman* filter, [14], is that here the channel parameters and $s_k(m)$'s are known and we do not need to recursively estimate them. So in simulations, we can compute from the beginning the matrix $\boldsymbol{R}(2L)$ and consequently $\boldsymbol{R}^{-1}(2L)$. During the simulation, the random data for each user are generated by a random generator and multiplied by their known signature codes. At this point a random delay is picked for each user and through equation Eq. (4.2) the received signal, $r(t)$, is generated. The received signal is sampled twice per spreading chip to get $r(m)$. During the detection, one of the users whose information bits are ahead of other users is considered as reference (without loss of generality we assume the user #1 is the reference user). At the end of each bit interval of user #1, the matrix $\boldsymbol{D}$ and consequently $\boldsymbol{C}(2L)$ are computed. Finally, from Eq. (4.9), the data bits are obtained. The received sequences model is shown in Fig.4.7.

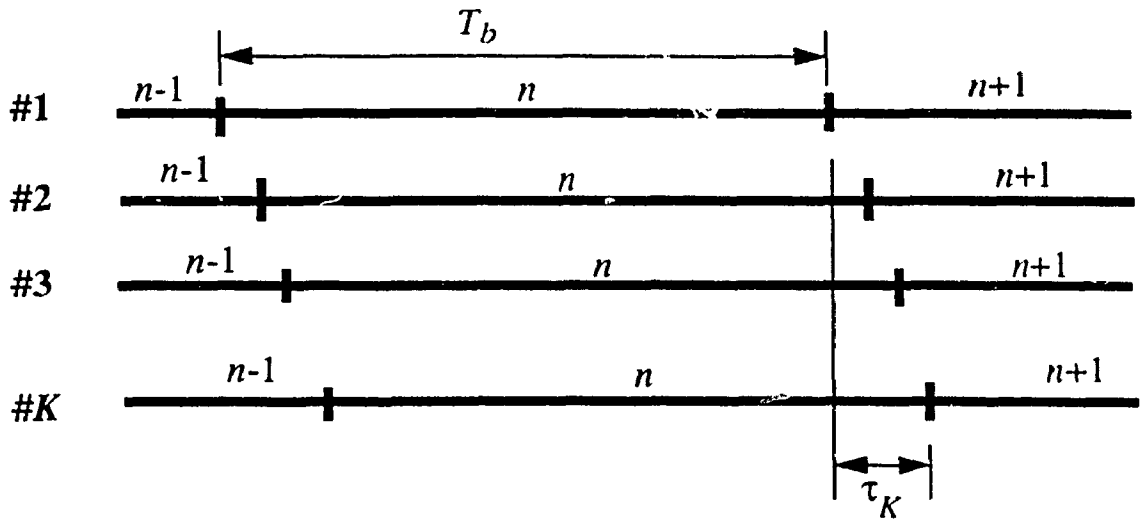

Fig. 4.7: Received Sequences Model

As the first case, simulations have been done for both single user and multi-user detection for different SNR's. The single user detection, for user k, is simply done by multiplying the received signal, $r(t)$ in Eq. (4.2) by $s_k(t+\tau_k)$ and integrating over one bit period as in Eq. (4.10). Also two cases of synchronous ($\tau_k = 0$ in Eq. (4.1) to Eq. (4.10)), and asynchronous (Bit Asynchronism) cases have been considered in the simulations.

The detected bits of user k in the single user detection case are obtained from:

$$\hat{b}_k = \text{sgn}\left(\int_0^{T_b} r(t)\, s_k(t+\tau_k)\, dt\right) \tag{4.10}$$

In the second phase of the simulations, the focus was on the performance of multi-user receiver when all the users are not active during the whole transmission time, i.e., there are silence periods as in voice traffic for example. Each user is assumed to send data in packets and during each time interval (packet length) the state of each user (active or silent) is a random variable and the users might change their states randomly at the end of

each packet. This process is shown in Fig.4.8.

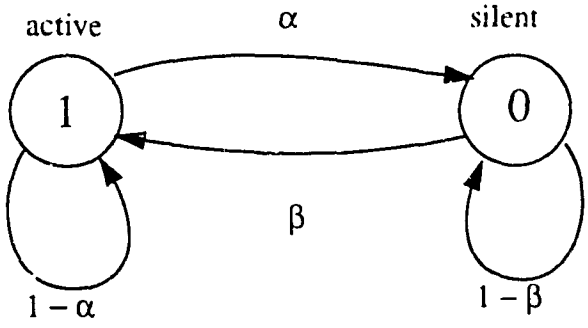

Fig. 4.8: State diagram of each user

where:

α : the probability that a user changes its state from active to silent at the end of a packet.

β : the probability that a user changes its state from silent to active at the end of a packet.

To compute the parameters α and β, suppose P_A and P_S are the steady state probabilities in active and silence periods, respectively. Then:

$$\alpha P_A = \beta P_S \tag{4.11}$$

$$P_A + P_S = 1 \tag{4.12}$$

so:

$$P_A = \frac{\beta}{\alpha+\beta}, \quad P_S = \frac{\alpha}{\alpha+\beta} \tag{4.13}$$

In a voice channel usually in about 1/3 of the time the user is in active mode, i.e., $P_A \approx 1/3$ and $P_S \approx 2/3$.

The active period length is Geometrically distributed so if $Pr\{X= i\}$ is the probability that a user is in active period for i packets, the mean active period will be:

$$(mean\ active\ period) = \left[\sum_{i=1}^{\infty} i(1-\alpha)^{i-1}\alpha\right]T_P \tag{4.14}$$

where T_P is the packet transmission time:

$$T_P = \frac{Packet\ length}{Capacity}\ , \text{but}\ \sum_{i=1}^{\infty} i(1-\alpha)^{i-1}\alpha = \frac{1}{\alpha}$$

so:

$$\alpha = \frac{T_P}{mean\ active\ period} \tag{4.15}$$

similarly:

$$\beta = \frac{T_P}{mean\ silence\ period} \tag{4.16}$$

In practical cases the mean active and silence periods are 350 *msec.* and 650 *msec.*, respectively, in the period of one second. In our simulations we assumed that:

Packet length = 500 bits,

Data transmission rate (Capacity) = 100000 bits/sec,

$$\therefore \qquad T_P = \frac{500}{100000} = 5\ m\text{sec}$$

and, $$\alpha = \frac{5\times 10^{-3}}{350\times 10^{-3}} = \frac{1}{70}, \qquad \beta = \frac{5\times 10^{-3}}{650\times 10^{-3}} = \frac{1}{130}$$

Also it is assumed that the data packets of all users are synchronous, for network objectives, even if there is bit asynchronism (considering the packet size this is a fair assumption), also the bit asynchronism was considered in evaluation of BER during the simulations.

Two different cases have been considered for simulations. One case is when the users do not transmit any data during OFF (silence) periods or the transmitted data are not important, i.e., the users are not completely off during these periods and transmit some power but it's not detected, so the average BER results pertain only to active users bursts.

The second case is when the users transmit data during OFF periods and their data are detected by the receiver, so the BER results are averaged over both silence and active bursts of all users (as a possible practical scenario, the data detection is needed for code acquisition and tracking during OFF periods). Simulations have been done for both cases for different power levels during the OFF periods and by assuming different kinds of codes as signature codes.

Two kinds of maximal sequence and Gold code were used in the simulations. The maximal sequence was generated by the feedback shift register, shown in Fig.4.9 (page 85), with *characteristic polynomial* $f(x) = 1 + x^3 + x^7$. The family of Gold codes was generated by combining the output of two feedback shift registers, as in Fig.4.10 (page 86), with *characteristic polynomials*: $f_1(x) = 1 + x + x^7$, and $f_2(x) = 1 + x^3 + x^7$.

For interested readers, some of the simulation programs used for this section are listed in Appendix on page 102.

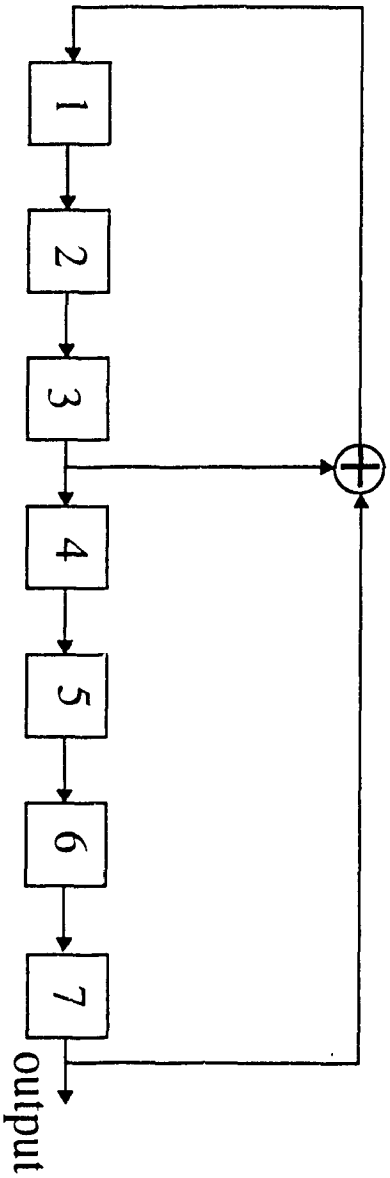

Fig. 4.9: Maximal sequence generator of length 127 (n=7)

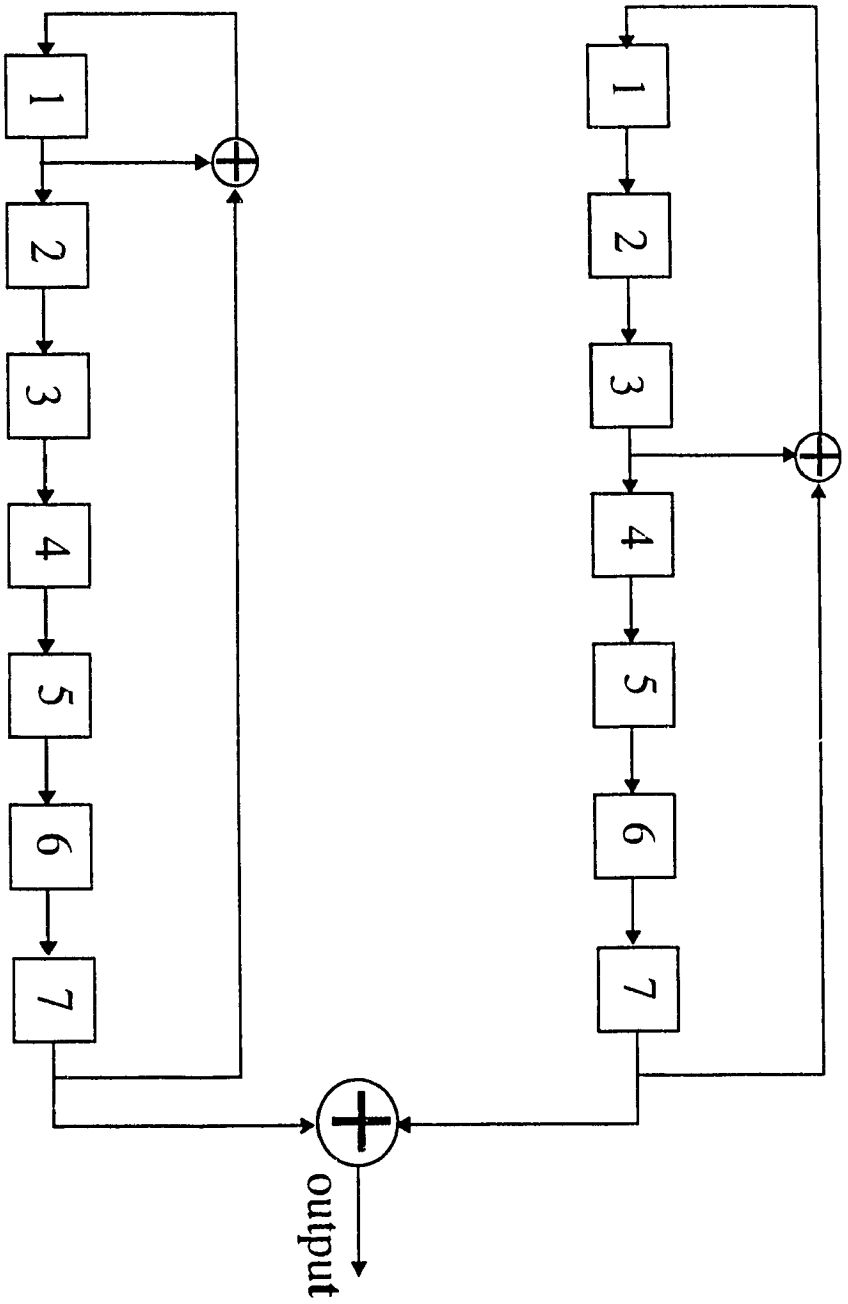

Fig. 4.10: Gold code generator of length 127 (n=7)

4.4 Simulation Results

In Fig.4.11 - Fig.4.15, (pages 89-93), the average BER for single user and sub-optimum multi-user receivers employing Gold codes and Maximal sequences in two synchronous and asynchronous cases with different SNR's (SNR=10 and SNR=1), are shown. The interesting observation from Fig.4.12 (page 90) and Fig.4.15 (page 93) is that the sub-optimum multi-user detection doesn't necessarily perform better than single user detection in all cases[1]. It is clear from these figures that for low SNR, high AWGN, single user detection performs better, so the necessity of employing two kinds of detection, single user and multi-user and comparing the detected data from both of them and choosing the most adequate one, in the proposed hybrid receiver of Fig.4.5, (page 77), are obvious. Fig.4.13, (page 91), shows the performance of single user, multi-user and the hybrid receiver for different levels of noise (SNR). Again it is clear that the hybrid receiver by taking advantage of both single user and multi-user detection, performs better in different noise environment.

Another observation from Fig.4.14 and Fig.4.15, (pages 92-93), is that the multi-user detection employing maximal sequences might be very unreliable in the asynchronous case. When different phases of one maximal sequence are used as signature codes for different users, if the maximum delay for the users is more than the difference in users' signature phases (the case of these figures), it might happen that the signature codes of two or more users look completely alike at the receiver[2]. In a single user receiver this problem may only destroy the received data of those users with the same signature codes, but in multi-user detection because of the nature of this kind of detection the error will distribute

1. This is due the fact that the multi-user detection, employed in this system, is sub-optimum.

2. It should be noticed that for this part of simulations only one set of delays is randomly chosen for all users. For some values of K, (total number of users), some of these delays are equal to phase difference between signature codes which results very high BER in multi-user detection.

and prevail among all users and the received data from all users might be destroyed (BER=0.5 as in Fig.4.14 and Fig.4.15). Again in such cases is better to rely on the results from single user detection.

The average BER for multi-user detection (30 users) when users have ON (active) and OFF (silence) periods like voice traffic, for instance, for two cases of detecting and ignoring the transmitted data by OFF users are shown in Fig.4.16 and Fig.4.17, (pages 94-95). As it was expected, the average BER is higher in the case of detection during OFF periods because of low SNR during these periods. BER decreases when the power level for OFF users (SNR for OFF users) increases.

When there is no detection during OFF periods (Fig.4.17) the average BER is much better and opposite to previous case, because of multiple-access interference, the BER might increase when the power level for OFF users (SNR for OFF users) increases. So when there is no need to detect the transmitted data by OFF users it is better to completely shut them off during these periods (no power is transmitted during OFF periods). This conclusion stands in contrast with TIA standard, [28], which necessitate power transmission during OFF periods to ease the recognition the variable user rate (VBR).

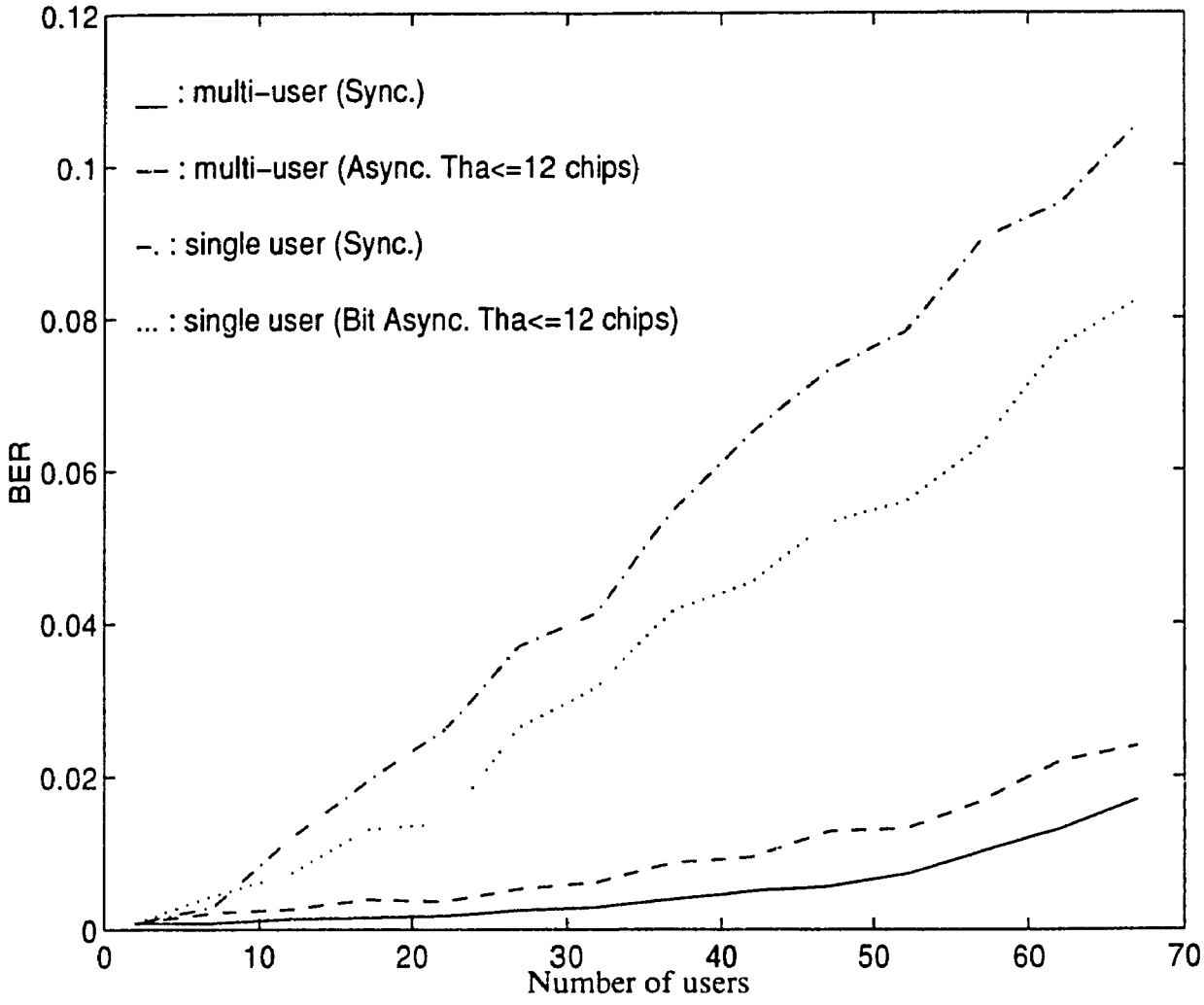

Fig. 4.11: BER for single and multi user receivers using Gold Codes (n=7), SNR=10. Note: multi-user detection performs better so the performance of hybrid receiver is as multi-user detection.

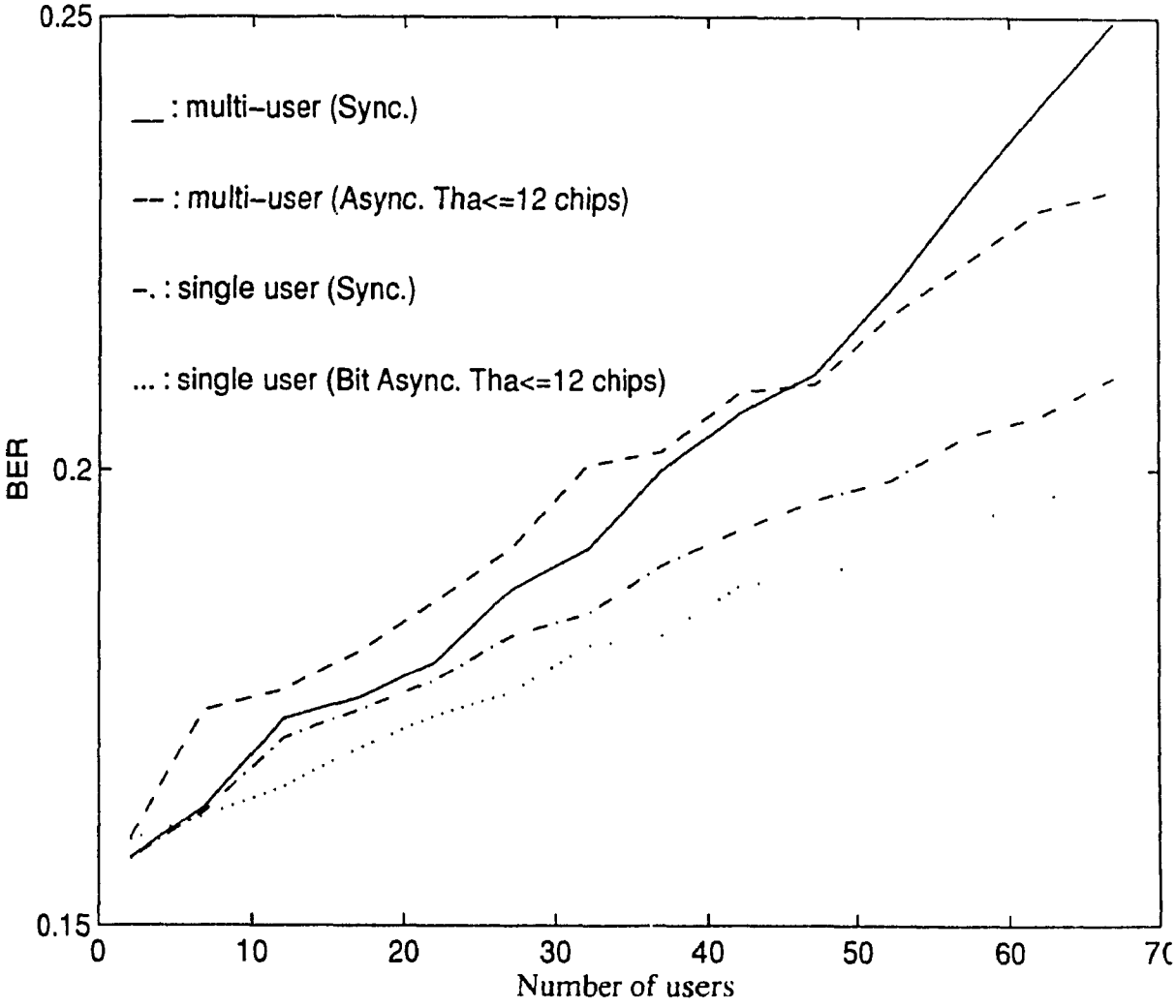

Fig. 4.12: BER for single and multi user receivers using Gold Codes (n=7), SNR=1. Note: single user detection performs better so the performance of hybrid receiver is as single user detection.

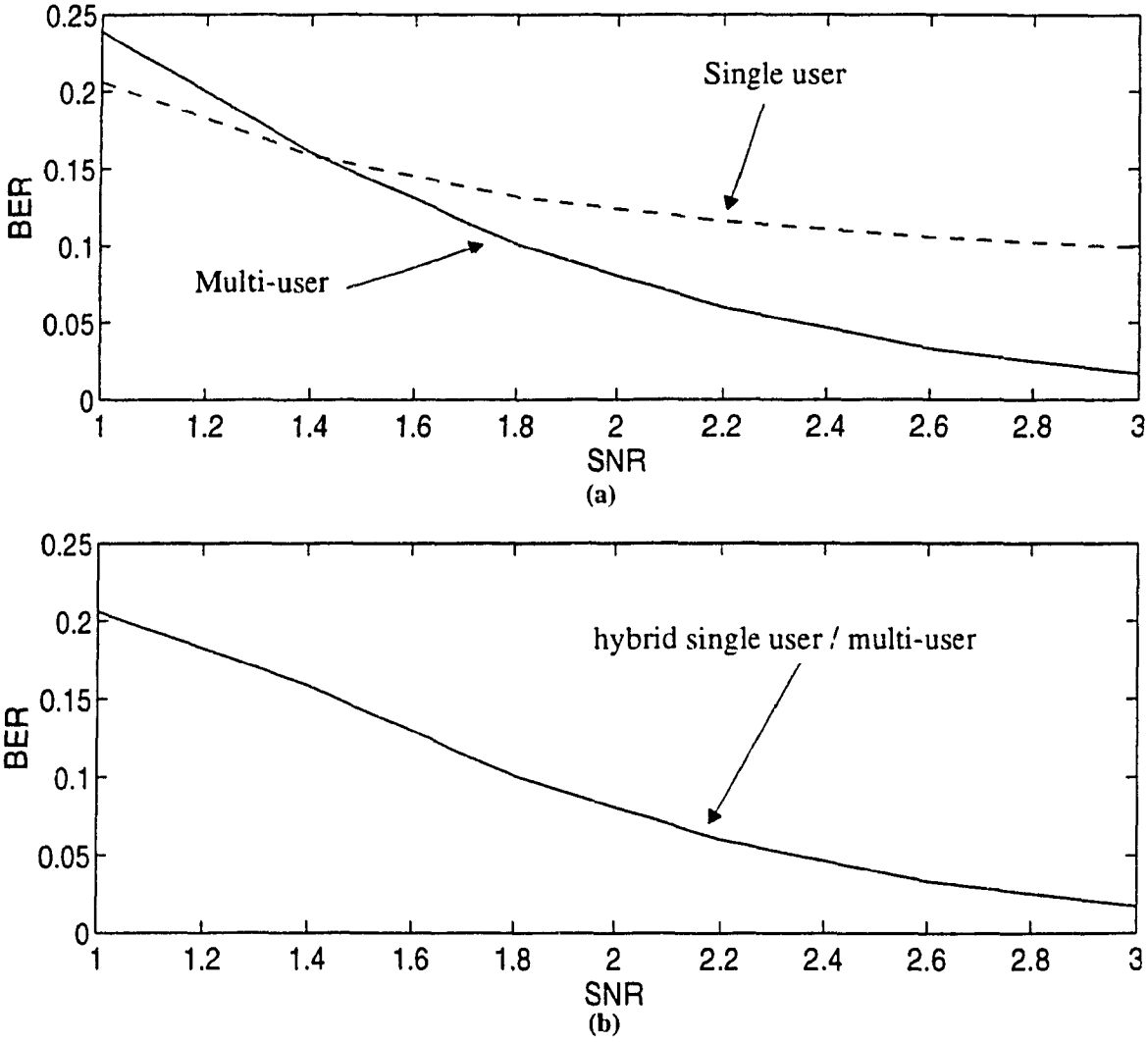

Fig. 4.13: BER for 62 users using Gold codes (n=7) with low SNR in (a): single user and multi-user detection, (b): hybrid single user / multi-user detection (proposed system)

Note: High probability of error is due to very low SNR and large number of users, (62 users for the code length 127).

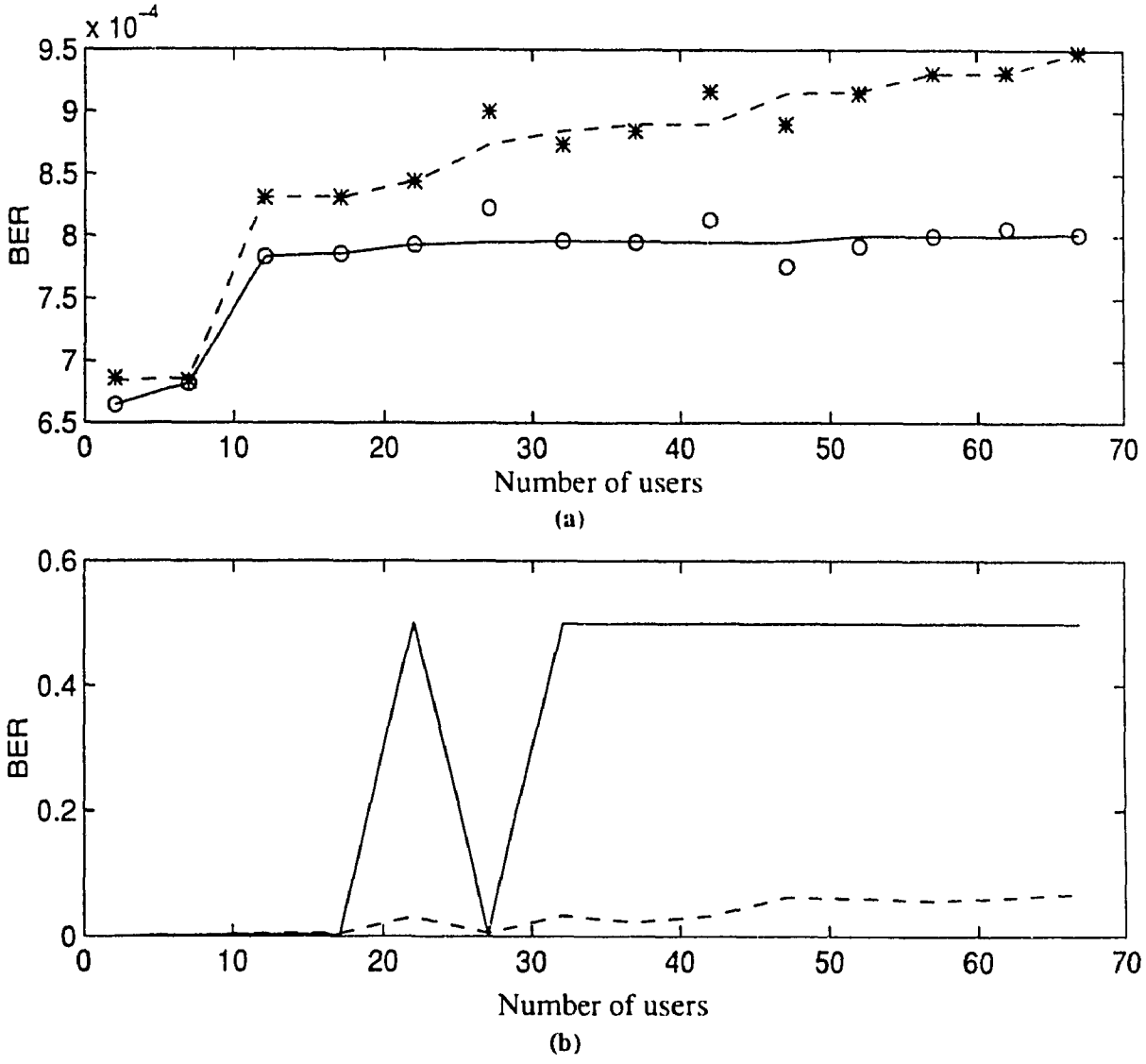

Fig. 4.14: BER for single and multi user receivers using maximal sequences (n=7), SNR=10, (a): Sync. case, (b): Async. case ($\tau_k \leq 12$ chips), '__' (o): multi-user, '--' (*): single user

Note: In asynchronous case, (b), only one set of delays for $\tau_k \leq 12$ is chosen for all users at the beginning of simulations. In case of K=22 and $K \geq 32$ some of the delays are equal to the phase shift between the signature codes so there is high BER for multi-user detection. for K=27 it didn't happen and system has good BER.

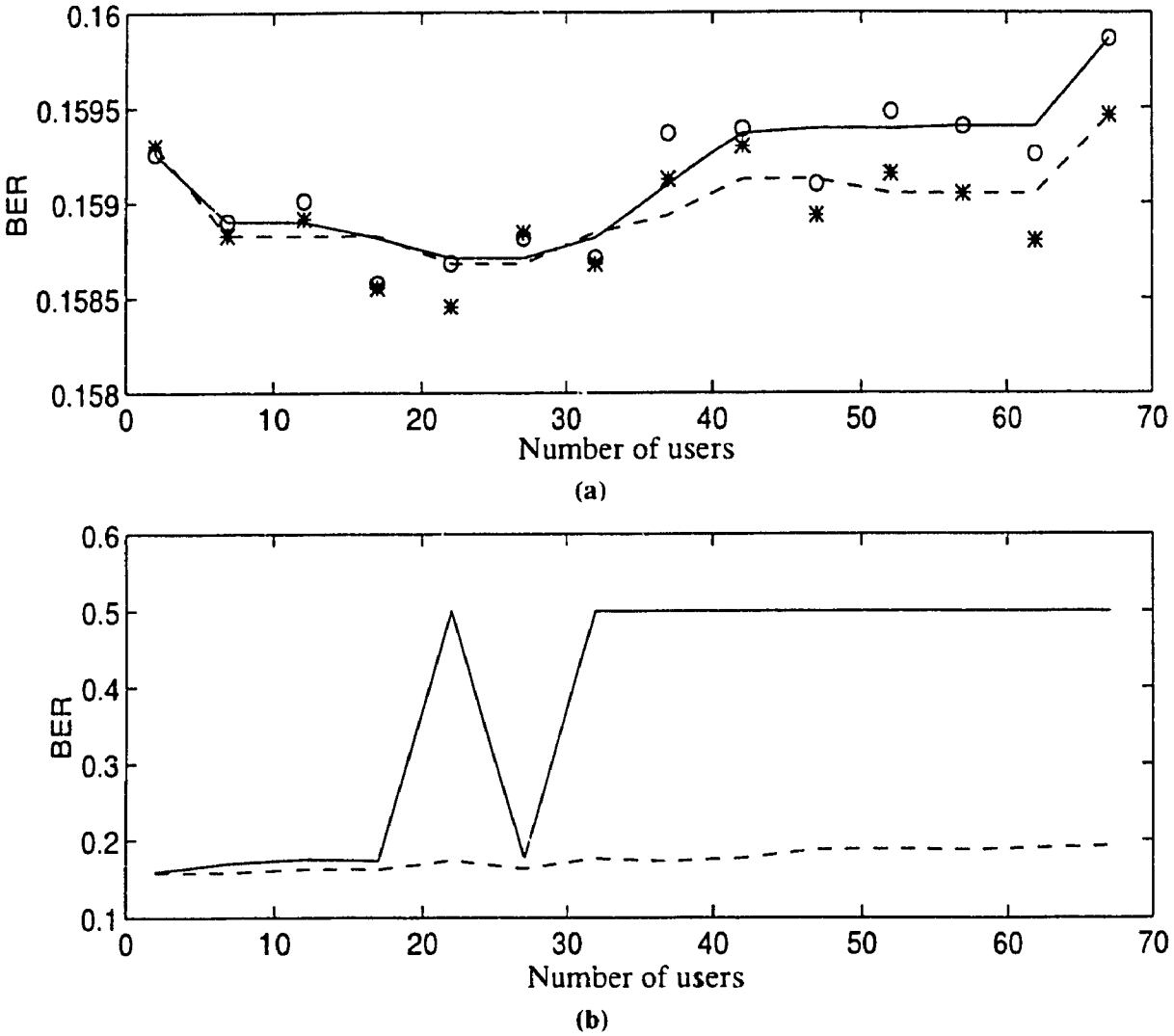

Fig. 4.15: BER for single and multi user receivers using maximal sequences (n=7), SNR=1, (a): Sync. case, (b): Async. case ($\tau_k \leq 12$ chips), '__' (o): multi-user, '--' (*): single user

Note: In asynchronous case, (b), only one set of delays for $\tau_k \leq 12$ is chosen for all users at the beginning of simulations. In case of K=22 and $K \geq 32$ some of the delays are equal to the phase shift between the signature codes so there is high BER for multi-user detection. for K=27 it didn't happen and system has good BER.

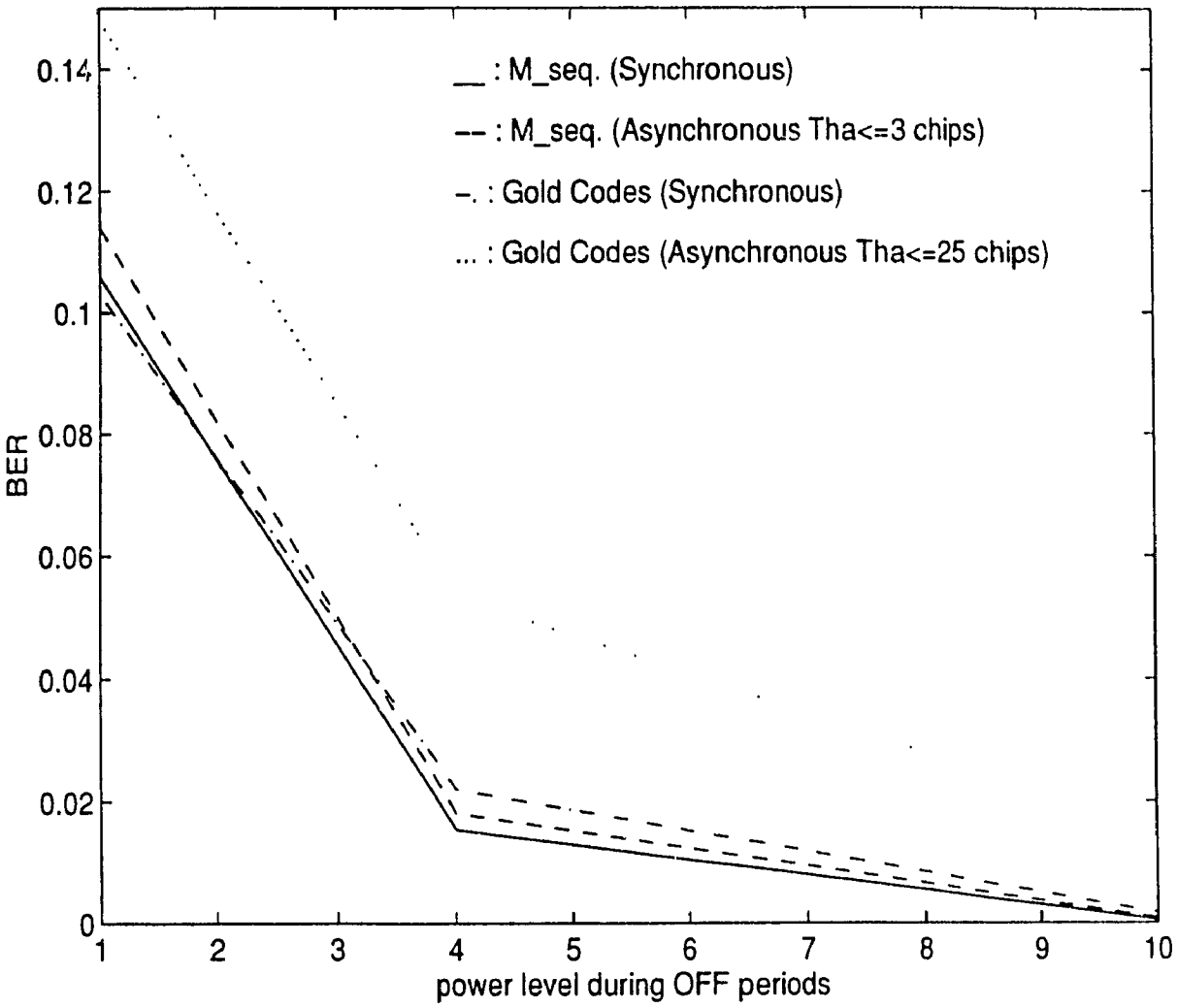

Fig. 4.16: BER for 30 users in multi-user receiver considering ON and OFF periods: Detecting the transmitted data by OFF users.

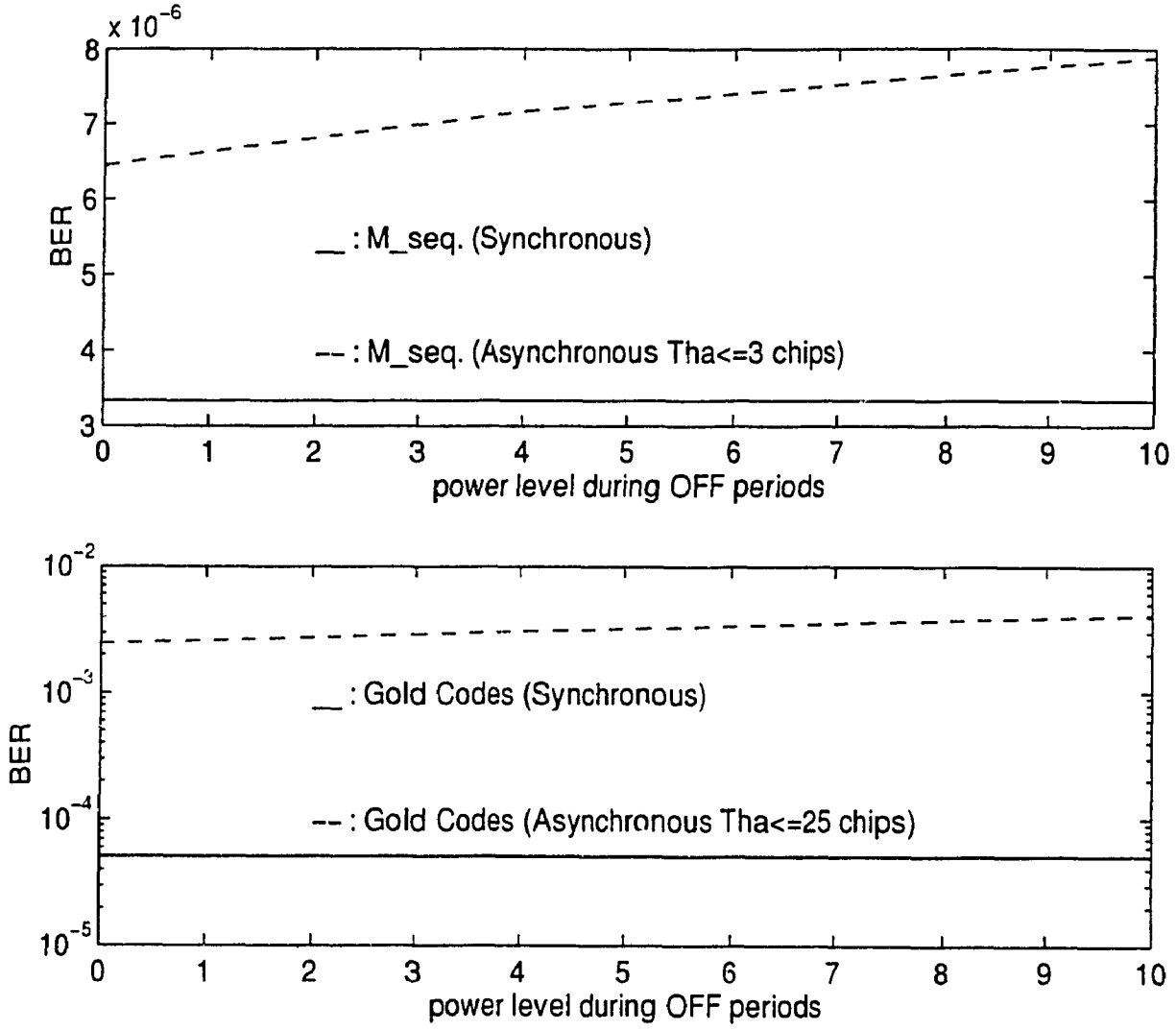

Fig. 4.17: BER for 30 users in multi-user receiver considering ON and OFF periods: Ignoring the transmitted data by OFF users.

CHAPTER 5

SUMMARY AND CONCLUSIONS

In chapter 3, the effects of selecting different kinds of codes as signature codes on the performance of multi-user receiver were investigated. Maximal sequence codes, Gold codes and the combination of one of these codes with Walsh functions were the codes which were considered as signature codes in simulations for this part of the thesis. The cross-correlation properties of these codes were explained in details and in the case of Walsh functions, the cross-correlations were calculated by the computer.

The simulation results showed that using codes with less cross-correlations provides better SNR. Also it was demonstrated by simulations that employing a combination of orthogonal functions and short linear codes would improve the SNR in multi-user detection.

In chapter 4, a new hybrid single user/multi-user detection scheme was introduced. Since this receiver took advantage of both single user and multi-user detection, it was necessary to examine the performance of single user and multi-user receiver in different noise levels (SNR) with employing different kinds of signature codes. In the simulations, besides the synchronous case, the asynchronous case was also considered.

The simulation results showed that in low SNR (high noise level) the single user receiver performed better than multi-user receiver. So, the necessity of employing both of them in the hybrid receiver was established. It was shown by simulations that the hybrid receiver in overall performed better than each of the single user and multi-user receivers. A very important and interesting observation in the simulation results, was the effect of the case that two or more signature codes look alike at the receiver. This might happen

when different phases of one maximal signature code are used as signature codes in asynchronous case when the maximum delay is more than the minimum of the difference in phase between two signature codes. The simulation results showed that this could destroy completely the reliability of multi-user detection but did not have serious effects, in overall, on BER of single user receiver. Again our hybrid receiver is almost immune of this danger.

In the rest of this chapter, the performance of multi-user detection in voice transmission, was studied. In this kind of information transmission, users are not active whole the time and there are silent or OFF periods. The model for this ON and OFF transmission was described. Two different cases were considered in the simulations for this part. The first case was when the users transmitted the data during OFF periods and the data was detected by the receiver. Results showed that for having better BER users should transmit more power during OFF periods, because the information transmitted during these periods is important.

The second case was the time that there was no detection during OFF periods. In this case, according to the simulation results, to have better BER users should transmit less power during OFF periods. So in this case, it is better not to transmit any power during OFF periods. This conclusion is in contrast with TIA standard [28], which necessitate power transmission during OFF periods to ease the recognition of the variable user rate (VBR).

Suggestions for Future Works:

- In our work we didn't consider fading. So as a possible continuation of this work, the performance of the hybrid receiver can be examined in different fading environments.

- The performance of the hybrid receiver can be improved by employing better multi-user detection scheme.

- In Sec.4.3, we considered only voice transmission. It is interesting to study the performance of multi-user detection in multimedia transmission.

REFERENCES

[1] M. B. Pursley, "The Role of Spread Spectrum in Packet Radio Networks", *Proc. IEEE*, Vol. 75, no. 1, pp. 116-134, Jan. 1987.

[2] R. Ziemer and R. Peterson, *Digital Communication and Spread Spectrum Systems*, New York, Macmillian, 1985

[3] Don J. Torrieri, *Principles of Secure Communication Systems*, Artech House, 1992.

[4] R. C. Dixon, *Spread Spectrum Systems*, John Wiley and Sons, New York, 1985.

[5] R. C. Dixon, "Why Spread Spectrum ", *IEEE Communications Society Magazine*, Vol. 13, pp. 21-25, July 1975.

[6] S. Verdu, "Recent Progress in Multiuser Detection", *Multiple Access Communications: Foundations for Emerging Technologies*, Edited by Norman Abramson, IEEE Press, pp. 164-175.

[7] S. Verdu, "Minimum Probability of Error for Asynchronous Gaussian Multiple-Access Channels", *IEEE Trans. Inform. Theory*, Vol. IT32, pp. 85-96, Jan. 1986.

[8] R. Lupas and S. Verdu, "Linear Multiuser Detectors for Synchronous Code Division Multiple Access Channels." *IEEE Trans. Inform. Theory.*, Vol. IT-35, pp. 123-136, Jan 1989.

[9] H. L. Van Trees, *Detection, Estimation and Modulation Theory, Part I*, John Wiley and sons, New York, 1968, page 29.

[10] M. Barkat, *Signal Detection and Estimation*, Artech House, Boston, 1991, page 128.

[11] S. Verdu, "Computational Complexity of Optimum Mutliuser Detection", *Algorithmica*, Vol. 4, 1989.

[12] K. S. Schneider, "Optimum Detection of Code Division Multiplexed Signals",

IEEE Trans. Aerosp. Electron. Syst., Vol. AES-15, pp. 181-185, Jan. 1979.

[13] D. S. Chen and S. Roy, "An Adaptive Multi-User Receiver for CDMA Systems", *IEEE Journal on Selected Areas in Comm.*, Vol. 12, No 5, pp. 808-816, June 1994.

[14] J. G. Proakis, *Digital Communications*, McGraw-Hill 1989

[15] M. K. Varanasi, and B. Aazhang, "Near-Optimum Detection in Synchronous Code Division Multiple Access Systems", *IEEE Trans. on Comm.*, Vol. COM-38, pp. 509-519, April 1990.

[16] P. Patel, and J. Hotzman, "Analysis of a Simple Successive Interference Cancellation Scheme in DS/CDMA System", *IEEE Journal on Selected Areas in Comm.*, Vol. 12, No 5, pp. 796-807, June 1994.

[17] P. R. Patel, and J. M. Holtzman, "Analysis of a DS/CDMA Successive Interference Cancellation Scheme Using Correlations", *Proceedings*, Globecom 93, pp. 76-80

[18] M. B. Pursley, "Performance Evaluation for Phase-Coded Spread Spectrum Multiple Access Communication-Part I: System Analysis", *IEEE Trans. on Comm.*, Vol. COM-25, 1977.

[19] J. Holtzman, "On Calculating DS/SSMA Error Probabilities", *Proceedings*, International Symposium on Spread Spectrum Techniques and Applications (ISSSTA), Yokohama, Japan, Dec. 92.

[20] A. Papoulis, *Probability, Random Variables, and Stochastic Processes*, Third Edition, McGraw-Hill, 1991, Page 54

[21] J. Blanz, A. Klein, M. Nasshan, and A. Steil, "Performance of a cellular hybrid C/ TDMA mobile radio system applying joint detection and coherent receiver diversity", *IEEE Journal on Selected Areas in Comm.*, Vol. 12, No 4, pp. 568-579, May 1994.

[22] A. D. Whalen, *Detection of Signals in Noise*, New York, Academic Press, 1971.

[23] A. Klein, and P. W. Baier, "Linear Unbiased Data Estimation in Mobile Radio Systems Applying CDMA", *IEEE Journal on Selected Areas in Communications*, Vol. 11, pp. 1058-1066, 1993.

[24] A. K. Elhakeem, M. A. Rahman, P. Balasubramanian, and T. Le-Ngoc, "Modified Sugar/DS: A New CDMA Scheme", *IEEE Journal on Selected Areas in Comm.*, Vol. 10, No 4, pp. 690-704, May 1992.

[25] E. Rezaaifar, and A. K. Elhakeem, "Signature Code Selection for Multi-User Detection Scheme in CDMA Systems", *Proceedings*, 1995 Canadian Conference on Electrical and Computer Engineering, Montreal, Canada, pp. 661-664, Sep. 95.

[26] R. L. Pickholtz, D. L. Schiling, and L. B. Milstein, "Theory of Spread Spectrum Communications - A Tutorial", *IEEE Trans. Comm.*, Vol. COM-30, No. 5, pp. 855-884, May 1982.

[27] J. J. Spilker, *Digital Communications by Satellite*, Prentice-Hall, New Jersey, 1977, page 605.

[28] "An Overview of the Application of Code Division Multiple Access (CDMA) to Digital Cellular Systems and Personal Cellular Networks", QUALCOMM Inc., May 1992.

[29] *IEEE Journal on Selected Areas in Comm.*, Special Issue, May, June 1994, Editor: A. K. Elhakeem.

[30] P. B. Rapajic, and S. Vucetic, "Adaptive Receiver Structures for Asynchronous CDMA Systems", *IEEE Journal on Selected Areas in Comm.*, Vol. 12, No 4, pp. 685-697, May 1994.

[31] R. A. Iltis, and L. Mailaender, "An Adaptive Multiuser Detector with Joint Amplitude and Delay Estimation", *IEEE Journal on Selected Areas in Comm*, Vol. 12, No 5, pp. 774-785, June 1994.

APPENDIX

The simulations in this thesis have been done employing MATLAB. Considering different cases in simulations demanded writing a large number of programs and sub-routines. Here for interested readers a few of the programs and sub-routines used for part of simulations described in chapter 4, are listed.

---

mseq7.m: The program to generate a maximal sequence of the degree 7. The characteristic polynomial for the linear feedback shift register is: $f(x) = 1 + x^3 + x^7$

```
% Maximal sequence generator of degree 7
% f(x)=1+x^3+x^7

  C=[1 0 1 0 0 0 1]; % initial conditions
  n=length(C);
  clear out
  for i=1:(2^n-1),
     out(i)=C(n);
     feed=xor(C(3),C(7));
     for j=n:-1:2,
        C(j)=C(j-1);
     end
     C(1)=feed;
  end
```

---

shift.m: The function to make a circular shift in the input vector

---

```
% this function provides a circular shift in a vector

 function y = shift(v,i)
   m=length(v);
   vi=v;
  if i >= m
      while i >= m
       i=i-m;
       end
```

```
end
if i ~= 0
    vi((i+1):m)=v(1:(m-i));
    vi(1:i)=v((m-i+1):m);
end
y=vi;
```

---

bal.m: The function to change the codes which are the sequence of zeros and ones to the codes of the sequence of 1's and -1's

---

```
% this function change the code of zeros and
% ones to 1 and -1 's.

function y = bal(v),
 for i=1:length(v),
     w(i)=1;
     if v(i)==0,
        w(i)=-1;
     end
 end
 y=w;
```

---

signat.m: The program to create and save the signature codes for all users. Different phases of a maximal sequence code are used as signature codes

---

```
% this file creates signature codes for defined number of users

usern=10; %number of users
mseq7
s1=bal(out);
for i=1:length(out),
    j=2*i-1;
    s(j)=s1(i);
    s(j+1)=s(j);
end
del=round(round(length(s)/usern)/2-0.1)*2
```

```
for i=1:usern,
   S(i,:)=shift(s,del*(i-1));
end
S=S/sqrt(length(s));
save signat7  usern S del
```

---

bin.m: The function to change a decimal number to binary

```
% This function changes a number to binary with the length n

function y=bin(a,n)
  b=zeros(1,n);
 for i=1:n,
    b(i)=rem(a,2);
    a=fix(a/2);
 end
 y=fliplr(b);
```

---

goldfun.m: The function to generate Gold codes. The input to the function is the initial values for two linear shift register. The characteristic polynomials for two linear shift registers are: $f_1(x) = 1 + x^3 + x^7$ and $f_2(x) = 1 + x + x^7$

```
% This function generate Gold sequence as the output. The input
% is the initial values for two linear code generators
% f1(x)=1+x^3+x^7 , f2(x)=1+x+x^7

 function y = goldfun(C1,C2),
   n=length(C1);
  clear out
  for i=1:(2^n-1),
     out1(i)=C1(n);
     out2(i)=C2(n);
     feed1=xor(C1(3),C1(7));
     feed2=xor(C2(1),C2(7));
     for j=n:-1:2,
```

```
        C1(j)=C1(j-1);
        C2(j)=C2(j-1);
    end
  C1(1)=feed1;
  C2(1)=feed2;
  end
  y=xor(out1,out2);
```

---

gold7.m: The program to generate different Gold codes of a family of gold codes of the length 127 for different users.

```
% Gold code generator of degree 7 for defined # of users
% f1(x)=1+x^3+x^7 , f2(x)=1+x+x^7

  C1=[1 0 1 0 0 0 1];
  usern=127;
  for k=1:usern,
     C2=bin(k,7);
     s1 = bal(goldfun(C1,C2));
     for i=1:length(s1),
         j=2*i-1;
         s(j)=s1(i);
         s(j+1)=s(j);
     end
      S(k,:)=s/sqrt(length(s));
  end
  save g7sig  S usern
```

---

goldtest.m: The program to find the BER for single user and multi-user detection scheme. Different number of active users using Gold codes in synchronous case are considered.

```
  clear
  note='Ber for single user and multiuser receiver for different # of users using Gold n=7'
  load g7sig
```

```
S1=S;
datal=50000;
ls=length(S(1,:));
p=1;
w=2:5:67;
for usern=2:5:67,
    usern
    clear S
    usesig=select(usern);
    for i=1:usern,
        S(i,:)=S1(usesig(i),:);
    end
    E=sqrt(10)*ones(1,usern); % power for each user
    SNR=10
    lambda=1; % forgetting factor (0,1]
    err=zeros(1,usern);% error for multi-user detection
    singerr=zeros(1,usern); % error for single user detection
    Rn=0;
    for m=1:ls,
      Rn=Rn+lambda^(ls-m)*S(:,m)*S(:,m)';
    end
    Rninv=inv(Rn);
    for ii=1:datal,
      d=datk(usern);% determining one bit of data for each user
      r=zeros(1,ls);
      for l=1:usern, % determining the arriving vector for each bit
          r=r+E(l)*d(l)*S(l,:);
      end
      r=r+randn(1,ls);
      usedata=zeros(1,usern);
      for q=1:usern,
           usedata(q)=r*S(q,:)';
      end
      singdata=sign(usedata);
      Dn=0;
      for m=1:ls,
          Dn=Dn+lambda^(ls-m)*r(m)*S(:,m);
      end
     Cn=Rninv*Dn;
     data=sign(Cn);
     for k=1:usern,
          if data(k) ~= d(k)
              err(k)=err(k)+1;
          end
          if singdata(k) ~= d(k)
              singerr(k)=singerr(k)+1;
```

```
        end
      end
    end
    Ber(p)=ber(err,usern,datal)
    singBer(p)=ber(singerr,usern,datal)
   save Case53 Ber singBer note w SNR
   p=p+1;
 end
```

---

goldAsync.m: Asynchronous case

```
clear
note='Ber for single user and multiuser receiver for different # of users using Gold n=7,
Async. case, max delay 12 chips'
 load g7sig
S1=S;
datal=50000;
ls=length(S(1,:));
p=1;
w=2:5:102;
Thaset=round(24*rand(1,102));
Thaset(1)=0
for usern=2:5:102,
   usern
   clear S
    usesig=select(usern);
    for i=1:usern,
       S(i,:)=S1(usesig(i),:);
    end
    Ss=S;
    E=sqrt(10)*ones(1,usern); % power for each user
    SNR=10;
    lambda=1;  % forgetting factor  (0,1]
    err=zeros(1,usern);
    singerr=zeros(1,usern);
    Rn=0;
    Tha=Thaset(1:usern)
    d = sign(rand(3,usern)-0.5);
    for i=1:usern,
    S(i,:)=shift(S(i,:),Tha(i));
    end
    for m=1:ls,
       Rn=Rn+lambda^(ls-m)*S(:,m)*S(:,m)';
```

```
end
Rninv=inv(Rn);
for ii=1:datal,
    d(1,:)=d(2,:);
    d(2,:)=d(3,:);
    d(3,:)=datk(usern);
    SS1=S;
    SS2=S;
   for i=1:usern,
     for j=1:Tha(i),
        SS1(i,j)=d(1,i)*d(2,i)*3S1(i,j);
        SS2(i,j)=d(2,i)*d(3,i)*SS2(i,j);
     end
   end
   if ii==1,
     r1=zeros(1,ls);
     for l=1:usern,
         r1=r1+E(l)*d(2,l)*SS1(l,:);
     end
     r1=r1+randn(1,ls);
     else
     r1=r2;
   end
   r2=zeros(1,ls);
   for l=1:usern,
     r2=r2+E(1)*d(3,l)*SS2(l,:);
   end
   r2=r2+randn(1,ls);
   usedata=zeros(1,usern);
   for q=1:usern,
      qd=ls-Tha(q);
      r(1:qd)=r1(Tha(q)+1:ls);
      r(qd+1:ls)=r2(1:Tha(q));
      usedata(q)=r*Ss(q,:)';
   end
   singdata=sign(usedata);
   Dn=0;
   for m=1:ls,
       Dn=Dn+lambda^(ls-m)*r1(m)*S(:,m);
   end
   Cn=Rninv*Dn;
   data=sign(Cn);
   for k=1:usern,
       if data(k) ~= d(2,k)
          err(k)=err(k)+1;
       end
```

```
            if singdata(k) ~= d(2,k)
                singerr(k)=singerr(k)+1;
            end
        end
    end
    Ber(p)=ber(err,usern,datal)
    singBer(p)=ber(singerr,usern,datal)
    save Case50 Ber singBer note w SNR Thaset
    p=p+1;
end
```

---

onoffG1.m: Program to find the BER for multi-user detection when there is voice transmission, i.e. there is ON and OFF periods. The users using Gold codes and there is detection during OFF periods. Synchronous case.

```
clear
Alpha1=1/70; % Probability to go from active to silent
Beta1=1/130; % Probability to go from silent to active
note='Ber multiuser receiver considering on and off periods using Gold n=7'
note1='Eon/Eoff = 20 / 1, Detecting during off periods'
Eon=20
Eoff=1
packsize=500;
packno=300;
load g7sig
S1=S;
ls=length(S(1,:));
usern=30
clear S
usesig=select(usern);
for i=1:usern,
    S(i,:)=S1(usesig(i),:);
end
userstat=fix(rand(1,usern)+0.5) % zero status means silent mode
lambda=1;  % forgetting factor  (0,1]
err=zeros(1,usern);
Rn=0;
for m=1:ls,
    Rn=Rn+lambda^(ls-m)*S(:,m)*S(:,m)';
end
Rninv=inv(Rn);
```

```
for Packet=1:packno,
   E=sqrt(Eon)*ones(1,usern); % power for each user in active period
   changeprob=rand(1,usern); % random # to change the status
   for i=1:usern,
      if userstat(i)==0,
         E(i)=sqrt(Eoff); % power for each user in silent period
         if changeprob(i) < Beta1
            userstat(i)=1;
         end
      elseif userstat(i)==1,
         if changeprob(i) < Alpha1
            userstat(i)=0;
         end
      end
   end
   for ii=1:packsize,
      d=datk(usern);% determining one bit of data for each user
       r=zeros(1,ls);
      for l=1:usern, % determining the arriving vector for each bit
         r=r+E(l)*d(l)*S(l,:);
      end
      r=r+randn(1,ls);
      Dn=0;
      for m=1:ls,
         Dn=Dn+lambda^(ls-m)*r(m)*S(:,m);
      end
      Cn=Rninv*Dn;
      data=sign(Cn);
      for k=1:usern,
         if data(k) ~= d(k)
            err(k)=err(k)+1;
         end
       end
   end
end
Ber=ber(err,usern,packsize*packno)
save Case45 Ber note  err usern packsize packno Alpha1 Beta1 userstat note1
```

---

onoffG2.m: Ignoring data during OFF periods.

```
clear
```

```
Alpha1=1/70; % Probability to go from active to silent
Beta1=1/130; % Probability to go from silent to active
note='Ber multiuser receiver considering on and off periods using Gold n=7'
note1='Eon/Eoff = 20 / 1 , ignoring the data in off periods'
Eon=20
Eoff=1
bitno=0;
packsize=500;
packno=300;
load g7sig
S1=S;
ls=length(S(1,:));
usern=30
clear S
usesig=select(usern);
for i=1:usern,
   S(i,:)=S1(usesig(i),:);
end
userstat=fix(rand(1,usern)+0.5) % zero status means silent mode
lambda=1;  % forgetting factor  (0,1]
err=zeros(1,usern);
Rn=0;
for m=1:ls,
   Rn=Rn+lambda^(ls-m)*S(:,m)*S(:,m)';
end
Rninv=inv(Rn);
for Packet=1:packno,
   E=sqrt(Eon)*ones(1,usern); % power for each user in active period
   bitno=bitno+sum(userstat);
   changeprob=rand(1,usern); % random # to change the status
   for i=1:usern,
      if userstat(i)==0,
         E(i)=sqrt(Eoff); % power for each user in silent period
         if changeprob(i) < Beta1
            userstat(i)=1;
         end
      elseif userstat(i)==1,
          if changeprob(i) < Alpha1
            userstat(i)=0;
          end
       end
   end
   for ii=1:packsize,
      d=datk(usern);% determining one bit of data for each user
      r=zeros(1,ls);
      for l=1:usern, % determining the arriving vector for each bit
```

```
        r=r+E(l)*d(l)*S(l,:);
    end
    r=r+randn(1,ls);
    Dn=0;
    for m=1:ls,
        Dn=Dn+lambda^(ls-m)*r(m)*S(:,m);
    end
    Cn=Rninv*Dn;
    data=sign(Cn);
    for k=1:usern,
        if (E(k) ~= sqrt(Eoff)) & (data(k) ~= d(k))
            err(k)=err(k)+1;
        end
    end
  end
end
Ber=sum(err)/(bitno*packsize)
save Case46 Ber note  err usern packsize packno Alpha1 Beta1 userstat note1
```